

Synthesis of Geosynthetic Reinforced Soil (GRS) Design Topics

PUBLICATION NO. FHWA-HRT-14-094

FEBRUARY 2015



U.S. Department of Transportation
Federal Highway Administration

Research, Development, and Technology
Turner-Fairbank Highway Research Center
6300 Georgetown Pike
McLean, VA 22101-2296

FOREWORD

Geosynthetic reinforced soil (GRS) for load-bearing applications has been identified by the Federal Highway Administration (FHWA) as a proven, market-ready technology and is being actively promoted through the agency's Every Day Counts initiative. With the publication of the FHWA interim design guidance for GRS abutments and integrated bridge systems, presented in *GRS Integrated Bridge System (IBS) Interim Implementation Guide* (FHWA-HRT-11-026), FHWA took the first steps to differentiate the design of GRS and conventional, larger-spaced geosynthetic mechanically stabilized earth (GMSE). This was based on considerable research and the change in behavior observed when reinforcement is closely spaced (i.e., less than about 12 inches (30.48 cm)). Because of its similarities to GMSE walls, however, there are some misconceptions about the design and behavior of closely spaced GRS systems. This synthesis report outlines the background and research for some of the most pertinent changes related to the design differences between GRS and GMSE: embedment length, reinforcement pullout, eccentricity, lateral earth pressures and connection strength, the W equation for required reinforcement strength, and long-term reduction factors for geosynthetic materials. This report can be used by transportation agencies to support design changes related to closely spaced GRS systems.

Jorge E. Pagán-Ortiz
Director, Office of Infrastructure
Research and Development

Notice

This document is disseminated under the sponsorship of the U.S. Department of Transportation in the interest of information exchange. The U.S. Government assumes no liability for the use of the information contained in this document.

The U.S. Government does not endorse products or manufacturers. Trademarks or manufacturers' names appear in this report only because they are considered essential to the objective of the document.

Quality Assurance Statement

The Federal Highway Administration (FHWA) provides high-quality information to serve Government, industry, and the public in a manner that promotes public understanding. Standards and policies are used to ensure and maximize the quality, objectivity, utility, and integrity of its information. FHWA periodically reviews quality issues and adjusts its programs and processes to ensure continuous quality improvement.

TECHNICAL REPORT DOCUMENTATION PAGE

1. Report No. FHWA-HRT-14-094	2. Government Accession No.	3. Recipient's Catalog No.	
4. Title and Subtitle Synthesis of Geosynthetic Reinforced Soil Design Topics		5. Report Date February 2015	
		6. Performing Organization Code: HRDI-40	
7. Author(s) Jonathan T.H. Wu and Phillip S.K. Ooi		8. Performing Organization Report No.	
9. Performing Organization Name and Address Department of Civil and Environmental Engineering, University of Hawaii at Manoa, 2540 Dole Street, Honolulu, HI 96822 Civil Engineering Department, University of Colorado—Denver, Denver, CO 80217		10. Work Unit No.	
		11. Contract or Grant No. N/A	
12. Sponsoring Agency Name and Address Office of Infrastructure R&D FHWA Research, Development and Technology 6300 Georgetown Pike McLean, VA 22101		13. Type of Report and Period Covered Technical	
		14. Sponsoring Agency Code	
15. Supplementary Notes The FHWA Contracting Officer's Technical Representative was Mike Adams, HRDI-40. FHWA technical reviewers were Jennifer Nicks, Daniel Alzamora, and Khalid Mohamed.			
16. Abstract This report synthesizes six topics related to geosynthetic reinforced soil (GRS) design: embedment length, pullout check, eccentricity, lateral pressures, the W-equation for GRS capacity and required reinforcement strength, and geosynthetic reduction factors. The synopsis for each topic includes a summary of the relevant research and a review of pertinent issues. The intent is not to provide recommendations but to explain the methodology behind the Federal Highway Administration's (FHWA) composite design for GRS, which is different than that for geosynthetic mechanically stabilized earth. The synopses support the FHWA's <i>GRS Integrated Bridge System (IBS) Interim Implementation Guide</i> , (FHWA-HRT-11-026).			
17. Key Words Geosynthetic reinforced soil, pullout, embedment length, eccentricity, overturning, connection strength, required reinforcement strength, abutment, integrated bridge system, geotextile		18. Distribution Statement No restrictions. This document is available to the public through the National Technical Information Service, Springfield, VA 22161. http://www.ntis.gov	
19. Security Classif. (of this report) Unclassified	20. Security Classif. (of this page) Unclassified	21. No. of Pages 86	22. Price

SI* (MODERN METRIC) CONVERSION FACTORS

APPROXIMATE CONVERSIONS TO SI UNITS

Symbol	When You Know	Multiply By	To Find	Symbol
LENGTH				
in	inches	25.4	millimeters	mm
ft	feet	0.305	meters	m
yd	yards	0.914	meters	m
mi	miles	1.61	kilometers	km
AREA				
in ²	square inches	645.2	square millimeters	mm ²
ft ²	square feet	0.093	square meters	m ²
yd ²	square yard	0.836	square meters	m ²
ac	acres	0.405	hectares	ha
mi ²	square miles	2.59	square kilometers	km ²
VOLUME				
fl oz	fluid ounces	29.57	milliliters	mL
gal	gallons	3.785	liters	L
ft ³	cubic feet	0.028	cubic meters	m ³
yd ³	cubic yards	0.765	cubic meters	m ³
NOTE: volumes greater than 1000 L shall be shown in m ³				
MASS				
oz	ounces	28.35	grams	g
lb	pounds	0.454	kilograms	kg
T	short tons (2000 lb)	0.907	megagrams (or "metric ton")	Mg (or "t")
TEMPERATURE (exact degrees)				
°F	Fahrenheit	5 (F-32)/9 or (F-32)/1.8	Celsius	°C
ILLUMINATION				
fc	foot-candles	10.76	lux	lx
fl	foot-Lamberts	3.426	candela/m ²	cd/m ²
FORCE and PRESSURE or STRESS				
lbf	poundforce	4.45	newtons	N
lbf/in ²	poundforce per square inch	6.89	kilopascals	kPa

APPROXIMATE CONVERSIONS FROM SI UNITS

Symbol	When You Know	Multiply By	To Find	Symbol
LENGTH				
mm	millimeters	0.039	inches	in
m	meters	3.28	feet	ft
m	meters	1.09	yards	yd
km	kilometers	0.621	miles	mi
AREA				
mm ²	square millimeters	0.0016	square inches	in ²
m ²	square meters	10.764	square feet	ft ²
m ²	square meters	1.195	square yards	yd ²
ha	hectares	2.47	acres	ac
km ²	square kilometers	0.386	square miles	mi ²
VOLUME				
mL	milliliters	0.034	fluid ounces	fl oz
L	liters	0.264	gallons	gal
m ³	cubic meters	35.314	cubic feet	ft ³
m ³	cubic meters	1.307	cubic yards	yd ³
MASS				
g	grams	0.035	ounces	oz
kg	kilograms	2.202	pounds	lb
Mg (or "t")	megagrams (or "metric ton")	1.103	short tons (2000 lb)	T
TEMPERATURE (exact degrees)				
°C	Celsius	1.8C+32	Fahrenheit	°F
ILLUMINATION				
lx	lux	0.0929	foot-candles	fc
cd/m ²	candela/m ²	0.2919	foot-Lamberts	fl
FORCE and PRESSURE or STRESS				
N	newtons	0.225	poundforce	lbf
kPa	kilopascals	0.145	poundforce per square inch	lbf/in ²

*SI is the symbol for the International System of Units. Appropriate rounding should be made to comply with Section 4 of ASTM E380.
(Revised March 2003)

TABLE OF CONTENTS

CHAPTER 1. INTRODUCTION	1
CHAPTER 2. EMBEDMENT LENGTH	3
RESEARCH AND CASE HISTORIES	3
Reinforced Soil Walls With Uniform Reinforcement Lengths.....	3
Reinforced Soil Walls With Nonuniform Reinforcement Lengths.....	6
DISCUSSION	9
CHAPTER 3. PULLOUT CHECK	11
RESEARCH AND CASE HISTORIES	12
Pullout Tests.....	12
Case Histories of Geosynthetic Pullout	12
Assessment of Pullout Stability	14
DISCUSSION	16
CHAPTER 4. ECCENTRICITY	19
ECCENTRICITY, BEARING PRESSURE DIAGRAM, AND FOOTING LIFTOFF ..	19
OVERTURNING VERSUS LIFTOFF	23
OVERTURNING DESIGN REQUIREMENTS FOR REINFORCED SOIL WALLS ..	25
SUMMARY	28
CHAPTER 5. LATERAL PRESSURES	29
COMPACTION-INDUCED STRESSES	29
MEASUREMENTS OF LATERAL PRESSURES IN REINFORCED SOIL	33
MEASUREMENTS OF LATERAL PRESSURES AGAINST THE FACE OF REINFORCED WALL SYSTEMS	34
METHODS FOR ESTIMATING LATERAL EARTH PRESSURES ON GRS WALL FACING	41
Wu's Procedure (2001)	41
Soong and Koerner's Procedure (1997).....	43
COMPARISON OF PREDICTED AND MEASURED LATERAL PRESSURES	45
FIELD CRITIQUE OF RANKINE ACTIVE THRUST THEORY	46
LATERAL PRESSURES DUE TO APPLIED LOADS	47
SUMMARY	49
CHAPTER 6. W EQUATION	51
W EQUATION	51
RELIABILITY OF THE W EQUATION	54
CHAPTER 7. REDUCTION FACTORS	57
RESEARCH AND CASE HISTORIES	57
Degradation.....	57
Installation Damage	58
Creep.....	58

DISCUSSION	61
Long-Term Degradation	61
Installation Damage	62
Creep	62
Current Practice	62
REFERENCES	65

LIST OF FIGURES

Figure 1. Drawing. Pullout failure, exaggerated for purposes of illustration	11
Figure 2. Illustration. Effects of facing connection condition on tensile force distribution in reinforcement	14
Figure 3. Illustration. Sequence of cutting of the PWRI test wall	15
Figure 4. Chart. The resulting horizontal movement of the PWRI test wall.	15
Figure 5. Chart. Lateral stress/pressure on different sections of a GRS wall.	17
Figure 6. Drawing. Free body diagram, cantilever wall system for overturning calculations.....	19
Figure 7. Equation. Estimated maximum bearing pressure, σ subscript max	19
Figure 8. Equation. Estimated minimum bearing pressure, σ subscript min.....	20
Figure 9. Equation. Simplified estimated maximum bearing pressure, σ subscript max.	20
Figure 10. Equation. Simplified estimated minimum bearing pressure, σ subscript min	20
Figure 11. Equation. Resultant force from the toe, χ subscript R	20
Figure 12. Drawing. Bearing pressure diagram—resultant force within middle third.	21
Figure 13. Drawing. Bearing pressure diagram—resultant force on middle third.	21
Figure 14. Drawing. Bearing pressure diagram—resultant force outside middle third.....	22
Figure 15. Equation. Resultant ratio, RR	22
Figure 16. Equation. Percent area of footing in compression, A subscript f_c (in percent)	22
Figure 17. Drawing. Forces on a rectangular rigid wall	23
Figure 18. Equation. Vertical component of resultant force at offset e , $R_{v,e}$	24
Figure 19. Equation. Force e	24
Figure 20. Equation. Safety factor, F	24
Figure 21. Equation. Footing width, B	24
Figure 22. Equation. Value of footing width B for liftoff to occur.....	24
Figure 23. Photo. First negative batter GRS wall constructed in Colorado for CDOT.	26
Figure 24. Photo. GRS wall in New Zealand with a negative.	27
Figure 25. Photo. Research on negative batter GRS walls in Japan	27
Figure 26. Chart. Residual lateral stress induced by vibratory plate compaction.....	30
Figure 27. Chart. Vertical stress distribution at 6-kN (1.35-kips) vertical load on the GRS (a) without and (b) with reinforcement.....	31
Figure 28. Chart. Horizontal stress distribution at 6-kN (1.35-kips) vertical load on the GRS (a) without and (b) with reinforcement.....	32
Figure 29. Chart. Shear stress distribution at 6-kN (1.35-kips) vertical load on the GRS (a) without and (b) with reinforcement.....	33

Figure 30. Drawing. Founders/Meadows bridge abutment cross-section and instrumentation....	36
Figure 31. Drawing. GRS mini-pier elevation plan.....	37
Figure 32. Drawing. GRS mini-pier elevation plan.....	38
Figure 33. Chart. Measured increase in lateral pressures on the facing of GRS mini-piers during load test in kPa.....	39
Figure 34. Charts. Measured increase in lateral pressures on the facing of GRS mini-piers during load test in kN/m^2	40
Figure 35. Diagram. Bin pressure diagram.....	42
Figure 36. Equation. Total lateral thrust, F subscript bin, as a function of the spacing between reinforcements, S subscript v , and peak bin pressure σ subscript h	42
Figure 37. Equation. Total lateral thrust, F subscript bin, in terms of the coefficient of active earth pressure.	42
Figure 38. Drawing. GMSE wall configuration showing nonreinforced backfill zones	43
Figure 39. Drawing. Lateral earth pressure distribution against wall facing exerted by the nonreinforced backfill.....	44
Figure 40. Equation. Connection force F	44
Figure 41. Photo. Grand County, Colorado, wall with a maximum height of 55 ft (16.8 m).....	47
Figure 42. Equation. Increase in lateral pressure $\Delta\sigma$ subscript h	47
Figure 43. Drawing. Definition of angles α and δ	48
Figure 44. Chart. Increase in lateral stress due to 4,000-psf (191.5-kPa) vertical stress on a 4-ft- (1.2-m-) wide footing with a 1-ft (.3-m) setback.....	48
Figure 45. Drawing. Mohr circles for unreinforced and reinforced soil.....	52
Figure 46. Equation. Major principal stress σ subscript 1	52
Figure 47. Equation. Confining stress due presence of reinforcement σ subscript 3R	52
Figure 48. Equation. Capacity of the GRS σ subscript 1R.....	53
Figure 49. Equation. Additional confining stress as function of reinforcement tensile strength divided by the reinforcement spacing $\Delta\sigma$ subscript 3.	53
Figure 50. Equation. Modified version of the equation in figure 49 for additional confining stress, $\Delta\sigma$ subscript 3 imposed with the W factor.	53
Figure 51. Equation. W factor	53
Figure 52. Equation. Capacity of the GRS, σ subscript 1R.....	54
Figure 53. Equation. Expansion of the equation in figure 52 for the capacity of the GRS, σ subscript 1R, to include cohesion.....	54
Figure 54. Graph. Predicted versus measured capacity of large-scale GRS tests using the equation in figure 52.	56

Figure 55. Graph. Predicted versus measured capacity of large-scale GRS tests using the equation in figure 52 without the W term. 56

Figure 56. Equation. Allowable reinforcement design strength, T subscript a 57

Figure 57. Illustration. Schematic diagram of a SGIP test 61

LIST OF TABLES

Table 1. Research: walls and abutments with uniform “short” reinforcement lengths.	6
Table 2. Research: walls and abutments with “truncated base” reinforcement lengths.	8
Table 3. Resultant force location and impact on safety against overturning, base area in compression, and bearing pressure diagram.	23
Table 4. Key points relating to the need to limit the eccentricity in the design of GRS walls.	28
Table 5. Comparison of Wu’s versus Soong and Koerner’s calculated lateral thrusts as a function of reinforcement spacing.	45
Table 6. Predicted versus measured lateral pressures on reinforced soil wall facing.....	46
Table 7. Prediction data for large-scale tests.	55

ABBREVIATIONS

AASHTO	American Association of State Highway and Transportation Officials
ASD	Allowable Stress Design
CDOT	Colorado Department of Transportation
CIS	Compaction Induced Stresses
CMU	Concrete Masonry Unit
DACSAR	Deformation Analysis Considering Stress Anisotropy and Reorientation
FEM	Finite Element Model
FHWA	Federal Highway Administration
GMSE	Geosynthetic Mechanically Stabilized Earth
GRS	Geosynthetic Reinforced Soil
IBS	Integrated Bridge System
LRFD	Load and Resistance Factor Design
MARV	Minimum Average Roll Value
MSE	Mechanically Stabilized Earth
NCHRP	National Cooperative Highway Research Program
NCMA	National Concrete Masonry Association
NGI	Norwegian Geotechnical Institute
NHI	National Highway Institute
PWRI	Public Works Research Institute (Japan)
RRR	Reinforced Railroad/Road with Rigid facing
SGIP	Soil-Geosynthetic Interactive Performance
USACE	U.S. Army Corps of Engineers

CHAPTER 1. INTRODUCTION

This report provides technical synopses on six topics related to geosynthetic reinforced soil (GRS) systems: embedment length, pullout check, eccentricity, lateral pressures, the W equation, and reduction factors. The synopsis for each topic includes a summary of the relevant research and a review of pertinent issues. GRS refers to closely spaced layers of geosynthetic reinforcement and compacted granular fill material. The GRS systems examined included, but were not limited to, walls, abutments, and the integrated bridge system (IBS).

Embedment length refers to the length of reinforcement for GRS walls or load-bearing walls. The synopsis on this subject addresses the issues of structures with short reinforcement lengths—lengths less than 0.7 of a wall height at its face. The synopsis includes a review of research and case histories on short reinforcement. GRS walls involving a “constrained fill” zone (that is, where rock, heavily overconsolidated soil, or a nail wall is present behind a wall) are also discussed.

The pullout check refers to the implications of performing, or not performing, the check for geosynthetic pullout of a GRS wall or abutment. The pullout check is performed to determine required reinforcement length, but there is some uncertainty about the check’s efficacy. The synopsis examines the research and performance data, discusses the history of this particular design component in traditional geosynthetic mechanically stabilized earth (GMSE) theory, and considers the appropriateness of extending the pullout check to GRS technology.

Eccentricity is another name for overturning. As part of the design of conventional cantilever and gravity retaining walls with relatively rigid footings, overturning failure is commonly checked to determine whether the design meets the required margin of safety. This check typically consists of taking moments of all the stabilizing forces acting on the free body of the wall system about the toe of the wall and comparing them with the moments for the destabilizing forces about the same point. An alternative approach involves basing overturning criteria on a minimum base area in compression. This synopsis examines the purpose and theoretical justification of the eccentricity design component.

Lateral pressures at a GRS facing differ from those in the soil portion. The internal lateral stress in the GRS soil is governed by compaction-induced stresses and by supplementary confining effects that the reinforcement adds to the soil. The pressure at the facing is governed by those two factors as well as the movement of the facing, especially in facings with little or no connection strength. The synopsis discusses the effects of compaction-induced stresses on the internal lateral stress of both the unreinforced and reinforced soil. Measured thrusts against facing elements with and without purely frictional connection are presented. Methods for estimating this thrust are compared with the measured values.

The W equation is used to estimate the vertical capacity and required reinforcement strength of GRS walls and abutments. The W refers to a term or factor that attempts to explain why an increase in the reinforcement strength does not have the same effect as a proportional decrease in the reinforcement spacing. Proportional effects between strength and spacing have been assumed in simplified GMSE design. The synopsis discusses the various terms in the W equation and

previous research and theory leading to its development. Based on load test results from the literature, the reliability of the equation is considered.

Lastly, the topic of reduction factors is examined. The synopsis includes a summary of the research and associated theory behind the reduction factors of creep, degradation—or durability—and installation damage. Deficiencies in current practices are also discussed. The reviewed literature includes reports on the impact of the use of various polymer types.

CHAPTER 2. EMBEDMENT LENGTH

Uniform reinforcement lengths of 0.6 to $0.7H$ (H is the wall height at face) have commonly been used for reinforced soil walls and abutments. This is a result of three major design guidelines: the American Association of State Highway and Transportation Officials (AASHTO) Standard Specifications for Highway Bridges, the Federal Highway Administration (FHWA) National Highway Institute (NHI) manual, and the National Concrete Masonry Association (NCMA) manual.^(1,2,3) The NCMA design manual, widely used in the private sector, requires a minimum reinforcement length of $0.6H$. A minimum length of $0.7H$, on the other hand, has been specified in the FHWA and AASHTO guidelines that are used routinely in the public transportation sector. The standard of practice in Europe and Asia uses a similar criterion for minimum reinforcement length: $0.7H$ for routine applications and $0.6H$ for low lateral load applications with a minimum length of 9.84 ft (3 m).^(4,5) Brazilian guidelines, perhaps the most conservative of all, require a minimum length of $0.8H$.

Despite the popularity of the 0.6 to $0.7H$ rule, uniform reinforcement lengths as small as 0.3 to $0.4H$ have been employed with good success for construction of GRS walls.⁽⁶⁾ The subject of short reinforcement lengths is important because such lengths can result in significant cost savings, especially in situations where construction involves excavation of existing ground. Another important design issue with reinforcement length is nonuniform reinforcement lengths (truncated base walls). In situations where excavation into rock or stiff deposits to allow for uniform reinforcement lengths involves significant costs, the use of nonuniform reinforcement lengths in the lower part of the wall may prove beneficial. There are, however, design concerns with this practice.

RESEARCH AND CASE HISTORIES

This synopsis addresses the issues of short reinforcement length and design implications as they relate to GRS walls and abutments with short reinforcement lengths. The synopsis includes a review of research and case histories on short reinforcement and a discussion of the issues. Both uniform and nonuniform reinforcement lengths are addressed. GRS walls involving a “constrained fill” zone (i.e., where rock, heavily overconsolidated soil, or a nail wall is present behind a wall) are also discussed.

Reinforced Soil Walls With Uniform Reinforcement Lengths

When considering the subject of short reinforcement lengths, the case histories and research by Tatsuoka and his associates in collaboration with Japan Railway are perhaps the most noteworthy.^(7,8,9) Beginning in the mid-1980s, Tatsuoka and his associates developed a GRS wall system with full-height rigid facing, referred to as the reinforced railroad/road with rigid (RRR) facing system. Because of its superior performance during earthquakes and heavy rainfalls compared with conventional cantilever walls and metallic-reinforced soil walls, the RRR system has become the “default” retaining wall type in Japan railway construction. To date, more than 74.5 mi (120 km) of RRR walls have been built for railway embankments in Japan with great success.

The RRR system involves a two-stage construction procedure. First, a GRS wall with geosynthetic reinforcement of approximately $0.3H$ in length, at typical spacing of .98 ft (0.3 m), is constructed using gravel gabions as facing. The wall is allowed to deform under its self-weight before the second-stage construction is begun, which involves installing full-height rigid concrete facing (cast-in-place) over the gabion face. The rigid concrete facing is attached to the reinforced soil mass via extruded steel bars that are embedded in the soil mass. In spite of the very short reinforcement lengths of 0.3 to $0.4H$, no failure has ever been observed during construction. It is important to note that both granular and cohesive backfills have been used in the construction of the RRR system. (Nonwoven–woven composite geotextiles were used for cohesive backfills to facilitate drainage while maintaining sufficiently high tensile capacity.)⁽⁷⁾ Tatsuoka et al. suggest that overturning may be the most critical mode of failure for an GMSE wall with short reinforcement lengths of 0.3 to $0.4H$, while sliding typically governs for conventional GMSE walls with reinforcement lengths of 0.6 to $0.7H$.⁽⁷⁾

Segrestin of Terre Armée International, in a rebuttal to Tatsuoka’s many comments regarding RRR walls versus reinforced earth walls, stated that a number of reinforced earth walls with reinforcement lengths as low as $0.45H$ had been constructed successfully.⁽¹⁰⁾ Segrestin also cited a 34.4-ft- (10.5-m-) high instrumented reinforced earth wall with reinforcement length as short as $0.48H$. Segrestin maintained that the basic mechanism and behavior of reinforced soil structures with reinforcement lengths between $0.4H$ and $0.7H$ are identical, as has been suggested by a finite element model (FEM) parametric study conducted by Terre Armée.⁽¹⁰⁾

Bastick conducted FEM analysis of MSE walls undergoing changes due to reduced reinforcement length.⁽¹¹⁾ It was found, similar to Terre Armée’s study, that the performance of an MSE wall would remain quite similar as long as the reinforcement lengths were kept above 0.4 to $0.5H$ and the reinforcement spacing stayed the same.⁽¹⁰⁾ The finding was confirmed by a full-scale experiment with reinforcement length of $0.48H$ loaded to an average surcharge of 121.83 psi (840 kPa).

Other cases of using short reinforcement lengths have typically been associated with (a) walls with “constrained fill zone,” where there is the presence of a rock or heavily over-consolidated soil outcrop, or an existing nailed wall, and the space constraint makes commonly used reinforcement lengths of 0.6 to $0.7H$ impractical, and (b) walls with reinforcement anchored by metal plates or geosynthetic loops.^(12,13,14) Case (a) is in line with the scope of this synopsis and will be elaborated in the following discussion.

Lawson and Yee proposed a design-and-analysis method for reinforced soil retaining walls involving a constrained fill zone.⁽¹²⁾ Within the constrained reinforced fill zone, the full active failure wedge is unable to develop because of the relative close proximity of the rigid zone behind the reinforced fill. In the method, the magnitude of horizontal thrust acting on the wall face, P_h , is evaluated by the following equation: $P_h = 0.5 K\gamma H^2$. For walls with reinforcement lengths greater than $0.5H$, the Rankine active wedge can fully develop within the granular fill zone; hence, K is equal to K_a . However, for reinforcement lengths less than $0.5H$, the full active wedge cannot develop fully, and the magnitude of K decreases with decreasing reinforcement lengths.

An extreme example of reduced lateral thrust for walls with a constrained fill zone is a very tall wall constructed by Lin et al. of Taiwan, a region with very heavy seasonal rainfall.⁽¹⁵⁾ The wall was 129.6 ft (39.5 m) high, constructed in six tiers (with three 26.2-ft- (8-m-) high tiers and three shorter tiers). The geogrid reinforcement length was 4.9 ft (1.5 m), or $0.19H$. All tiers, despite having to carry the soil-weight from upper tiers, performed satisfactorily even with the very short reinforcement length.

It is interesting to note that the reinforcement length of $0.19H$ happens to agree with the finding of a numerical study for a reinforcement spacing of 1.3 ft (0.4 m).⁽¹⁶⁾ Vulova's numerical study also agrees with Tatsuoka's assertion that overturning will be the controlling failure mode for an GMSE wall with short reinforcement lengths.

Morrison et al. performed centrifuge tests on shored GMSE walls.⁽¹⁷⁾ The results were the following: (a) reinforcement lengths in the range of 0.25 to $0.6H$ generally produced stable wall systems; (b) reinforcement lengths of $0.25H$ or shorter generally produced outward deformation followed by an overturning collapse of the GMSE mass under increasing gravitational levels; (c) at reinforcement lengths less than $0.6H$, deformation produced a "trench" at the shoring interface, interpreted to be the result of tension because the trench was observed with reinforcement lengths of $0.6H$ or longer; and (d) a conventional GMSE wall with retained fill and a reinforcement length of $0.3H$ was stable up to an acceleration level of 80 g, which represented a prototype height of approximately 88.6 ft (27 m).

It has been suggested that a shorter reinforcement length may result in larger lateral displacements and likely more settlement as well. A FEM study conducted by Chew, et al. showed that shortening reinforcement length from 0.7 to $0.5H$ caused about a 50-percent increase in lateral deformation.⁽¹⁸⁾ Ling and Leshchinsky reported that, with a reinforcement length of $0.5H$, a reinforced soil wall would give satisfactory performance considering the maximum displacement mobilized in the reinforcement layers.⁽¹⁹⁾ A recent study by Liu suggests that the larger lateral displacement is due to larger lateral deformation of the soil behind the reinforced zone.⁽²⁰⁾

It is of interest to note that a soil mass reinforced by closely spaced reinforcement (i.e., spacing not more than 0.82 to 0.98 ft (0.25 to 0.30 m)) will likely behave as a coherent mass. This behavior is clearly evidenced in two loading tests of full-scale segmental facing GRS bridge abutment walls, referred to as the National Cooperative Highway Research Program (NCHRP) GRS test abutments.^(21,22) Two different woven geotextiles were used as reinforcement, each 10.33 ft (3.15 m) long and at 0.66-ft (0.2-m) spacing. The backfill was a nonplastic silty sand, and the abutment was loaded by applying increasing vertical loads via a strip footing near the wall face. A tension crack was observed on the wall crest in both tests. The tension crack was first detected exactly where the reinforced zone ended (i.e., 10.33 ft (3.15 m) from the back face of the facing) under an applied pressure of 21.8 to 29.0 psi (150 to 200 kPa). The location of the tension cracks suggests that the reinforced soil mass behaves as a coherent mass. The coherent soil mass behavior is particularly prevalent for GRS walls with closely spaced reinforcement. This also explains why overturning has been the most critical failure mode with short reinforcement lengths of 0.3 to $0.4H$, especially with closely spaced reinforcement. The exception is when a constrained fill zone is involved.

Table 1 summarizes highlights of the case histories and case studies with uniform short reinforcement lengths (reinforcement lengths $\leq 0.5H$).

Table 1. Research: walls and abutments with uniform “short” reinforcement lengths.

<i>L/H</i> (length/height ratio)	<i>H</i> (wall height)	<i>S_v</i> (reinforcement spacing)	Key Findings	Notes	References
0.3 (typical)	16.4– 39.4 ft (5–12 m) (typical)	1 ft (0.3 m) (typical)	Two-stage construction (wrapped-face wall with gravel-gabion in first stage, and full-height panel in second stage). Wall movement in the first stage is not of concern; no failure has ever been observed.	Both granular and cohesive backfills have been used; more than 74.5 mi (120 km) of railroad railway walls and abutments have been built with excellent performance under static and seismic loads and heavy rainfalls.	7, 8, and 9
0.48	34.4 ft (10.5 m)	not reported	Performed satisfactorily under an average surcharge of 121.8 psi (840 kPa).	A FEM study conducted by Terre Armée indicated reinforcement lengths between $0.4H$ and $0.7H$ would perform approximately the same.	10 and 11
0.19	129.6 ft (39.5 m) in 6 tiers (tallest tier was 26.2 ft (8 m))	6.6 ft (2.0 m)	Performed satisfactorily, even in a region with very heavy seasonal rainfall.	Walls constructed in a “constrained fill” condition (constructed over a nailed wall); $L = 0.19H$ happens to match FDM analysis results of minimum reinforcement length with $S_v = 1.31$ ft (0.4 m).	15 and 16
0.3	88.6 ft (27 m) (equiv.)	.78 inches (20 mm) (typical)	Stable up to an acceleration level of 80 g.	Centrifuge modeling; $L/H = 0.25$ to 0.6 generally produces a stable wall system in a “constrained fill” condition.	17

FEM = Finite Element Model

FDM = Finite Difference Model

Reinforced Soil Walls With Nonuniform Reinforcement Lengths

Nonuniform reinforcement lengths in a reinforced soil wall, also known as a truncated base wall, typically have reduced reinforcement lengths in the lower part of the wall. A truncated base wall is employed when costs of excavation to allow for uniform reinforcement lengths are significant and construction may be difficult. The reduction in length takes the following two forms: stepped wall (reducing lengths in groups of two to four layers) and trapezoidal wall (reducing lengths at almost every layer).

Nonuniform reinforcement lengths for GMSE walls are allowed in the FHWA NHI manual.⁽²⁾ The manual provides general design guidelines for a truncated-base wall and states that this provision should only be considered if the base of the GMSE wall is founded on rock or

competent soil; competent soil is soil that will exhibit minimal post-construction settlement. For foundation soil that is less than competent, ground improvement techniques may be used prior to GMSE construction.

The British standard BS 8006 design manual for GMSE walls also allows the use of a truncated base.⁽⁵⁾ It states that a trapezoidal wall should only be considered where foundations are formed by excavation into rock or where other competent foundation conditions exist. The manual prescribes a minimum reinforcement length of $0.4H$ for the lower portion of the wall. In Asia, Hong Kong's Geoguide 6 follows the FHWA NHI manual, except it also stipulates that soil arching needs to be accounted for in design.⁽⁴⁾

Japan Railway has employed reinforcement with truncated lengths in the lower part of a GRS wall when the costs of excavation to allow for full length reinforcement are high.^(7,23,24) The walls constructed with truncated base have performed satisfactorily during heavy rainfalls and severe earthquake events.

Segrestin reported applications of truncated base walls with steel-strip reinforcement in constrained fill situations.⁽¹⁰⁾ It was reported that wider metal strips, or a more closely spaced, increased number of strips, have been employed in truncated base walls.

The Colorado Department of Transportation (CDOT) constructed a 24.9-ft- (7.6-m-) high GRS wall with a truncated base in DeBeque Canyon along Interstate 70.⁽²⁵⁾ For comparison purposes, a 32.8-ft (10-m) section was constructed with full-length reinforcement. A road base material was used for backfill, and the wall was situated over a firm foundation. Measurements of lateral displacements along a full-length reinforcement section (reinforcement length = 16.4 ft (5 m)) and along a truncated-base section (reinforcement length at base = 3.61 ft (1.1 m), or $0.14H$), taken 6 months after construction, were very similar—both on the order of 0.12 to 0.23 inches (3 to 6 mm), with a maximum displacement of about 0.31 inches (8 mm). Adams et al. of the FHWA reported a number of GRS abutments with a truncated base.⁽⁶⁾ The GRS abutments have performed satisfactorily.

Thomas and Wu conducted FEM analysis on the behavior of GRS walls with a truncated base.⁽²⁶⁾ Major findings of the study were threefold. First, when designing a GRS wall with a truncated base, external stability should be thoroughly checked. Truncated-base walls are more likely to experience sliding failure, and the length of reinforcement at the lowest level should be at least $0.35H$ or 0.9 m. Second, soil type and compaction of the backfill play a significant role in the performance of a GRS wall with a truncated base. The use of cohesive backfill should be avoided for a truncated-base wall. Third, the foundation soil needs to be sufficiently stiff for a truncated-base wall. Other numerical studies have also indicated that truncated base walls can perform equally well as full-length walls under certain conditions. (See references 11, 16, 26, 27, 28, and 29.)

Lee et al. conducted a forensic study on a series of failed walls founded on rock with rock forming the back-slope for the lower reinforcements, and concluded that the resistance against sliding failure is reduced by a truncated base due to a smaller base area.⁽³⁰⁾ They noted that soil arching due to the rock behind the fill would reduce vertical stress above the back of lower reinforcements and hence lead to overestimation of resistance to pullout failure.

Table 2 summarizes highlights of the case histories and case studies with “truncated base” reinforcement lengths (reinforcement lengths $\leq 0.5H$).

Table 2. Research: walls and abutments with “truncated base” reinforcement lengths.

L_B (reinforcement length at base)	H (wall height)	S_v (reinforcement spacing)	Key Findings	Notes	References
4.6 ft (1.4 m) (0.27H)	17.1 ft (5.2 m)	1 ft (0.3 m)	The truncated base wall has performed satisfactorily.	This is one of the many truncated base walls constructed by Japan Railway. Of the 74.5 mi (120 km) of GRS walls constructed by Japan Railway, only a handful of truncated base walls are reported in the literature, all with base cut into stiff sloping ground.	7
3.6 ft (1.1 m) (0.14H)	24.9 ft (7.6 m)	0.7 ft (0.2 m)	The difference in performance between truncated base wall and full-length wall was found to be insignificant. Lateral displacements measured 6 months after construction for both walls were typically on the order of 0.12 to 0.23 inches (3 to 6 mm), with maximum displacement of 0.31 inches (8 mm).	This is the only full-scale field tests on truncated base walls. A 32.8-ft (10-m) section of the wall was constructed with full-length reinforcement for comparisons with truncated base wall.	25
4.6 ft (1.4 m) (0.38H)	12.1 ft (3.7 m)	0.4 m	A truncated base wall deforms slightly more than full-length wall in the lower half of the wall, with 5- to 10-percent larger lateral displacement.	FEM analysis results using a sophisticated FEM code Deformation Analysis Considering Stress Anisotropy and Reorientation (DAC SAR).	29
8.2 ft (2.5 m) (0.4H)	19.7 ft (6 m) (approx.)	Not reported	The truncated base wall has performed satisfactorily.	When using a truncated base, wider metal strip reinforcement or, more often, increased number of strips have been employed.	10

L_B (reinforcement length at base)	H (wall height)	S_v (reinforcement spacing)	Key Findings	Notes	References
4.9 ft (1.5 m) (0.11H)	44.3 ft (13.5 m)	1 ft (0.3 m) (within 4.9 ft (1.5 m) of the wall face)	The truncated base wall has performed satisfactorily.	Reinforcement spacing was 0.98 ft (0.3 m) for shorter (4.92 ft (1.5 m)) reinforcement; longer reinforcement (with a truncated base) was used at 29.5 ft (0.9 m) spacing. Cement mixed gravel was used as backfill in the reinforced soil zone.	23
4.92 ft 1.5 m (0.11H)	43.3 ft (13.2 m)	1 ft (0.3 m)	The truncated base wall has performed satisfactorily.	The truncated base was installed into stiff sloping ground in steps.	17

GRS = Geosynthetic Reinforced Soil

FEM = Finite Element Model

DACSAR = Deformation Analysis Considering Stress Anisotropy and Reorientation

DISCUSSION

A minimum reinforcement length of 0.6 to $0.7H$ (H = height of wall at wall face) has been used in most designs of GRS/GMSE walls. However, reinforcement lengths as short as 0.3 to $0.4H$ have been shown to be stable under certain conditions, and studies have suggested that GRS walls with reinforcement lengths between 0.4 and $0.7H$ behave approximately the same. For situations where a uniform reinforcement length is to be employed, a minimum reinforcement length of $0.6H$ is well justified. Care must be exercised to prevent tension crack on the wall crest if the wall is to carry significant vertical loads near the wall face (e.g., bridge abutments). Extending the top one or two reinforcement layers well beyond the assumed failure plane based on a design analysis should help reduce the tension cracks.

Use of uniformly shorter reinforcement, with a reinforcement length of 0.35 to $0.5H$, may result in larger lateral movement and is acceptable only if (a) the wall will not be subject to heavy edge loads such as a bridge abutment, (b) a granular backfill is employed and well compacted, (c) the foundation is competent (to minimize post-construction settlement), and (d) external stability, especially against overturning, is satisfied.

Use of a truncated base wall is a viable approach when costs of excavation to allow for uniform reinforcement lengths are significant and the foundation material is competent. There is strong evidence offered by case histories and research that a truncated base wall will perform satisfactorily as long as the base of a reinforced soil wall is founded on a competent foundation, and external stability, especially against sliding, is assured. The reinforcement length at the lowest level should generally be at least $0.3H$.

CHAPTER 3. PULLOUT CHECK

Pullout and rupture of reinforcement are two modes of failure that have been identified for checking the internal stability (stability within reinforced zone) in the design of a reinforced soil wall or abutment. The pullout check is performed to determine required reinforcement length, whereas the rupture check is conducted to determine required reinforcement strength. The need to check pullout failure stems from the fundamental design concept of GMSE systems in which the reinforcement is considered as tiebacks acting as tension members to “hold” an assumed failure wedge in place (see figure 1), thus preventing it from sliding down and away from the rest of the reinforced soil mass.

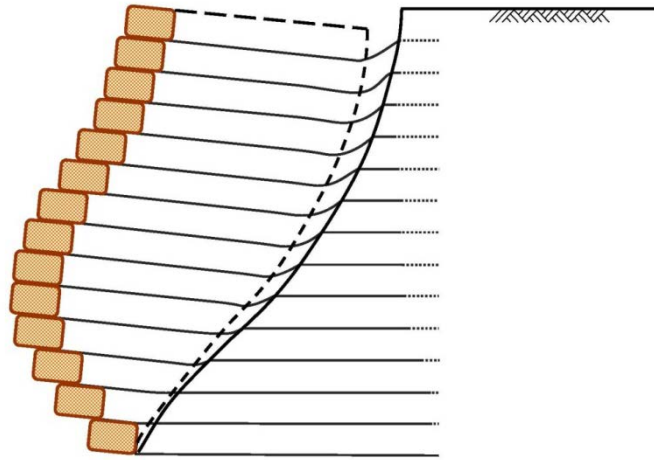


Figure 1. Drawing. Pullout failure, exaggerated for purposes of illustration.

In the three major design guidelines for reinforced soil walls and abutments—AASHTO *Standard Specifications for Highway Bridges*, FHWA NHI manual, and NCMA design manual—the check of reinforcement pullout is performed by requiring the reinforcement be long enough that the “resisting force” (resulting from soil-reinforcement interface friction/interlocking resistance) beyond an assumed slip plane be sufficiently greater than the “driving force” (earth thrust within the tributary zone) for “any” level of a reinforcement layer.^(1,2,3) A minimum safety factor of 1.5 and a minimum anchored length of 2.95 ft (0.9 m) have typically been specified to assure pullout failure will not occur.

The driving force at a given reinforcement layer is evaluated by multiplying the reinforcement spacing by the lateral stress in the tributary zone along an assumed critical slip plane. On the other hand, the resisting force of a geosynthetic reinforcement layer is determined by multiplying the unit interface shear resistance by the length of reinforcement behind the assumed slip plane. Both forces require a realistic assumption of the location of the most critical slip plane, which may be a function of, among other factors, soil friction angle and facing rigidity.

To develop a sound design concept, checking reinforcement pullout of a GMSE system is needed. This is because if a tieback system does not have a sufficient anchor length, the system

is destined to fail. However, for a GRS system, the same is not true. Reinforcement length in a GRS system is determined by external stability. In a GRS system, geosynthetic reinforcement is considered to be tensile inclusion, which serves to improve soil stiffness and strength (through such reinforcing mechanisms as inducing apparent cohesion, increasing confinement, suppressing dilation, and reducing lateral deformation). Because geosynthetic reinforcement layers are not considered tieback members, the necessity to check geosynthetic pullout for a GRS system has become a debatable issue.

Those who insist that geosynthetic pullout failure should not be checked for a GRS system have stated that if the design protocol of a GRS system involves checking pullout failure, the design has resorted to the tieback concept, which violates the fundamental design concept of GRS systems—it is like “mixing apples and oranges.” In addition, the pullout check is confusing and redundant for GRS systems.

On the other hand, those who maintain that geosynthetic pullout should be checked have argued that checking geosynthetic pullout failure is a simple step in a design, and therefore, it would not be a drawback to perform that extra step to ensure pullout stability. Although this argument sounds reasonable, it is perhaps not so simple.

RESEARCH AND CASE HISTORIES

Pullout Tests

A great deal of research effort has been expended on the determination of reinforcement length to ensure stability against pullout failure. Since the 1980s, hundreds of studies have been conducted on the subject of a simple test called the “pullout test.” Huang collected 478 sets of pullout tests for a statistical analysis.⁽³¹⁾ In a pullout test, a reinforcement element (metallic strip, metallic mesh, geosynthetic strip, geosynthetic sheet, etc.) is confined in soil under a constant surcharge, inside a test bin, and is subject to increasing tensile loads. Pullout tests that have been performed range from small- to large- to field-scale tests, from short- to long-term tests, from static to cyclic tests, from laboratory to field tests, from drained to undrained tests, from unsaturated to saturated tests, from finite element/difference analysis to close-form solution, and include centrifuge model tests.(See references 32 through 37.)

It is to be noted that pullout tests in fact only address the interface shear resistance that occurred beyond an assumed slip surface. In a pullout test, the location of the failure surface is not of concern; i.e., it does not address the question of the available resisting force in its entirety. For a GRS wall, it has been tacitly assumed that the Rankine or Coulomb active failure surface for a “uniform” soil mass is applicable to a reinforced soil mass that contains layers of geosynthetic reinforcement (e.g., AASHTO, Berg et al., and NCMA).^(1,2,3)

Case Histories of Geosynthetic Pullout

After an exhaustive search of the literature, a single case of “in-service” reinforced soil wall, including both GMSE walls and GRS walls, was not found in which failure can be clearly attributed to pullout of reinforcement. Part of the reason pullout failure is difficult to identify is because, unless a distinct failure surface is fully developed, pullout of reinforcement is “buried” and not visible without careful reconnaissance work that involves removing the covering soil. It

is conceivable that pullout failure in a reinforced soil wall or abutment may occur under certain combinations of the following conditions: (a) reinforcement is very stiff and has very high strength; (b) backfill is loosely compacted, or cohesive and wet; (c) reinforcement spacing is large (say, greater than 1.97 ft (0.6 m)); and (d) reinforcement is relatively long (say, $\geq 0.6H$).

Suah and Goodings performed 27 centrifuge model tests of wrapped-faced geotextile walls, all with 100-percent clay backfill.⁽³⁸⁾ The reinforcement lengths varied from 0.5 to 1.5 H . All the tests were brought to failure. Wall failure in all the tests occurred by tensile breakage of the geotextile, and never by pullout. This is contrary to the popular perception that clayey backfill is highly susceptible to pullout failure, and often cited as the primary disadvantage of employing clayey backfill in construction of a reinforced soil wall. Suah and Goodings also indicated that when reinforcement was short (0.5 H), prefailure differential settlement at the front of the wall was pronounced, and failure by overturning was likely; when reinforcement was longer (1.0 to 1.5 H), differential settlement was less pronounced, and sliding along an inclined failure surface was more likely.

Woodruff performed a series of centrifuge model tests to examine potential failure surfaces of shored GMSE walls.⁽²⁷⁾ Yang et al. investigated the same subject using a limit equilibrium approach.⁽³⁹⁾ The two studies came to a similar conclusion that the critical failure plane for reinforcement length less than 0.7 H was bilinear. The inclination angle of the critical failure plane within a shored GMSE wall is 10- to 20-percent less than that of the Rankine theory and extends along the contact surface between the back of the reinforced wall and the shored wall.

It is interesting to note that Leshchinsky and Vulova conducted a parametric study, using a finite difference program, Fast Lagrangian Analysis of Continua, or FLAC, to examine the effects of various parameters on GMSE walls with segmental facing.⁽⁴⁰⁾ Factors such as backfill strength, foundation strength, reinforcement stiffness, soil-reinforcement interface strength, reinforcement spacing, and wall height were examined. The study indicates that for closely spaced reinforcement (spacing less than 1.31 ft (0.4 m) in their definition), the critical slip plane did not pass through the reinforced soil zone. They suggest that a method different from Rankine or Coulomb analysis is needed to assess internal stability of a closely spaced GMSE wall. They also argue that the reason many experiments were able to bring about internal failure was because those walls do not typically represent realistic prototypes. They offered the following analogous example:

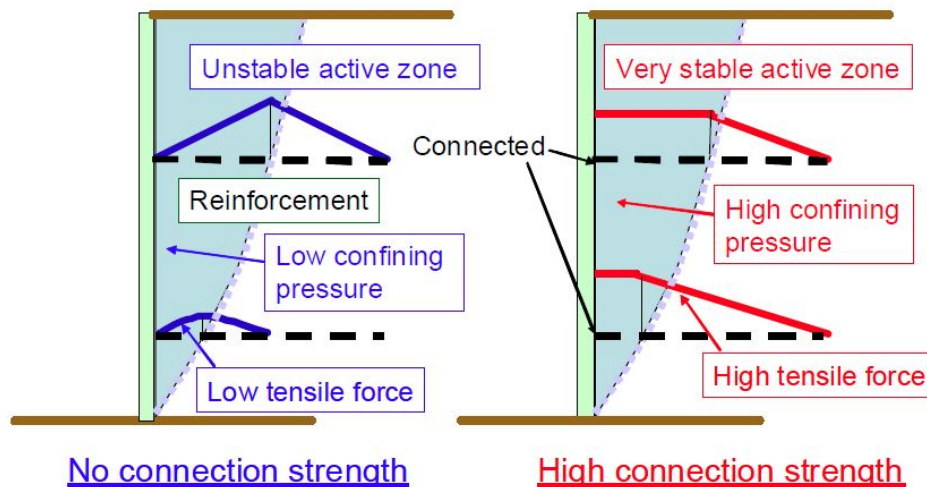
Consider the case of a rigid, non-yielding (unreinforced) retaining wall. Correct design would use at-rest lateral earth pressures reflecting the impossibility of an active wedge developing within the retained soil (a unrealistic failure mechanism). However, one can conduct an experiment on such a structure and impose the active case by exerting very large surcharges (i.e., cause yielding of the wall). Such an unrealistic experiment may lead to the incorrect conclusion that, for non-yielding walls, active soil pressures should be used. That is, the observed failure mechanism in the experiment is not necessarily relevant to the prototype. (page 363)⁽⁴⁰⁾

Assessment of Pullout Stability

As noted in earlier in this synopsis, evaluation of pullout failure involves calculations of driving forces and resisting forces, and both involve the knowledge of the location of the critical slip plane (often taken as the plane of maximum reinforcement loads). The following presents studies on the location of the critical slip plane and on the lateral thrust for the determination of the driving forces.

Critical Slip Plane

Tatsuoka pointed out that facing rigidity has a significant effect on the distribution of tensile forces induced in the reinforcement (see figure 2).⁽⁴¹⁾ For reinforcement securely connected to rigid facing, the largest tensile force occurs near the wall face; whereas it occurs away from the wall face if the connection force is small. The distribution of reinforcement loads, hence the location of the critical slip plane, is strongly affected by the rigidity of the facing.



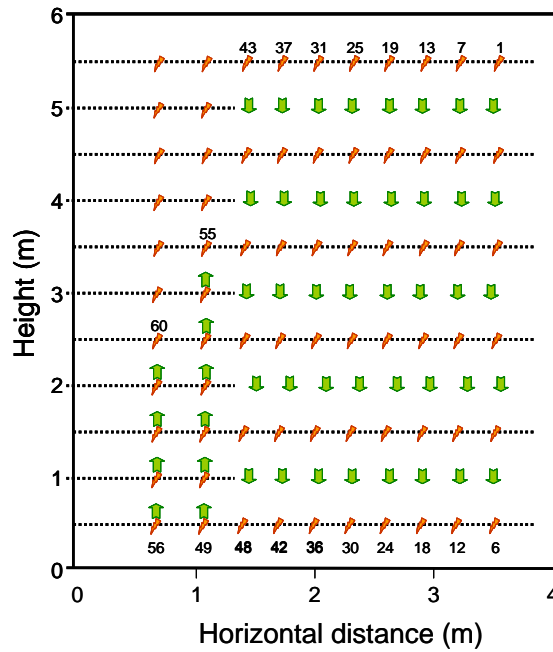
©F. Tatsuoka, O. Murata, and M. Tateyama

Figure 2. Illustration. Effects of facing connection condition on tensile force distribution in reinforcement.⁽⁷⁾

Yang et al. reported the behavior of a railway embankment wall constructed with a procedure similar to Japan Railway's RRR system. (See reference 42 and 7 through 9.) From measured maximum reinforcement strains in different layers, they conclude that the critical slip plane is likely curved, with the failure surface in the upper portion of the wall not deviating significantly from the $0.3H$ -distribution suggested by Schlosser and Long, and the slip plane in the lower portion of the wall being quite different from those of Rankine or Schlosser and Long.⁽⁴³⁾

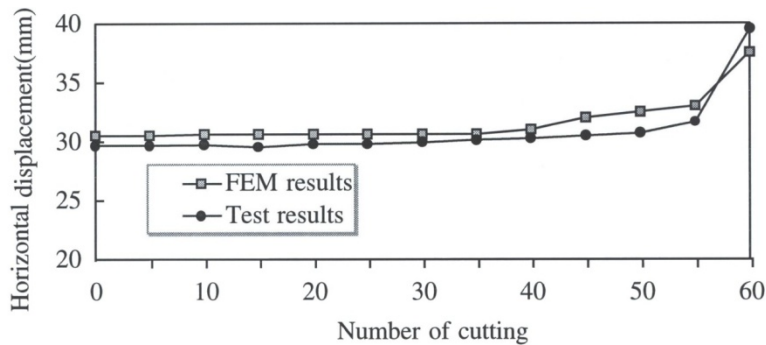
Perhaps the most extreme example to illustrate the deficiency concerning the critical slip planes is a full-scale experiment conducted by the Public Works Research Institute (PWRI), Japan. The experiment involves a 19.7-ft- (6-m-) high GRS wall with a segmental concrete blocks wall face, and the backfill was a sandy soil reinforced with six layers of 11.5-ft- (3.5-m-) long polymer grid. The reinforcement inside the wall was sequentially severed at pre-selected sections after

construction of the wall was completed. Figure 3 shows the sequence of cutting the reinforcements, and figure 4 shows the maximum horizontal movement corresponding to cutting of the reinforcements. It is seen that there was little movement due to the cutting of the reinforcements until Cut No. 55. Any current design methods of reinforced soil walls would have predicted a failure condition to occur long before Cut No. 55. In a tieback design method, cutting reinforcement is equivalent to shortening the tieback lengths. The cuts before Cut No. 55 would have rendered the tiebacks far shorter than the anchorage needed in any tieback design method (e.g., AASHTO, FHWA, NCMA).



1 m = 3.28 ft

Figure 3. Illustration. Sequence of cutting of the PWRI test wall.



1 m = 3.28 ft

Figure 4. Chart. The resulting horizontal movement of the PWRI test wall.

From the standpoint of an internally stabilized retaining wall, the observed behavior is not at all surprising. A sheet of reinforcement, whether continuous or not, offers a similar restraining

effect to lateral movement of soil, and hence will be able to achieve a stable composite. Note that the resulting stress distribution in the reinforcement will be rather different for continuous and discontinuous reinforcements. It should be noted that the observation of the PWRI experiment was supported by similar experiments by John in the United Kingdom and by the Amoco test wall in the United States.^(44,25)

Lateral Earth Thrust Along Critical Slip Plane

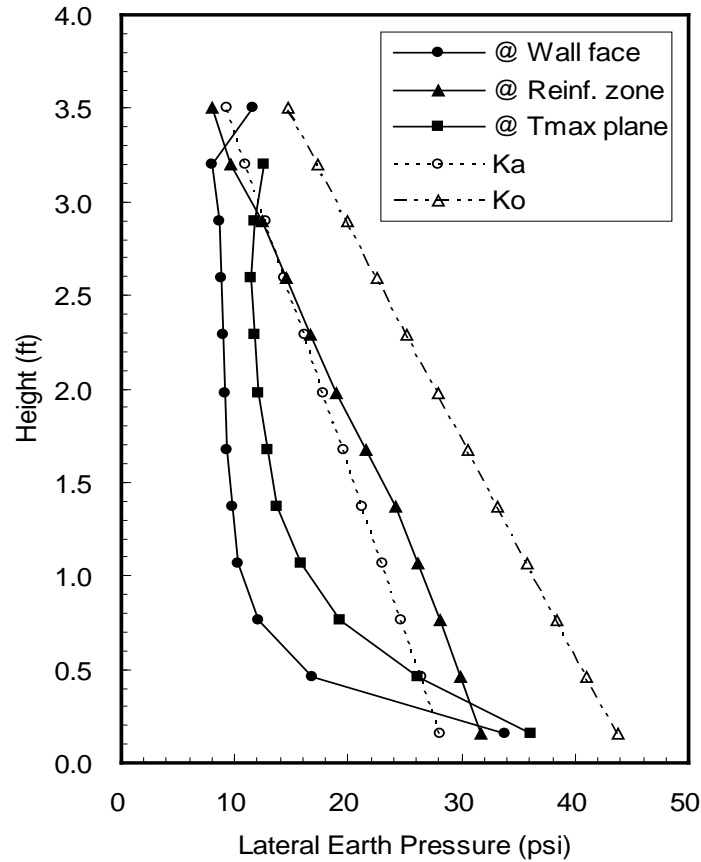
Calculation of the driving force in pullout stability analysis involves determination of lateral thrusts along the critical slip plane. The FHWA NHI manual and AASHTO guidelines use Rankine active earth pressure for calculation of the driving force for GMSE walls with extensible reinforcement. The NCMA design manual uses Coulomb earth pressure for the calculation of the driving force.

Similar to AASHTO guideline, the British standard BS 8006 includes two methods for internal design of GMSE walls: the tieback wedge method and the coherent gravity method.⁽⁵⁾ The former uses active earth pressure K_a for design; whereas the latter uses a K -value varying from the at-rest coefficient (K_o) to the active coefficient (K_a) in the upper 19.68 ft (6 m) of the wall, and K_a below 19.68 ft (6 m). The tieback wedge method is recommended when the short-term tensile strain exceeds 1 percent (e.g., polymeric reinforcement) while the coherent gravity method is recommended when the short-term tensile strain is less than 1 percent (e.g., steel reinforcement).

Chou and Wu conducted a study to investigate the performance of GRS walls with reinforcement at 0.98 ft (0.3 m) spacing by a sophisticated finite element code, DACSAR.⁽²⁹⁾ The lateral pressures and stresses along three separate sections were examined: earth pressure against wall face, earth pressure against the back of the reinforced soil mass, and lateral stresses along the plane of maximum tensile force in reinforcement, as shown in figure 5. The study showed that the lateral thrusts in the three sections are rather different. The lateral earth pressure, the smallest of the three, is nearly constant with depth except near the base of wall (where there is greater constraint to deformation). The lateral stresses along the plane of maximum reinforcement tensile force is almost parallel to the lateral earth pressure profile except the magnitude is somewhat larger. The study also showed that the earth pressure exerted on reinforced soil mass by the retained fill, i.e., the earth pressure commonly used for evaluation of external stability of reinforced soil walls, is close to the Rankine active earth pressure.

DISCUSSION

Pullout of reinforcement stems from the design concept of GMSE walls in which reinforcement serves as tiebacks. The reinforcement needs to be long enough to provide sufficient anchorage length to ensure internal stability of the reinforced zone of a GMSE wall or abutment. GRS walls/abutments, however, are designed based on a different concept. The reinforcement in a GRS structure serves to improve the stiffness and strength of the soil-reinforcement composite. Reinforcement length of a GRS wall is dictated by external stability. In a GRS wall, pullout of geosynthetic reinforcement is theoretically not a design issue.



©N.N. S. Chou and J.T.H. Wu

1 ft = .305 m
1 psi = 6.89 kPa

Figure 5. Chart. Lateral stress/pressure on different sections of a GRS wall.⁽²⁹⁾

A very large number of pullout tests have been conducted by many researchers and designers to help assess pullout capacity of geosynthetic reinforcement under various conditions. It is important to point out that a great majority of the failures of reinforced soil walls involve prolonged rainfall (see references 35 and 45 through 50). In view of these findings, for design purposes, it will be prudent to conduct pullout tests under saturated undrained condition.

Observation of field performance of GRS walls and abutments with closely spaced reinforcement has strongly suggested that pullout is not a probable failure mode for closely spaced GRS walls. Even though pullout failure is not impossible in a reinforced soil wall, a single case of in-service reinforced soil wall where failure can be clearly attributed to pullout of reinforcement has not yet been identified. Nonetheless, the reinforced soil system does not know whether the reinforcement is designed as tiebacks (as in a GMSE) or a tensile inclusion to improve soil stiffness and strength (as in a GRS). In other words, the reinforcement in a GMSE wall, even though designed as tiebacks, also serves to improve the stiffness and strength of the surrounding soil (although not as effectively because of the large reinforcement spacing); and conversely, the reinforcement in a GRS wall, even though designed as reinforcing inclusion, also serves as tiebacks. As a result, one can argue that it would not be a drawback to also check for pullout

stability in the design of a GRS wall or abutment. Longer reinforcement length will likely lead to smaller lateral movement of a wall, unless the wall is in a “constrained fill” condition (where a firm sloping ground is behind the wall).⁽²⁰⁾

The question then becomes: how to check for pullout failure if it is deemed warranted? The answer involves the knowledge of (a) the location of the critical slip plane in a reinforced soil mass and (b) the lateral thrust along the critical slip plane. The latter is less of an issue because the thrust can probably be assumed to be a combination of a K_a - or K_o -condition, depending on the desired degree of conservatism. The location of the critical slip plane, however, is a more troubling issue.

The location of the critical slip plane has traditionally been assumed to follow the Rankine theory. Based on studies by Tatsuoka and his associates, the location of a potential slip surface is a function of facing rigidity. The stiffer the facing, the closer the slip plane will be to the wall face.⁽⁴¹⁾ Also, the location of the slip plane has been known to be affected by the loading condition on the wall crest. When a GRS wall is subject to large edge loads (as in an abutment), the critical slip plane is likely to be quite different from the Rankine active slip plane. The experiment performed by PWRI of Japan, as described previously under the subheading Critical Slip Plane, has further cast doubts on the applicability of the Rankine active slip plane. Also, it is possible that such a slip plane does not exist for typical configurations, material properties, and loading conditions of GRS walls, as argued by Leshchinsky and Vulova.⁽⁴⁰⁾ As a final note, the NCHRP GRS test abutments with reinforcement spacing of 0.66 ft (0.2 m) and reinforcement length of $0.67H$, and with loads being applied near the wall face, did not show any sign of geosynthetic pullout when loaded to failure. The reinforced soil mass clearly behaved as a coherent mass as it was subject to front edge loads all the way to failure. This further suggests that geosynthetic pullout is likely not a probable failure mode for closely spaced GRS abutments.

The inability to compute the driving force and resisting force with confidence may cast doubts on the usefulness for checking geosynthetic pullout of a GRS wall or abutment. Moreover, the method for checking pullout failure as adopted in current design guidelines is unrealistically conservative. The current design guidelines require that the pullout safety factor at each reinforcement layer be greater than a prescribed value (typically 1.5).^(1,2,3) The fact is, pullout failure only occurs if a group of reinforcement layers experiences instability related to pullout. Pullout of any single reinforcement layer will never occur.

In summary, even though the extra design step of checking pullout failure will not harm the overall design of a GRS wall or abutment, two critical reasons—(a) pullout does not appear to be a probable failure mode, and (b) there is no reliable and realistic procedure for checking pullout—have rendered the reinforcement pullout check not particularly meaningful.

CHAPTER 4. ECCENTRICITY

As part of the design of conventional cantilever and gravity retaining walls with relatively rigid footings, overturning failure is commonly checked to determine whether the design meets the required margin of safety. This check typically consists of taking moments of all the stabilizing forces acting on the free body of the wall system about the toe (e.g., Point O for a cantilever wall shown in figure 6) and comparing them with the moments for the destabilizing forces about the same point. The required margin of safety for overturning is typically specified in the relevant code of practice.

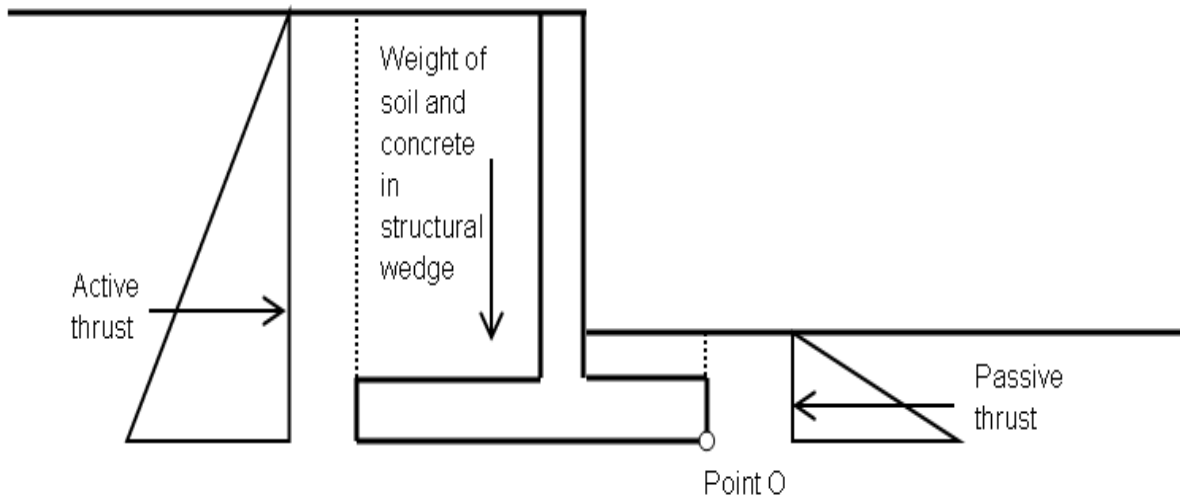


Figure 6. Drawing. Free body diagram, cantilever wall system for overturning calculations.

An alternative means of assessing the overturning potential of retaining walls has been proposed by the U.S. Army Corps of Engineers, (USACE).⁽⁵¹⁾ Rather than comparing the stabilizing and destabilizing moments, the overturning criteria are based on a minimum base area in compression, i.e., limiting the amount of footing “liftoff.” This technical synopsis examines the purpose and theoretical justification of this design component.

ECCENTRICITY, BEARING PRESSURE DIAGRAM, AND FOOTING LIFTOFF

For a wall supported on a rigid concrete footing, the amount of footing liftoff is determined from its bearing pressure diagram. If R and R_v are the resultant force and vertical component of the resultant force, respectively, acting on the free body of the wall system per unit length, the bearing pressure diagram can be determined for several possible resultant force locations. Key to this evaluation is the estimation of the maximum (σ_{\max}) and minimum (σ_{\min}) bearing pressures, calculated using the equations shown in figure 7 and figure 8:

$$\sigma_{\max} = \frac{R_v}{A} + \frac{Mc}{I}$$

Figure 7. Equation. Estimated maximum bearing pressure, σ subscript max.

$$\sigma_{\min} = \frac{R_v}{A} - \frac{Mc}{I}$$

Figure 8. Equation. Estimated minimum bearing pressure, σ subscript min.

A equals the footing area, which is the footing width, B , per unit length for a plane strain problem. The distance from the centroid of footing to extreme fiber is c , which equals $B/2$. I is the moment of inertia of footing, and equals $B^3/12$ per unit length. M is the moment about the footing centroid, and equals R_v times e , e being the eccentricity of the resultant force from the footing centroid. After simplifying, the equations in figure 7 and figure 8 become the equations in figure 9 and figure 10:

$$\sigma_{\max} = \frac{R_v}{B} \left(1 + \frac{6e}{B} \right)$$

Figure 9. Equation. Simplified estimated maximum bearing pressure, σ subscript max.

$$\sigma_{\min} = \frac{R_v}{B} \left(1 - \frac{6e}{B} \right)$$

Figure 10. Equation. Simplified estimated minimum bearing pressure, σ subscript min.

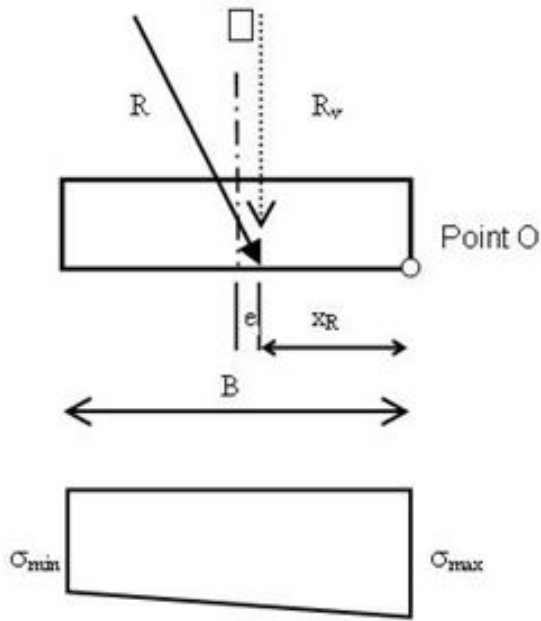
For no footing liftoff, σ_{\min} must be ≥ 0 . By setting σ_{\min} equal to 0 in the equation in figure 10, it can be seen that the resultant force acting on the free body of the wall system must lie within the middle third of the footing; i.e., $e \leq B/6$.

As shown in the equation in figure 11, the point of action of the resultant force from the toe (χ_R) is calculated by simply summing the moments about the toe of all the forces acting on the free body of the wall system and dividing by the vector sum of the vertical force components acting on the footing (R_v).

$$\chi_R = \frac{\sum \text{Moments about the toe}}{R_v}$$

Figure 11. Equation. Resultant force from the toe, χ subscript R.

If the resultant force acts within the middle third, the bearing pressure diagram is trapezoidal and 100 percent of the footing is in compression; i.e., no liftoff (see figure 12). If the resultant force acts on the middle third point, the bearing pressure diagram is triangular and spans the entire footing width (figure 13). There is still no footing liftoff in this case. If the resultant force acts outside the middle third but within the footing, the bearing pressure diagram is also triangular but the span of the triangle is less than the footing width. The remaining portion of the bearing pressure diagram is negative; i.e., $\sigma_{\min} < 0$ (figure 14). The portion of the footing that is outside the triangular bearing pressure diagram (i.e., when $\sigma < 0$) is in a state of tension or liftoff. Clearly, it is undesirable to allow any footing liftoff except perhaps during temporary live loading or during extreme events such as earthquakes.

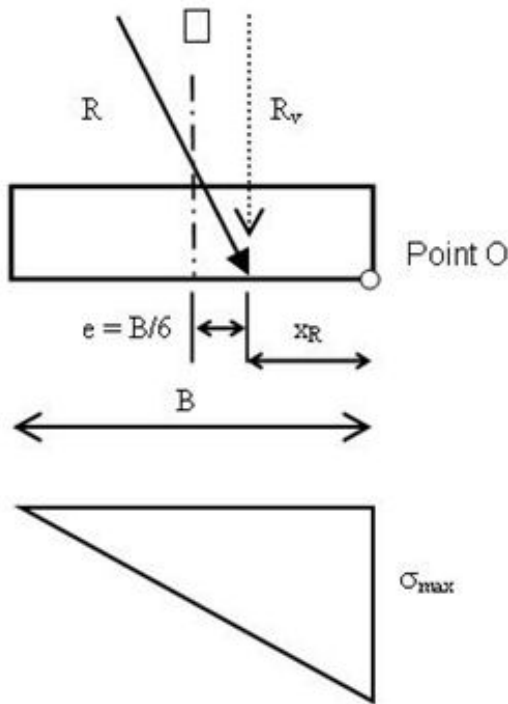


(a) Within middle third ($e < B/6$)
100% base in compression

$$\sigma_{\max} = \frac{R_v}{B} \left(1 + \frac{6e}{B} \right)$$

$$\sigma_{\min} = \frac{R_v}{B} \left(1 - \frac{6e}{B} \right)$$

Figure 12. Drawing. Bearing pressure diagram—resultant force within middle third.



(b) On middle third
100% base in compression

$$\sigma_{\max} = q = \frac{2R_v}{B}$$

$$\sigma_{\min} = 0$$

Figure 13. Drawing. Bearing pressure diagram—resultant force on middle third.

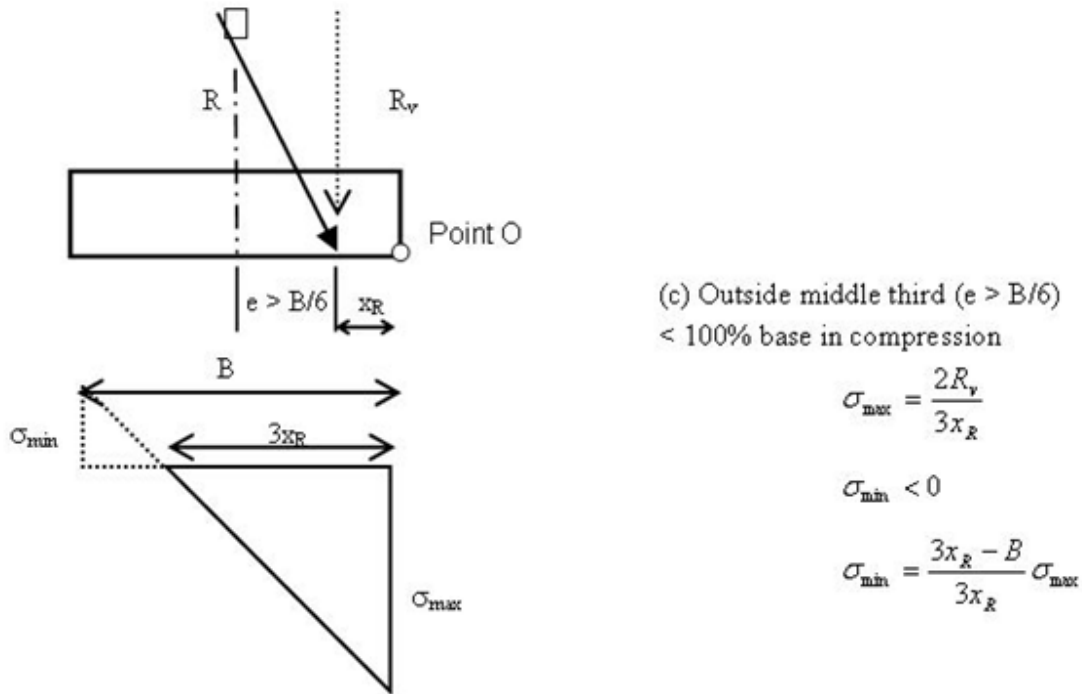


Figure 14. Drawing. Bearing pressure diagram—resultant force outside middle third.

The area of the footing in compression can be calculated by first computing the resultant ratio, RR , as shown in the equation in figure 15:

$$RR = \chi_R/B$$

Figure 15. Equation. Resultant ratio, RR .

The percent area of footing in compression (A_{fc}) can be estimated as shown in the equation in figure 16:

$$A_{fc} \text{ (in \%)} = 100 \quad \text{when } \frac{1}{3} \leq \chi_R/B \leq \frac{1}{2}$$

$$A_{fc} \text{ (in \%)} = 300 \times RR = 300\chi_R/B \quad \text{when } \chi_R/B < \frac{1}{3}$$

Figure 16. Equation. Percent area of footing in compression, A subscript fc (in percent).

It follows that the percent area of footing experiencing liftoff is 100 percent minus A_{fc} .

If the resultant force acts at the toe of the footing, the wall is on the verge of overturning; i.e., the destabilizing moment is just equal to the stabilizing moment and there is no margin of safety available. If the resultant force acts outside the footing, the wall will overturn. The USACE requires that, in designing for earthquake protection, the resultant force must lie within the footing for retaining walls.⁽⁵¹⁾ The various possible scenarios described above are summarized in table 3.

Table 3. Resultant force location and impact on safety against overturning, base area in compression, and bearing pressure diagram.

Resultant Force Location	Safety Against Overturning	Base Area in Compression, A_{fc}	Bearing Pressure Diagram
Within middle third	Very safe	100 percent	Trapezoidal and positive over entire footing width B
On middle third point	Safe	100 percent	Triangular and positive over entire footing width B
Outside middle third but within footing	Margin of safety diminishes as resultant pushes towards toe but stabilizing moment is still \geq overturning moment	$0 \text{ percent} < A_{fc} < 100 \text{ percent}$	Triangular and positive over front portion of footing; triangular and negative over back portion of footing
On footing toe	No margin of safety; i.e., stabilizing moment = overturning moment	0 percent	Negative over entire footing width B except at toe where $\sigma_{\max} \rightarrow +\infty$
Outside footing	Unsafe. Will overturn	0 percent	Negative over entire footing width B

OVERTURNING VERSUS LIFTOFF

In this section, a simple methodology is presented to determine when liftoff will control. Figure 17 depicts the simple case of the lateral (E_a is horizontal because the wall friction δ is assumed to be 0) and vertical (W) forces acting on a rectangular wall with a rigid base.

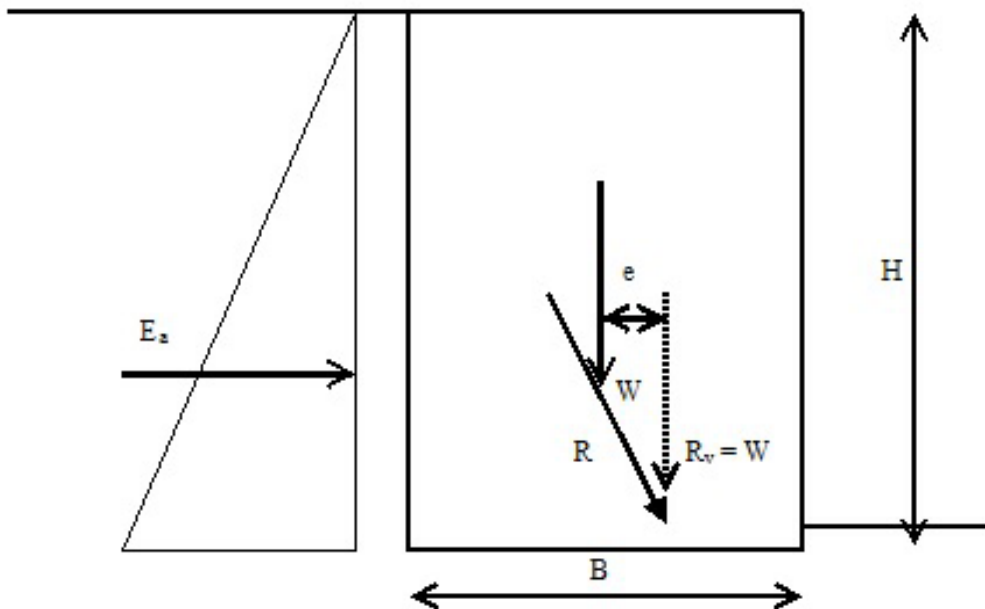


Figure 17. Drawing. Forces on a rectangular rigid wall.

The two forces—lateral and vertical—can be represented by a single resultant force, R , which is acting at an offset e from the centroid of the wall base. This eccentricity can be estimated by decomposing the resultant force into the vertical and horizontal (not shown) components at the base and summing moments about the centroid of the wall base as shown in the equation in figure 18:

$$R_v e = E_a \frac{H}{3}$$

Figure 18. Equation. Vertical component of resultant force at offset e , $R_v e$.

R_v is the vertical component of the resultant force, whose moment about the centroid of the wall base is not zero as opposed to the horizontal component. Therefore, the equation in figure 19 follows.

$$e = \frac{E_a H}{3R_v}$$

Figure 19. Equation. Force e .

The factor of safety against overturning can be obtained by summing moments about the toe as shown in the equation in figure 20:

$$F = \frac{WB/2}{E_a H/3} = \frac{R_v B/2}{E_a H/3} = \frac{B}{2e}$$

Figure 20. Equation. Safety factor, F .

Solving the equation in figure 20 for B gives the equation shown in figure 21:

$$B = 2eF$$

Figure 21. Equation. Footing width, B .

For liftoff to occur, the condition shown in figure 22 must be satisfied.

$$B < 6e$$

Figure 22. Equation. Value of footing width B for liftoff to occur.

By inspecting the equations in figure 21 and figure 22, it can be determined that liftoff occurs when the factor of safety against overturning is less than 3; i.e., liftoff is not an issue when the overturning factor of safety exceeds 3. This criterion is only true when no surcharge loads are acting on top of the wall. When surcharge loads act on top of the wall (as is the case in a GRS IBS), then the factor of safety against overturning for no liftoff will be less than 3. How much less than 3 depends on the magnitude of the load on top of the wall and its point of action.

OVERTURNING DESIGN REQUIREMENTS FOR REINFORCED SOIL WALLS

- **AASHTO.**⁽⁵²⁾ In the 1998 AASHTO *LRFD Bridge Design Specifications*, the practice of calculating the ratio of stabilizing moment to overturning moment as a check for overturning of bridge abutments and GMSE walls was replaced by the resultant location criteria coupled with a check for bearing pressure. The criteria state that the resultant force for walls with footings on soil and rock must lie within the middle third and middle half, respectively, for allowable stress design (ASD) (middle half and middle three quarter for load and resistance factor design (LRFD)).
- **FHWA.**⁽⁵³⁾ FHWA 1997 guidelines for GMSE structures state that “the flexibility of MSE walls should make the potential for overturning failure highly unlikely.” Unlike cantilever and gravity walls with relatively rigid footings, the base of GMSE or GRS walls have little or no flexural rigidity. The notion that they can support bending stresses with tensile contact pressures or liftoff developing seems counterintuitive and has not been observed in instrumented GMSE structures such as those studied by Simac et al. and Bathurst et al.^(54,55) Therefore, the FHWA 1997 guidelines omit overturning as a potential failure mode for GMSE structures. To control lateral deformation due to tilting, however, FHWA requires that the eccentricity of the resultant force be checked to determine whether it exceeds a maximum permissible value as prescribed by AASHTO.
- **NCMA.**⁽³⁾ NCMA indicates in its *Design Manual for Segmental Retaining Walls* (these are geosynthetic reinforced walls that use dry stacked interlocking modular masonry concrete units as a facing) that overturning about the toe should be considered as a potential failure mechanism, a view that differs from that of the FHWA. NCMA does not require consideration of the base eccentricity criteria.
- **Canadian Geotechnical Society.**⁽⁵⁶⁾ Like the NCMA, the *Canadian Foundation Engineering Manual* (Canadian Geotechnical Society, 2006) does require checking for overturning of reinforced walls.
- **British Standards Institution.**⁽⁵⁾ British standard BS 8006 (1995) does not require overturning of strengthened/reinforced soil and other fills be assessed during design. For external stability, the British standard does require a check for bearing capacity, sliding, and external slip. In checking for bearing capacity, the maximum bearing pressure (σ_{\max}) is compared with the bearing capacity. Because σ_{\max} increases with increasing eccentricity, the implication is that the eccentricity will be automatically limited by imposing a limit on the bearing capacity.
- **Designing With Geosynthetics.**⁽⁵⁷⁾ Koerner indicated that the factor of safety against overturning for geotextile reinforced walls is typically very high. He further points out that overturning is not a likely failure mechanism because of base flexibility. Therefore, “many engineers do not even include an overturning calculation in the design process.”
- **Retaining Wall-Dialog: “A Tale of Two Walls” and “GRS—A New Era in Reinforced Soil Technology.”**^(58,59) Barrett and Ruckman presented cases of GRS walls with negative batter being used or tested successfully in Colorado (figure 23), New

Zealand (figure 24), Japan (figure 25), and elsewhere. Barrett wrote “prevailing guidelines for internally supported MSE walls are based on translations from externally supported cantilever walls and are generally inappropriate.” GRS walls with negative batter that generally do not meet the overturning requirements are still performing well today.



Source: R.K. Barrett and A.C. Ruckman

Figure 23. Photo. First negative batter GRS wall constructed in Colorado for CDOT.⁽⁵⁹⁾



Source: R.K. Barrett and A.C. Ruckman

Figure 24. Photo. GRS wall in New Zealand with a negative.⁽⁵⁹⁾



Source: R.K. Barrett and A.C. Ruckman

Figure 25. Photo. Research on negative batter GRS walls in Japan.⁽⁵⁹⁾

SUMMARY

Table 4 offers key points relating to the need to limit the eccentricity in the design of GRS walls.

Table 4. Key points relating to the need to limit the eccentricity in the design of GRS walls.

Points that argue for the need for a limiting eccentricity criterion	Points that argue against the need for a limiting eccentricity criterion
It is prudent to consider a limiting eccentricity criterion.	The check that the bearing pressure meets the bearing capacity criterion requires σ_{\max} to be less than the bearing capacity with an adequate margin of safety. Because σ_{\max} increases with increasing eccentricity, it implies that the eccentricity will be automatically limited by imposing a limit on the bearing capacity.
GRS walls can be less wide at the base than GMSE walls according to different design methods (Adams et al., and Berg et al., respectively), and hence, the factors of safety pointed out by Koerner in GMSE structures may not be as high for GRS walls. ^(6,2,57)	Flexible reinforcing elements (e.g., geotextiles) do not reinforce the soil by any interaction involving bending or shear across their cross-sectional area. They merely interact with the soil by absorbing axial tension. Consequently, the base of GRS walls cannot be considered rigid. While overturning is a valid failure mechanism for walls with rigid bases, GRS walls cannot fail by overturning because bending moments cannot transfer to the toe of such a flexible system. Moreover, it is questionable whether the methodology and equations presented herein apply to a reinforced soil wall system with flexible bases.
	Even when the equations presented herein are used, Koerner points out that the factor of safety against overturning for geotextile reinforced walls is typically high. ⁽⁵⁷⁾
	FHWA 1997 guidelines require limiting the eccentricity of the resultant force only for the sake of limiting lateral deformation. It may be implied that lateral deflection increases with increasing eccentricity but such correlations are not readily available to decide on an acceptable eccentricity value for design.
	Barrett showed that GRS walls with negative batters have performed very well. ^(58,59)

GMSE = Geosynthetic Mechanically Stabilized Earth

GRS = Geosynthetic Reinforced Soil

Clearly, checking for limiting eccentricity is generally prudent. However, such a check is based on theories that really do not apply to flexible base systems. The check is intended as a failure mechanism that is feasibly impossible in a GRS and thus should be discontinued.

CHAPTER 5. LATERAL PRESSURES

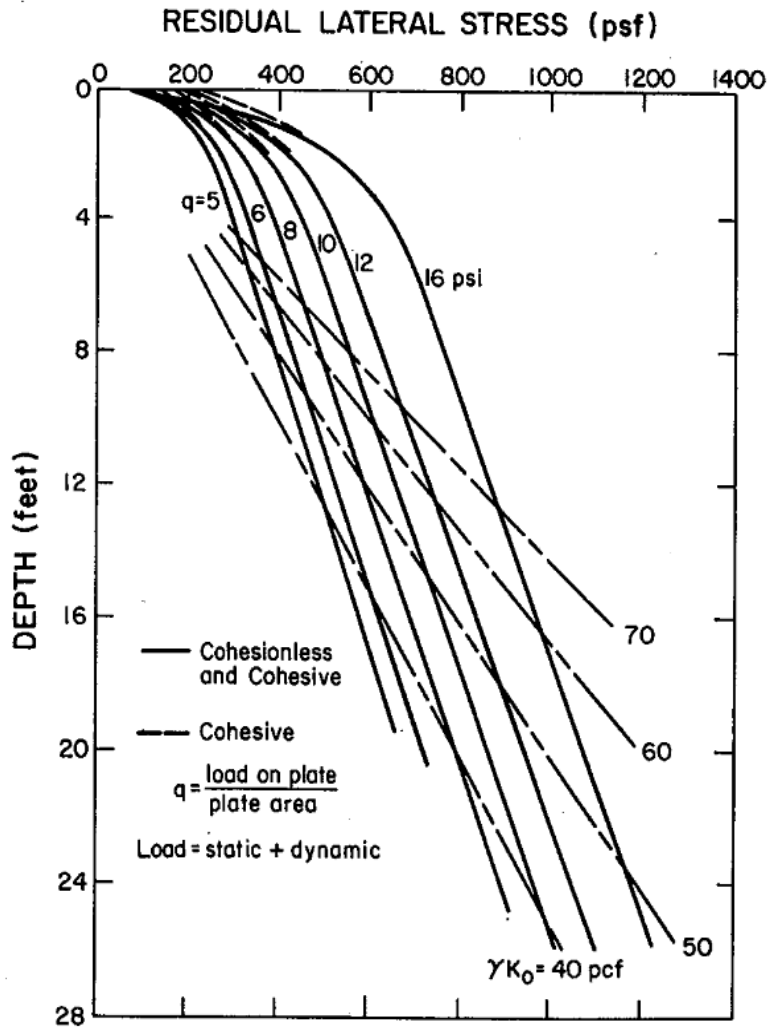
The lateral stress at a GRS facing is different from that in the soil portion. The internal lateral stress in the GRS soil is governed by compaction-induced stresses (CIS) and by additional confining effects that the reinforcement provides to the soil. The pressure at the facing is governed by these two factors as well as the movement of the facing especially in facings that have little or no connection strength. The effects of CISs on the internal lateral stress of both the unreinforced and reinforced soil is discussed. Measured thrusts against facing elements with and without purely frictional connection are presented. Methods for estimating this thrust are used to compare with the measured values.

COMPACTION-INDUCED STRESSES

Based on Duncan and Seed's work on CISs, Williams developed simple charts to estimate the residual lateral earth pressures on a nonyielding wall due to compaction.^(60,61) An example of a chart for residual lateral stress due to vibratory plate compactors, usually used in GRS construction, is shown in figure 26. At shallow depths, the CIS is a function of the load from the vibratory plate (q) and it exceeds the at-rest value. The family of curves represents different values of q ranging from 5 to 16 psi (34.5 to 110.3 kPa). At greater depths, the lateral pressures revert to the at-rest value once the overburden pressure exceeds the preconsolidation pressure generated during compaction (by the vibratory plate compactor). The family of dashed lines represents the at-rest stresses for varying soil unit weight and friction angles, ϕ ($K_o = 1 - \sin \phi$). Figure 26 is applicable to compaction of unreinforced soil.

CIS in GRS is likely to be higher than in the same soil unreinforced because the reinforcement-soil-interface friction restrains soil movement thereby producing larger values of soil confining stress, which manifests in the form of greater CIS. Evidence of increased lateral stress has been demonstrated by numerical analysis performed by Ketchart and Wu for a compacted GRS mass loaded to 6 kN (1.35 kips).⁽⁶²⁾ The vertical stress distribution in the loaded unreinforced soil and GRS are similar, as shown in figure 27. However, the horizontal (figure 28) and shear (figure 29) stresses are higher in the GRS than in the same soil unreinforced. They are higher near the reinforcement and decrease with increasing distance from the reinforcement. The increase in lateral stress will result in increased strength of the GRS. Based on these results, Ketchart and Wu recommended that reinforcement spacing be limited to 12 inches (30.48 cm) for improved performance—hence the advent of closely spaced reinforcement, more commonly called GRS.⁽⁶²⁾

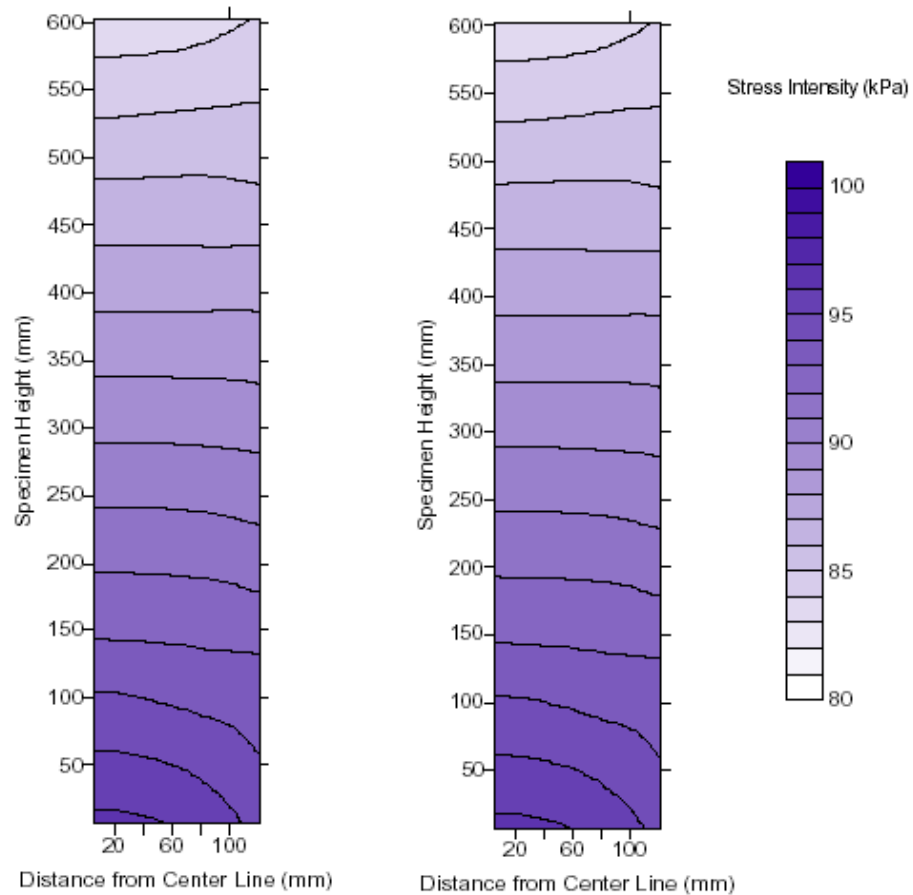
Even though CIS clearly adds an important contribution to the vertical capacity of a GRS wall, one drawback when considering CIS in design is that the compaction equipment is seldom known a priori. Therefore, any quantitative analysis of the contribution of compaction to enhance the lateral stresses, and hence capacity in a GRS in the field, is speculative at best.



Source: Francis Group LLC Books

1 ft = .305 m
 1 psf = .05 kPa
 1 psi = 6.89 kPa
 1 pcf = 16.02 kg/m³

Figure 26. Chart. Residual lateral stress induced by vibratory plate compaction.⁽⁶³⁾



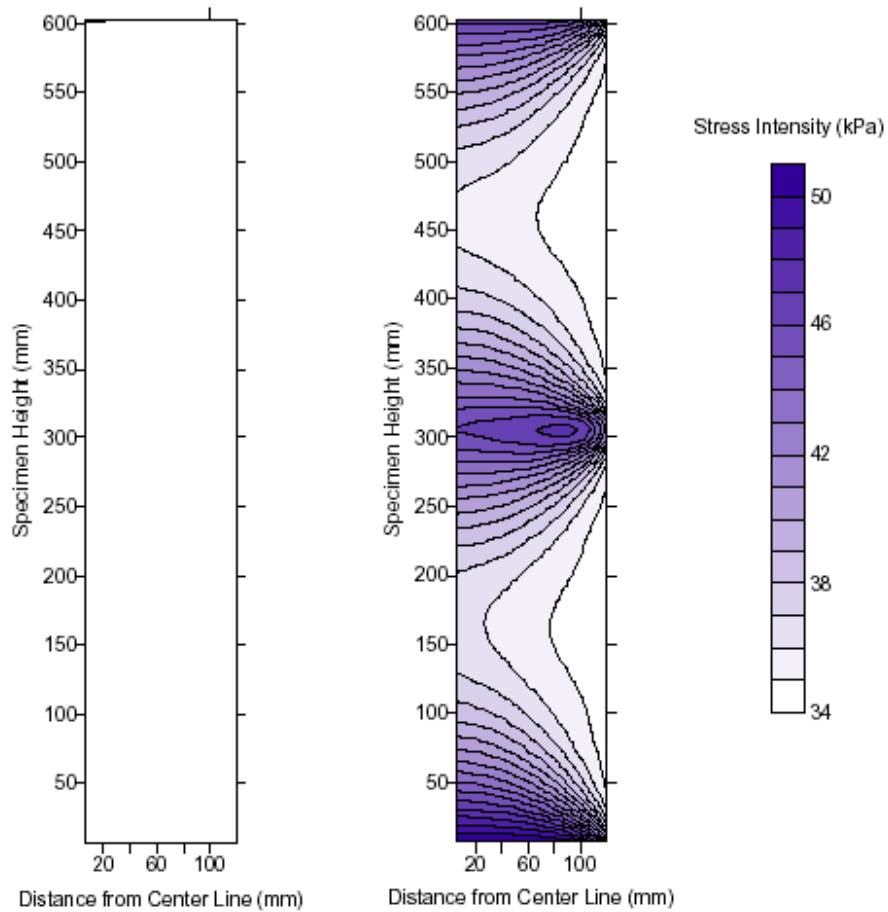
(a) Vertical Stress at 6 kN of Test P-M-RB

(b) Vertical Stress at 6 kN of Test P-M-(RB+2044)

©K. Ketchart and J.T.J.H. Wu

1 kPa = 20.89 psf
 1 mm = .039 inches
 1 kN = 0.23 kips

Figure 27. Chart. Vertical stress distribution at 6-kN (1.35-kips) vertical load on the GRS (a) without and (b) with reinforcement.⁽⁶²⁾



(a) Horizontal Stress at 6 kN of Test P-M-RB

(b) Horizontal Stress at 6 kN of Test P-M-(RB+2044)

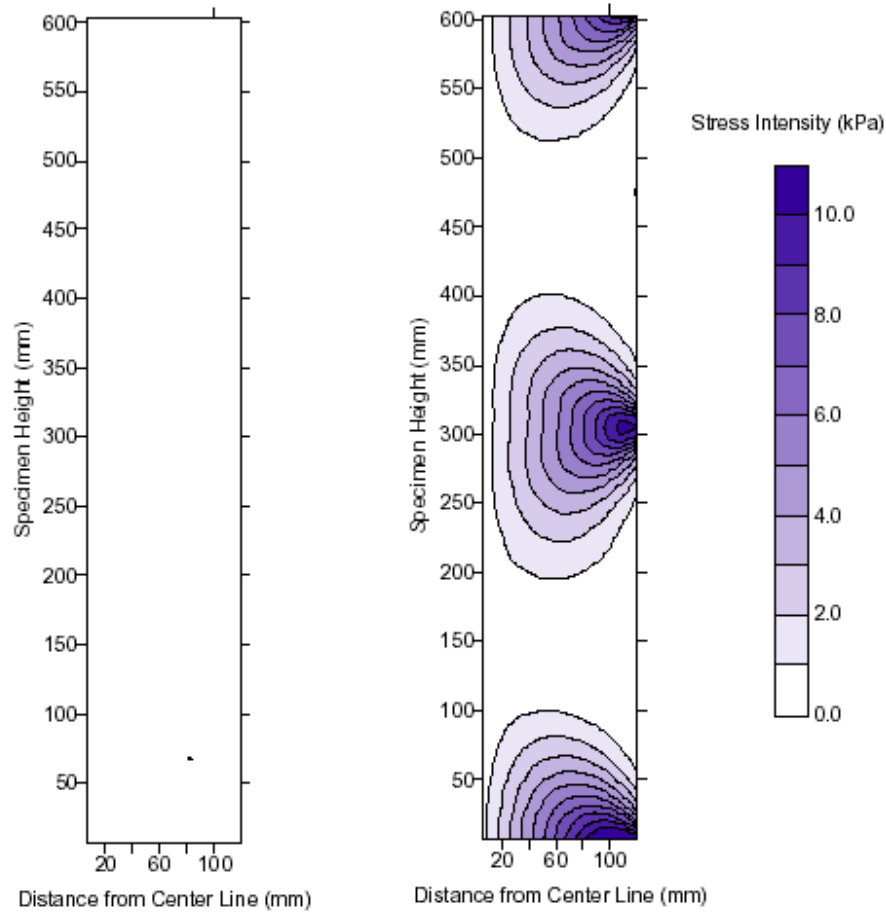
©K. Ketchart and J.T.J.H. Wu

1 kPa = 20.89 psf

1 mm = .039 inches

1 kN = 0.23 kips

Figure 28. Chart. Horizontal stress distribution at 6-kN (1.35-kips) vertical load on the GRS (a) without and (b) with reinforcement.⁽⁶²⁾



(a) Shear Stress(xy) at 6 kN of Test P-M-RB

(b) Shear Stress(xy) at 6 kN of Test P-M-(RB+2044)

©K. Ketchart and J.T.J.H. Wu

1 kPa = 20.89 psf
 1 mm = .039 inches
 1 kN = 0.23 kips

Figure 29. Chart. Shear stress distribution at 6-kN (1.35-kips) vertical load on the GRS (a) without and (b) with reinforcement.⁽⁶²⁾

MEASUREMENTS OF LATERAL PRESSURES IN REINFORCED SOIL

Lateral stresses in a reinforced soil mass were measured by Yang.⁽⁶⁴⁾ He conducted footing model tests on both reinforced and unreinforced soil using a rigid 8-inch- (20.3-cm-) diameter stainless steel plate as a footing. The soil consisted of a dry sand with an average density of 92 pcf (1,474 kg/m³) (corresponding to a relative density of 70 percent ($\gamma_{d \min} = 81.5$ pcf (1,306 kg/m³, and $\gamma_{d \max} = 96.5$ pcf (1,546 kg/m³)). This density was achieved by pluviation, raining the sand from a height of 9 inches (22.9 cm). Compaction-induced stresses were nonexistent in this study. Therefore, any difference in lateral stress between the reinforced and

unreinforced sand was purely a result of the effect of the reinforcement. The reinforcement consisted of six 20-inch-(50-cm-) diameter fiberglass nets having average tensile strengths of 202 lb/inch (35.4 kN/m) in one direction and 178.5 lb/inch (21.3 kN/m) in the other. The first reinforcing was placed 2 inches (5.1 cm) below the footing. The additional reinforcings were spaced at 2 inches (5.1 cm).

Lateral stresses were measured at several depths along the centerline of the footing using pressure cells that were 1.4 inches (3.6 cm) in diameter and 0.2 inches (0.5 cm) thick. To prevent damage to the pressure cells that were originally designed by the U.S. Bureau of Mines, the maximum applied stress on the footing was limited to 75 percent of the ultimate bearing capacity for the unreinforced sand. For the reinforced sand, the applied stress was kept below a level that corresponded to a maximum lateral pressure of 40 psi (276 kPa).

Based on the normalized measured lateral stress (lateral stress divided by the applied stress) versus the normalized depth (depth divided by the footing radius) in both the reinforced and unreinforced soil. Yang offered the following results.⁽⁶⁴⁾

- The unreinforced soil at two different stress levels clearly indicate that the radial stress to applied stress ratio increased with increasing stress level. For the reinforced soil, Yang indicated that the lateral stress ratio was independent of the applied stress level. He did caution that this might not be true as the applied stress approached the ultimate bearing capacity of the footing on the reinforced soil. However, in the interest of preserving the pressure cells, the tests did not reach such high loads.
- The lateral stress in the reinforced soil was fairly constant from a depth of 0.5 to 2.25 times the footing radius. The corresponding reduction in lateral stress in the unreinforced soil with increasing depth was more significant.
- The lateral stresses in the reinforced sand were in general higher than those in the unreinforced sand. A GRS is expected to be stronger than the same soil unreinforced. For this to occur, the confining stress in the soil must effectively increase due to the presence of the reinforcement, as shown numerically by Ketchart and Wu.⁽⁶²⁾ These data provide compelling evidence of this lateral stress increase.

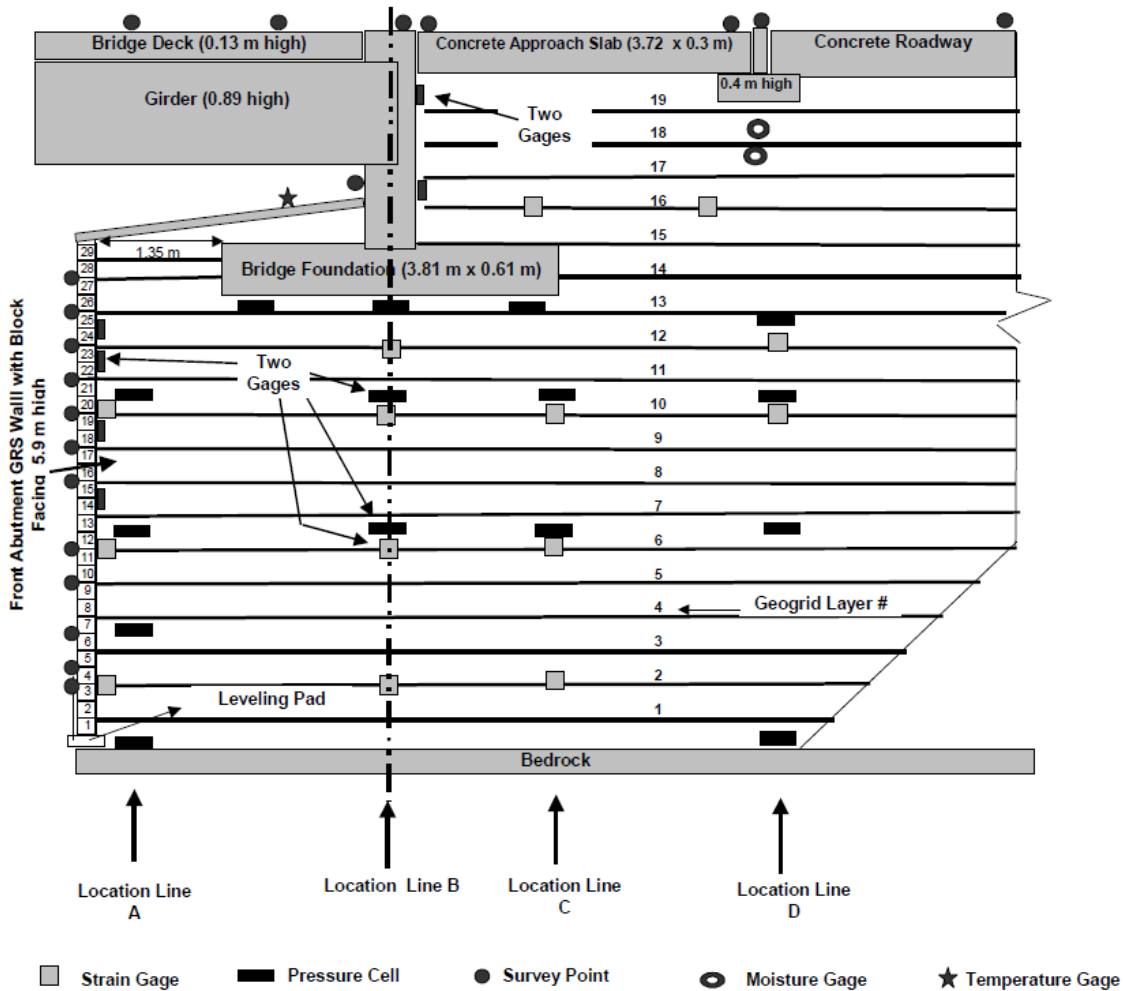
MEASUREMENTS OF LATERAL PRESSURES AGAINST THE FACE OF REINFORCED WALL SYSTEMS

Lateral stresses have been measured in many reinforced soil wall systems. They include systems with reinforcing elements that are both connected and not connected to the wall face. Among the those not connected, the wall systems consisted of a concrete wall at the end of a bridge (Warren and LeGrand), an aluminum plate (Ahmadi and Hajjalilue-Bonab), brick elements mortared together (Dalton, Walsh, and Pinto and Cousens), and gravity/rigid retaining walls (Saran et al., Garg and Saran, Mittal et al., and Garg et al.). (See references 65 through 73.) Among those that were connected, the wall systems consisted of a full-height plywood facing panel connected to geogrids (Shinde and Mandal), gabion walls connected to geogrids, woven and nonwoven geotextiles (Won and Kim), modular block facing frictionally connected to geogrids (Abu-Hejleh

et al. and Mitchell), and full-height-panel and incremental panel walls connected to geogrids (Yogarajah and Saad). (See references 74 through 78.)

Abu-Hejleh et al. reported lateral pressures on the facing of a 19.4-ft- (5.9-m-) high segmental retaining wall reinforced with 16-inch- (40.6-cm-) spaced Tensar® UX 6 geogrids at the Founders/Meadows bridge in Denver, Colorado (figure 30).⁽⁷⁶⁾ These pressures were only reported at the end of construction with the bridge superstructure loading the abutment. This is not a true GRS because the spacing was greater than 12 inches (30.48 cm). The abutment fill, described as a gravelly CDOT Class 1 backfill, had a measured unit weight of 141 pcf (2,259 kg/m³) with peak shear strength parameters from large-scale triaxial tests of $\phi = 39$ degrees and $c = 1,440$ psf (68.0 kPa).

Earth pressure cells were mounted above the 7th, 9th, 11th, and 12th geogrid layer from the bottom. Abu-Hejleh et al. indicated that the measured lateral pressures were significantly less (6 to 35 percent) than the Rankine active pressures plus the footing-induced pressure assumed a 2V:1H load spread (see table 6). Lateral pressures before placing the bridge footing were not reported.

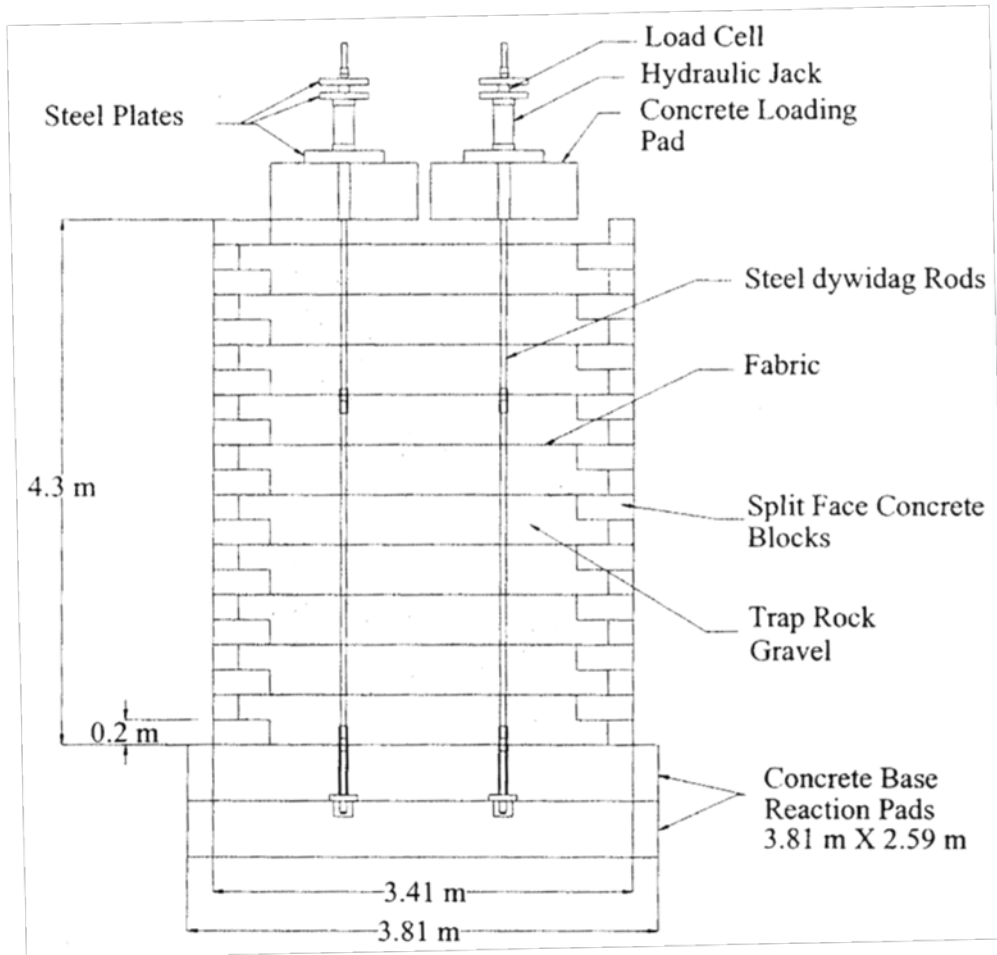


Source: N.M. Abu-Hejleh et al.

Figure 30. Drawing. Founders/Meadows bridge abutment cross-section and instrumentation.⁽⁷⁶⁾

Mitchell measured lateral pressures on the concrete masonry unit (CMU) facing of four GRS mini-piers (figure 31 and figure 32).⁽⁷⁷⁾ The reinforcement (Amoco 2006—wide-width tensile strength = 2,100 lb/ft(30.6 kN/m)) spacings were 24 inches (60.9 cm), 16 inches (40.6 cm), 8 inches (20.3 cm), and 32 inches (81 cm) in piers 1, 2, 3, and 4, respectively. The facing consisted of 99-lb (45.0-kg) split-face keystone retaining wall blocks that were 18 inches (46 cm) long, 5 inches (12.7 cm) wide, and 8 inches (20.3 cm) deep with a flange protruding to the inside of the piers. Corner blocks with slightly different weight and dimensions were used.

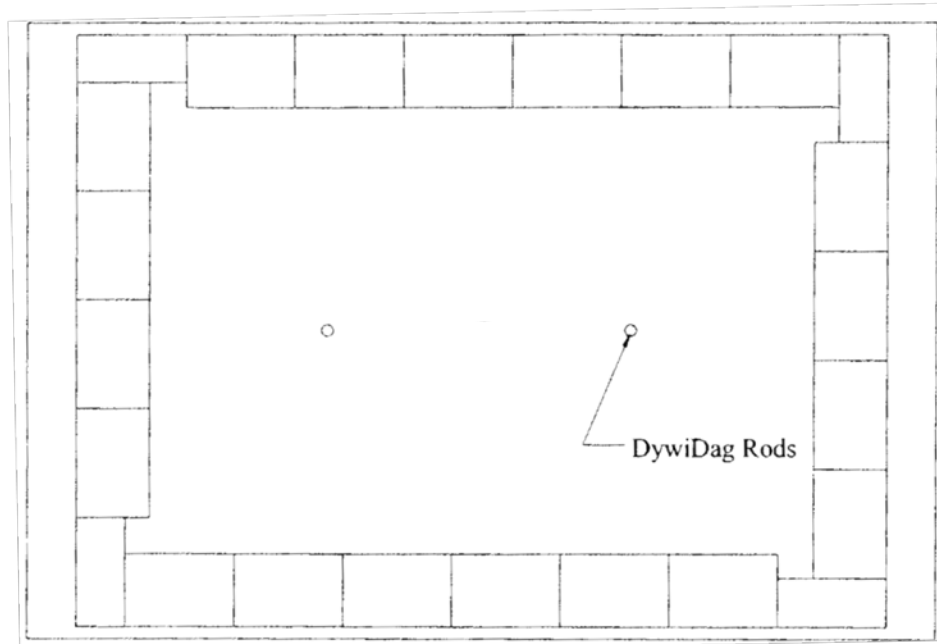
Known as trap rock gravel (32.1 percent gravel, 56.5 percent sand, and 11.5 percent fines; $C_u = 40$, $C_c = 3.2$, $G_s = 2.93$; Standard Proctor $\gamma_{d \max} = 144$ pcf (2,307 kg/m³); $w_{\text{opt}} = 8.75$ percent; Modified Proctor $\gamma_{d \max} = 150$ pcf (2,403 kg/m³); $w_{\text{opt}} = 6.5$ percent), the backfill had shear strength parameters of $\phi = 36$ degrees and $c = 637$ psf (30.5 kPa) based on a failure relative displacement of 10 percent of the shear box length as measured in a 12- by 12-inch (30.5- by 30.5-cm) direct shear box. The shear stress-displacement curves appear to be still strain hardening at the interpreted failure relative displacement.



Source: J.W. Mitchell

1 m = 3.28 ft

Figure 31. Drawing. GRS mini-pier elevation plan.⁽⁷⁷⁾

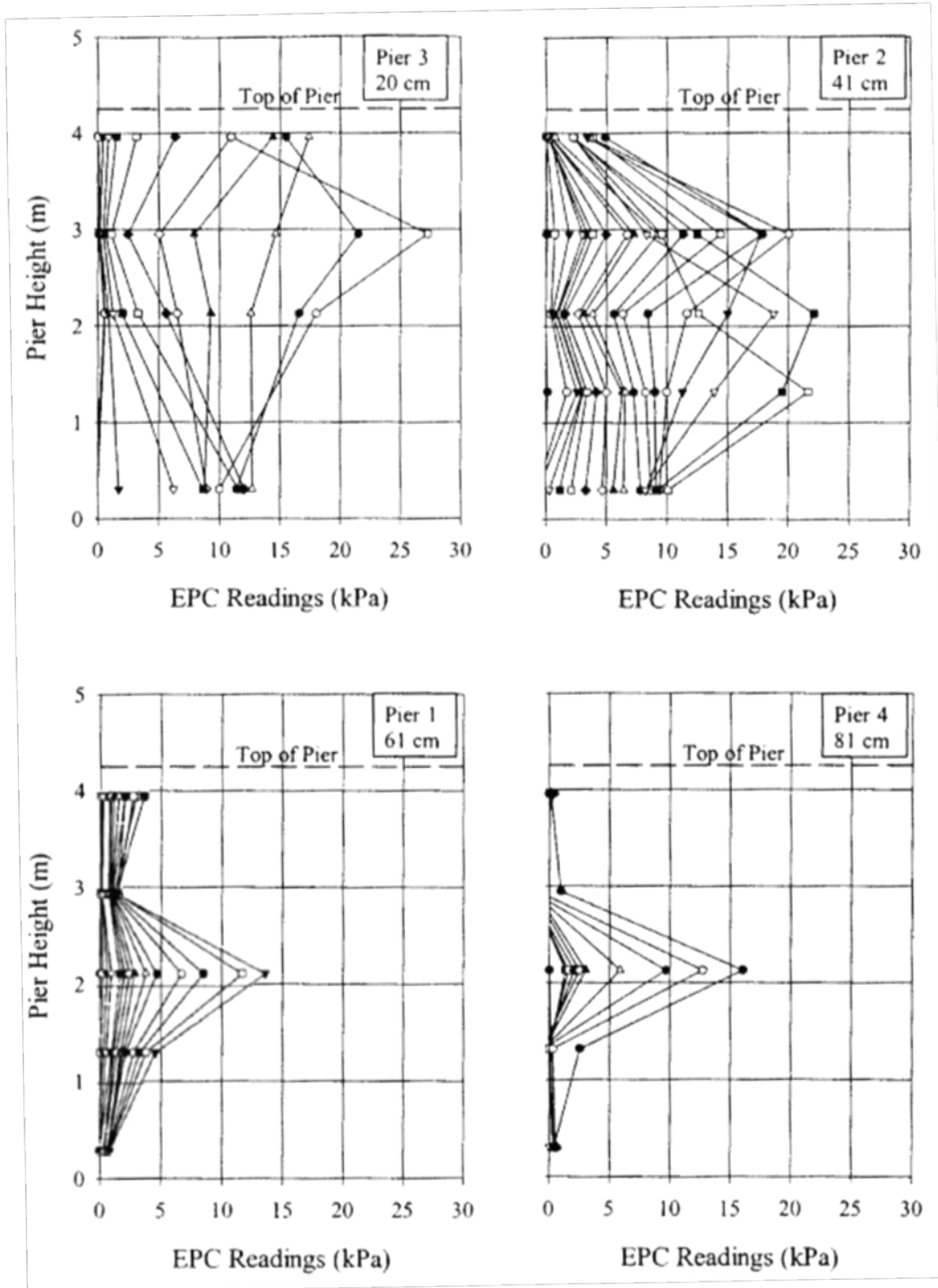


Source: J.W. Mitchell

Figure 32. Drawing. GRS mini-pier elevation plan.⁽⁷⁷⁾

Geokon™ vibrating wire pressure transducers were placed at five elevations (1 ft (0.3 m), 4.3 ft (1.3 m), 7 ft (2.1 m), 9.7 ft (3.0 m), and 13 ft (4.0 m) above base) along the GRS wall height. The measured lateral pressures are shown in figure 33 and figure 34. These pressure readings were zeroed at zero load and represent only the increase in the lateral pressures during the load test. Mitchell noted that with a decrease in reinforcement spacing, the lateral pressures increased and became more equally distributed over the wall height.⁽⁷⁷⁾

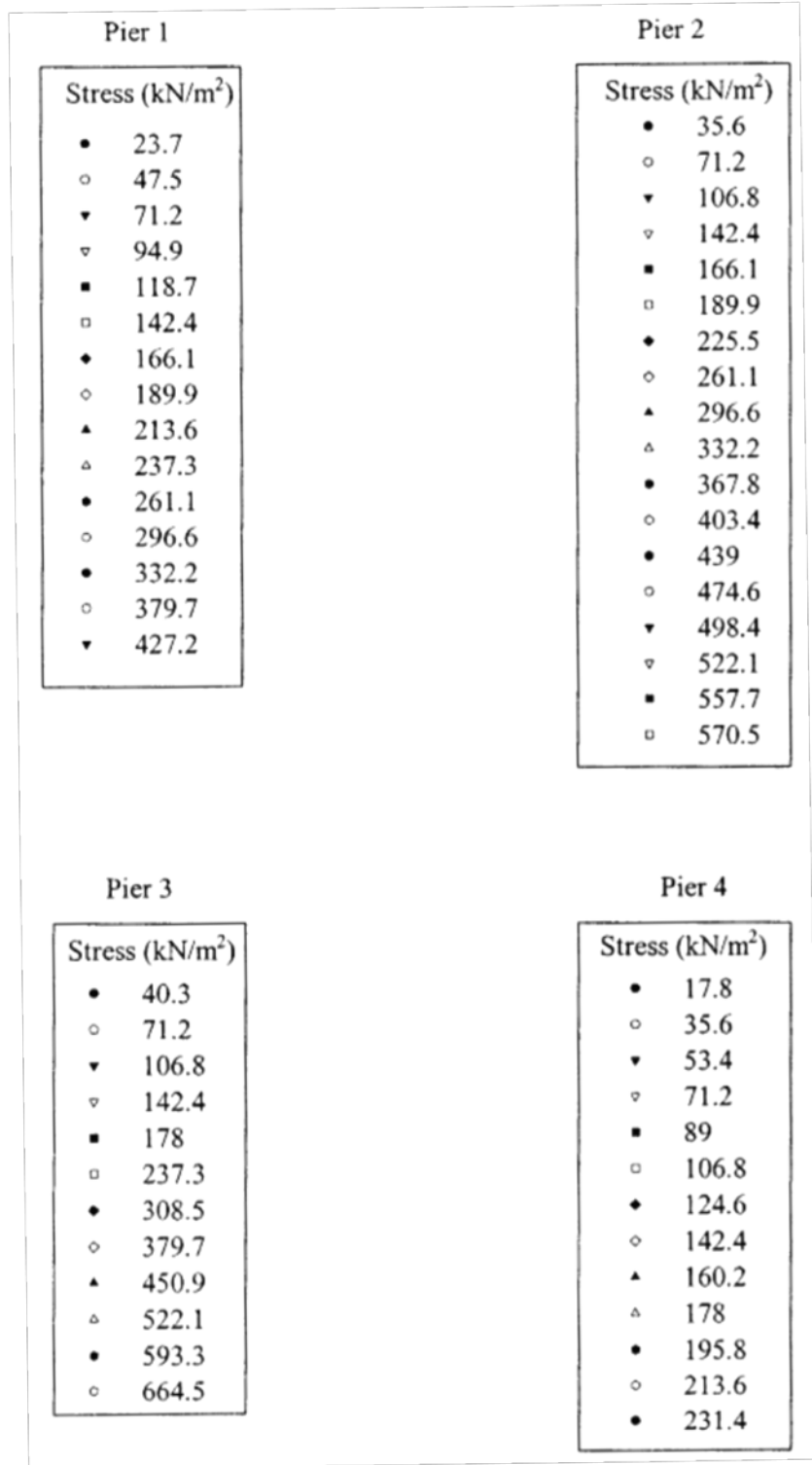
The actual measured lateral pressures at zero load were provided in appendix C of Mitchell's report and are shown in table 6. Unfortunately, they are mostly negative, with a few exceptions. When and how the zero readings were obtained could not be discerned from Mitchell's report.



Source: J.W. Mitchell

- 1 kPa = 20.89 psf
- 1 m = 3.28 ft
- 1 cm = 0.39 inches

Figure 33. Chart. Measured increase in lateral pressures on the facing of GRS mini-piers during load test in kPa.⁽⁷⁷⁾



Source: J.W. Mitchell

1 kN/m² = 20.9 lbs/ft²

Figure 34. Charts. Measured increase in lateral pressures on the facing of GRS mini-piers during load test in kN/m².⁽⁷⁷⁾

Yogarajah and Saad experimentally measured the lateral earth pressures on incremental panel walls backfilled with reinforced Leighton Buzzard sand.⁽⁷⁸⁾ The dry unit weight of the compacted sand was 104 pcf (16.4 kN/m³) corresponding to a relative density of 82 percent (peak and constant volume friction angles of 47 degrees and 34 degrees, respectively). The test walls were 5.9 ft (1.8 m) high and reinforced with three layers of 2.1-ft (0.63-m)-spaced Tensar® SR80 geogrid. Two wall configurations were used with the aid of three 4.5 in-(0.114-m)-thick wall panels. Known as single and multisegment, these two configurations include two wall panels that were 1.8 ft (0.55 m) wide and 5.9 ft (1.8 m) long. The third was 2.3 ft (0.7 m) wide and 5.9 ft (1.8 m) long. The reinforcement was attached to the facing panels through elongated holes to accommodate any vertical movement of the reinforcements during construction.

Each wall panel for the single configuration was propped vertical into position with struts at the 1 ft (0.3 m), 3.3 ft (1.0 m), and 5.3 ft (1.6 m) heights from the base. The struts were removed after construction. With the multisegment configuration, struts were used at five locations on each panel (four near the corners and one at the center) and removed once the backfill height reached the top of the panel. Hence, no more than one panel was propped at any one time during construction of the multisegment wall.

Lateral pressures were measured using six load cells placed flush with the facing. No surcharge loading was applied after strut removal. Consistent with Yang's observations on a reinforced soil wall, the lateral pressures on Yogarajah and Saad's geosynthetic reinforced wall appear to be fairly constant with depth below the top 2 ft (0.6 m).^(64,78) Also below the top 2 ft (0.6 m), the lateral pressures were significantly smaller than the predicted Rankine active values.

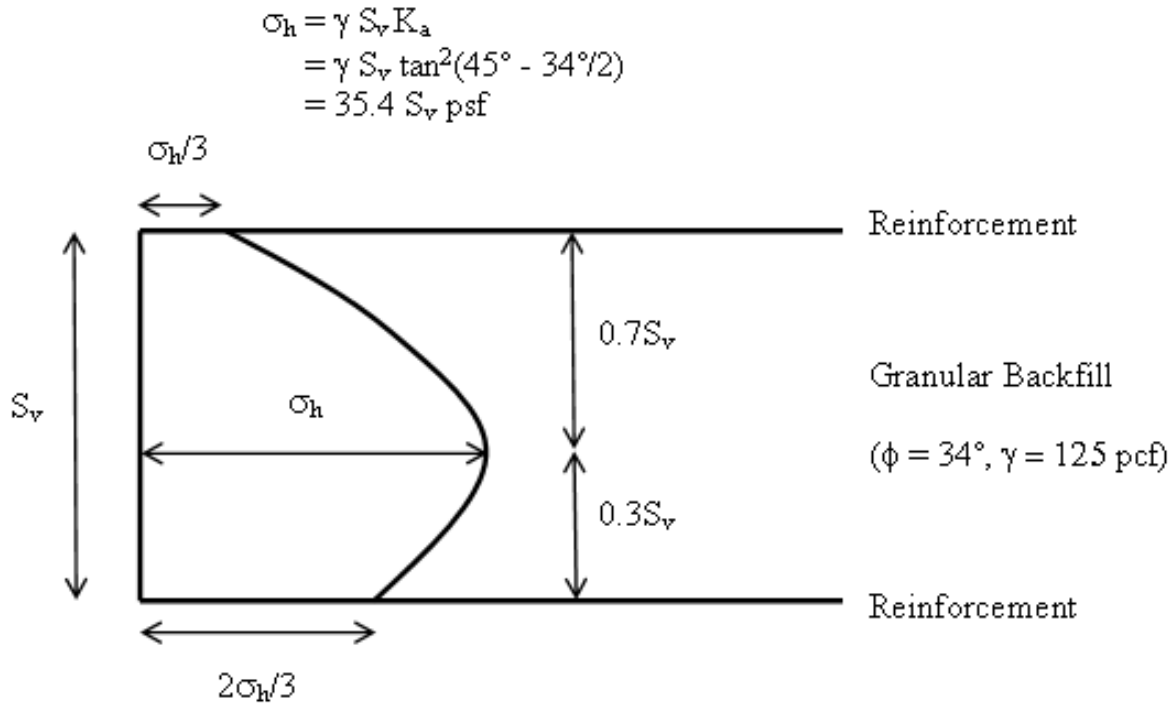
METHODS FOR ESTIMATING LATERAL EARTH PRESSURES ON GRS WALL FACING

Two methods involving the use of simple equations to estimate the lateral thrust on GRS wall facing are presented. They include the procedures developed by Wu, and Soong and Koerner.^(25,79) Ehrlich and Mitchell developed charts that are quite elegant for estimating the maximum tension in a reinforced soil.⁽⁸⁰⁾ This study is not presented further herein for four reasons. First, although the tension in the reinforcement can be related to the lateral stress, this lateral stress represents the value within a GRS mass rather than on the wall facing. Second, the study assumes that each reinforcement layer is responsible for equilibrium with the lateral stress, meaning the tensile strength divided by the vertical spacing is equal to the average lateral earth pressure within the tributary area of the reinforcement, which is not true for closely spaced GRS. Third, this method will predict a lateral pressure that increases with depth. Finally, the compaction equipment must be known a priori.

Wu's Procedure (2001)

For closely spaced systems, Wu indicated that the primary function of the facing is to prevent soil sloughing.⁽²⁵⁾ It also serves as a construction aid but is not a major load carrying element. Wu further postulated based on evidence from numerous case studies that the lateral thrust against the facing is independent of the wall height.⁽⁸¹⁾ Because the reinforcement effectively restrains lateral deformation of the soil, the lateral pressure on the facing is quite small in comparison to the lateral stress predicted from Rankine earth pressure theory. Its magnitude

depends on the reinforcement spacing, the soil shear strength parameters, and the rigidity of the facing. Calling the magnitude “bin pressure,” Wu proposed that the bin pressure diagram is near zero at the reinforcement elevation. It increases with depth below the reinforcement before decreasing to near zero at the reinforcement layer below (i.e., at the base of the facing). However, because the reinforcement may deform slightly and there may be imperfect bonding between the soil and reinforcement at the wall face, Wu proposed the bin pressure diagram as shown in figure 35.



©J.T.H. Wu

1 pcf = 16.02 kg/m³

1 psf = 0.05 kPa

Figure 35. Diagram. Bin pressure diagram.⁽²⁵⁾

The total lateral thrust (F_{bin}) can be calculated as the area under the bin pressure diagram as shown in the equations in figure 36 or figure 37⁽²⁵⁾:

$$F_{bin} = 0.72 S_v \sigma_h$$

Figure 36. Equation. Total lateral thrust, F subscript bin, as a function of the spacing between reinforcements, S subscript v , and peak bin pressure σ subscript h .

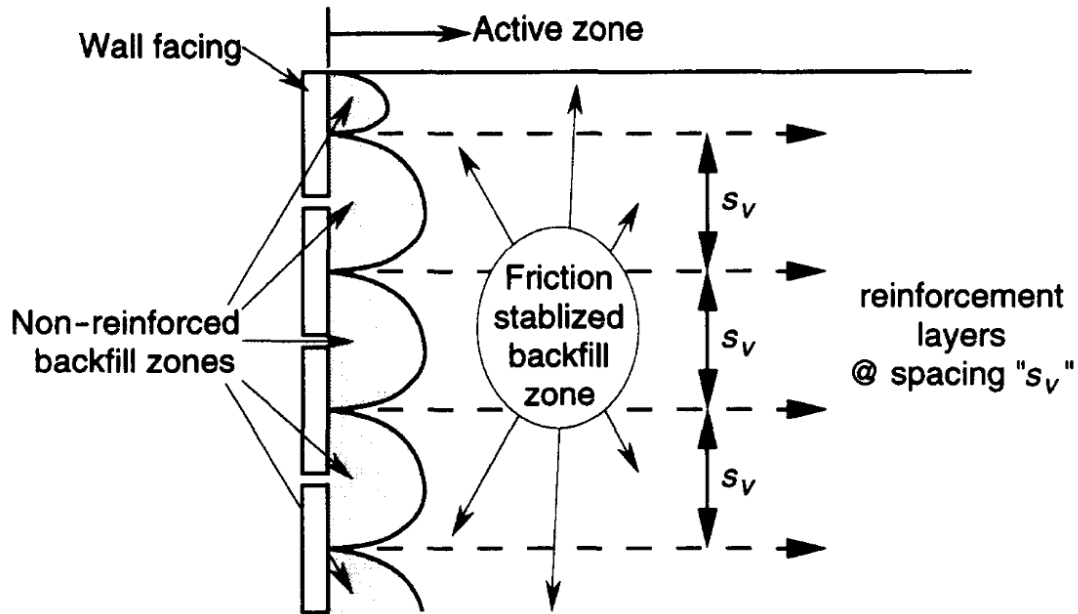
or

$$F_{bin} = 0.72 \gamma K_a S_v^2$$

Figure 37. Equation. Total lateral thrust, F subscript bin, in terms of the coefficient of active earth pressure.

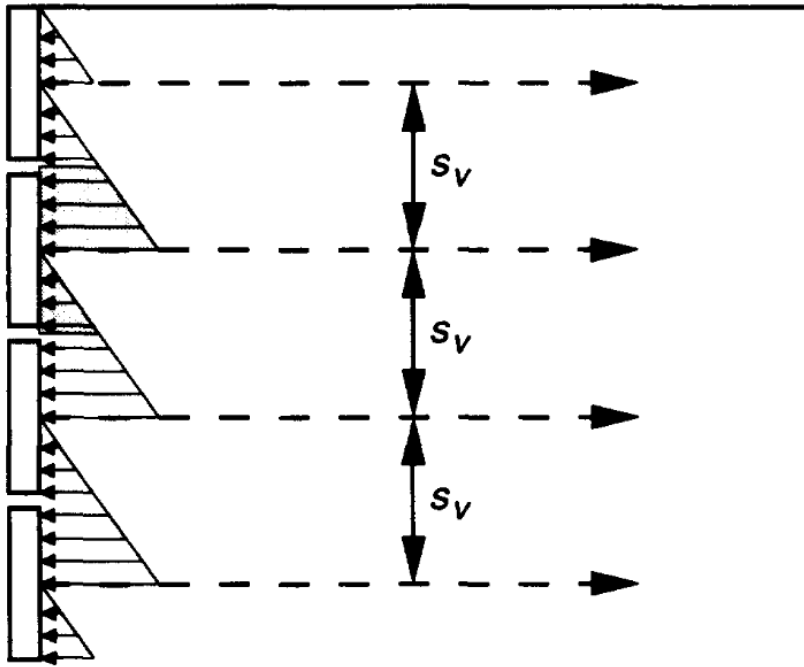
Soong and Koerner's Procedure (1997)

A similar concept was proposed by Soong and Koerner for GMSE walls where the reinforcement is connected to the middle of the back face of the wall facing as shown in figure 38.⁽⁷⁹⁾ While the reinforcements stabilize most of the soil mass through interface friction, Soong and Koerner postulated that there is a small zone of soil bearing against the wall facing that is not restrained by the reinforcement mobilized friction. Assuming that each layer acts independently from those above and below, they proposed a lateral earth pressure distribution as shown in figure 39.



Source: Elsevier Ltd.

Figure 38. Drawing. GMSE wall configuration showing nonreinforced backfill zones.⁽⁷⁹⁾



Source: Elsevier Ltd.

Figure 39. Drawing. Lateral earth pressure distribution against wall facing exerted by the nonreinforced backfill.⁽⁷⁹⁾

Soong and Koerner estimated the magnitude of the connection force using the equation in figure 40:

$$F = 0.5\gamma K_a S_v^2$$

Figure 40. Equation. Connection force F.

This equation produces a thrust that is 31-percent smaller than the equation in figure 37.

Table 5 shows the lateral thrust on the facing as a function of reinforcement spacing for both Wu's and Soong and Koerner's methods for a soil with $\gamma = 125$ pcf ($2,002 \text{ kg/m}^3$), $\phi = 34$ degrees and $c = 0$.

Table 5. Comparison of Wu’s versus Soong and Koerner’s calculated lateral thrusts as a function of reinforcement spacing.^(25,79)

Reinforcement Spacing, S_v (inches)	Lateral Thrust (lb/ft)	
	Wu ⁽²⁵⁾	Soong and Koerner ⁽⁷⁹⁾
4	2.83	1.96
8	11.3	7.85
12	25.4	17.7
16	45.2	31.4
24	102	70.7
36	229	159

Note: Assumes a backfill with $\gamma = 125$ pcf (2,002 kg/m³), $\phi = 34$ degrees and $c = 0$.

1 inch = 2.54 cm

1 lb/ft = 14.6 N/m

COMPARISON OF PREDICTED AND MEASURED LATERAL PRESSURES

When an earth pressure cell is placed at the mid-point between two reinforcement layers on the wall facing, the measured pressures should coincide with the pressure at the middle of the pressure distribution diagrams.⁽⁸²⁾ It is estimated that the pressures mid-way between reinforcements are about $0.8\sigma_h$ and $0.5\sigma_h$ for Wu’s bin pressure and Soong and Koerner’s triangular pressure distributions, respectively.^(25,79) A comparison of the calculated and measured lateral pressures is provided in table 6 for the case histories described previously and assuming no surcharge loading. The following should be noted:

- The measured lateral pressures from Abu-Hejleh include the effects of loading from the bridge superstructure.⁽⁷⁶⁾ Based on elastic theory (footing width = 12.5 ft (3.8 m) and setback = 4.43 ft (1.35 m), it is estimated that the increase in lateral pressures are 13 percent, 21 percent, 25 percent, and 21 percent of the applied footing stress for the 12th, 11th, 9th, and 7th geogrid layers, respectively, from the bottom. The applied stress on the Founders/Meadow bridge abutment footing was not reported by Abu-Hejleh to facilitate a proper comparison.
- Only Mitchell’s lateral pressures obtained at the end of construction and prior to load testing (i.e., zero surcharge load) are shown in table 6.⁽⁷⁷⁾ Mitchell’s measured lateral pressures at zero load were mostly negative. When and how the zero readings were obtained could not be discerned from the report.
- The earth pressure cells for the Yogarajah and Andrawes study were not mid-way between reinforcements.⁽⁸²⁾ However, the pressure distribution does appear constant with depth below the top 2 ft (0.6 m). The single segment wall is less representative of a GRS type wall with modular block facing elements than the multisegment wall. Nevertheless, the comparison between predicted and measured values agrees best in this study.

Table 6. Predicted versus measured lateral pressures on reinforced soil wall facing.

Reference	γ (pcf)	ϕ (degrees)	S_v (ft)	$0.8\sigma_h$ (psf)	$0.5\sigma_h$ (psf)	Measured (psf)
Abu-Hejleh et al. (2003)—12th geogrid	141	39	1.33	34	21	31 ^a
Abu-Hejleh et al. (2003)—11th geogrid North	141	39	1.33	34	21	177 ^a
Abu-Hejleh et al. (2003)—11th geogrid South	141	39	1.33	34	21	163 ^a
Abu-Hejleh et al. (2003)—9th geogrid	141	39	1.33	34	21	188 ^a
Abu-Hejleh et al. (2003)—7th geogrid	141	39	1.33	34	21	334 ^a
Mitchell (2002)—Pier 1—1 ft above base	120	36	24	50	31	-121 ^b
Mitchell (2002)—Pier 1—4.3 ft above base	120	36	24	50	31	-402 ^b
Mitchell (2002)—Pier 1—7 ft above base	120	36	24	50	31	-228 ^b
Mitchell (2002)—Pier 1—9.7 ft above base	120	36	24	50	31	-96 ^b
Mitchell (2002)—Pier 1—13 ft above base	120	36	24	50	31	-152 ^b
Mitchell (2002)—Pier 2—1 ft above base	124	36	16	34	21	-127 ^b
Mitchell (2002)—Pier 2—4.3 ft above base	124	36	16	34	21	-51 ^b
Mitchell (2002)—Pier 2—7 ft above base	124	36	16	34	21	-89 ^b
Mitchell (2002)—Pier 2—9.7 ft above base	124	36	16	34	21	-4 ^b
Mitchell (2002)—Pier 2—13 ft above base	124	36	16	34	21	60
Mitchell (2002)—Pier 3—1 ft above base	121	36	8	17	10	541
Mitchell (2002)—Pier 3—4.3 ft above base	121	36	8	17	10	33
Mitchell (2002)—Pier 3—7 ft above base	121	36	8	17	10	343
Mitchell (2002)—Pier 3—9.7 ft above base	121	36	8	17	10	113
Mitchell (2002)—Pier 3—13 ft above base	121	36	8	17	10	-25 ^b
Mitchell (2002)—Pier 4—1 ft above base	122	36	32	67	42	-99 ^b
Mitchell (2002)—Pier 4—4.3 ft above base	122	36	32	67	42	-222 ^b
Mitchell (2002)—Pier 4—7 ft above base	122	36	32	67	42	-19 ^b
Mitchell (2002)—Pier 4—9.7 ft above base	122	36	32	67	42	-653 ^b
Mitchell (2002)—Pier 4—13 ft above base	122	36	32	67	42	-125 ^b
Yogarajah and Andrawes (1994)—single seg.	104	47	2.07	27	17	13
Yogarajah and Andrawes (1994)—multi-seg.	104	47	2.07	27	17	38

^a Measured lateral pressures from Abu-Hejleh include the effects of loading from the bridge superstructure.⁽⁷⁶⁾ Lateral pressures before construction of the superstructure were not reported.

^b Mitchell's measured lateral pressures at zero load were mostly negative.⁽⁷⁷⁾ When and how the zero readings were obtained could not be discerned from the report.

1 pcf = 16.02 kg/m³

1 ft = 0.3 m

1 psf = 0.048 kPa

FIELD CRITIQUE OF RANKINE ACTIVE THRUST THEORY

Wu's and Soong and Koerner's calculated lateral thrusts are much smaller than the Rankine active thrust because they are a function of the reinforcement spacing and not the wall height.^(25,79) If it were true that the bin pressure were not a function of wall height, GRS walls can be safely constructed to very tall heights if desired (e.g., figure 41). If the Grand County wall in Colorado illustrated in figure 41 were an externally stabilized wall designed using strictly Rankine active earth pressure theory, as in GMSE design, it would have required an enormous footing embedment and connection requirement to resist the assumed loads, which is not the case in this GRS wall.^(2,81) This wall offers the most compelling field evidence that the lateral pressure exerted on the GRS facing is much smaller than that derived from classical earth pressure theory.



Source: R. Barrett

Figure 41. Photo. Grand County, Colorado, wall with a maximum height of 55 ft (16.8 m).⁽⁸³⁾

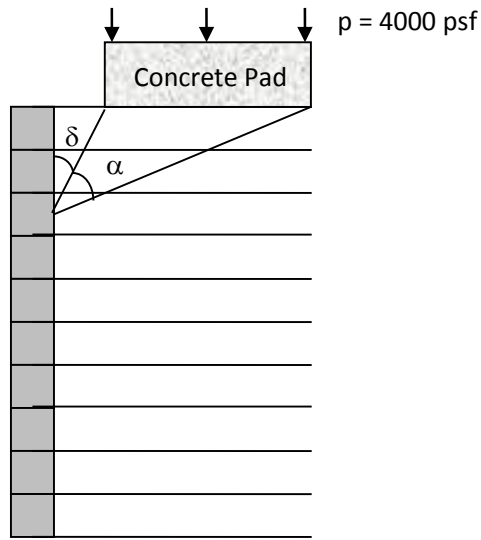
LATERAL PRESSURES DUE TO APPLIED LOADS

The lateral pressures on the facing of a GRS wall due to applied loading behind the facing (e.g., bridge footing on a GRS abutment) will increase with increasing footing load as seen in Mitchell's study.⁽⁷⁷⁾ Using linear elastic theory, the increase in lateral pressure can be approximated using Carother's equation in figure 42.⁽⁸⁴⁾ Assuming an allowable maximum applied bearing stress on a GRS abutment of $p = 4,000$ psf (191.5 kPa), the increase in lateral pressure ($\Delta\sigma_h$) on the CMU blocks can be calculated as shown in figure 42:

$$\Delta\sigma_h = p/\pi [\alpha - \sin \alpha \cos(\alpha + 2\delta)]$$

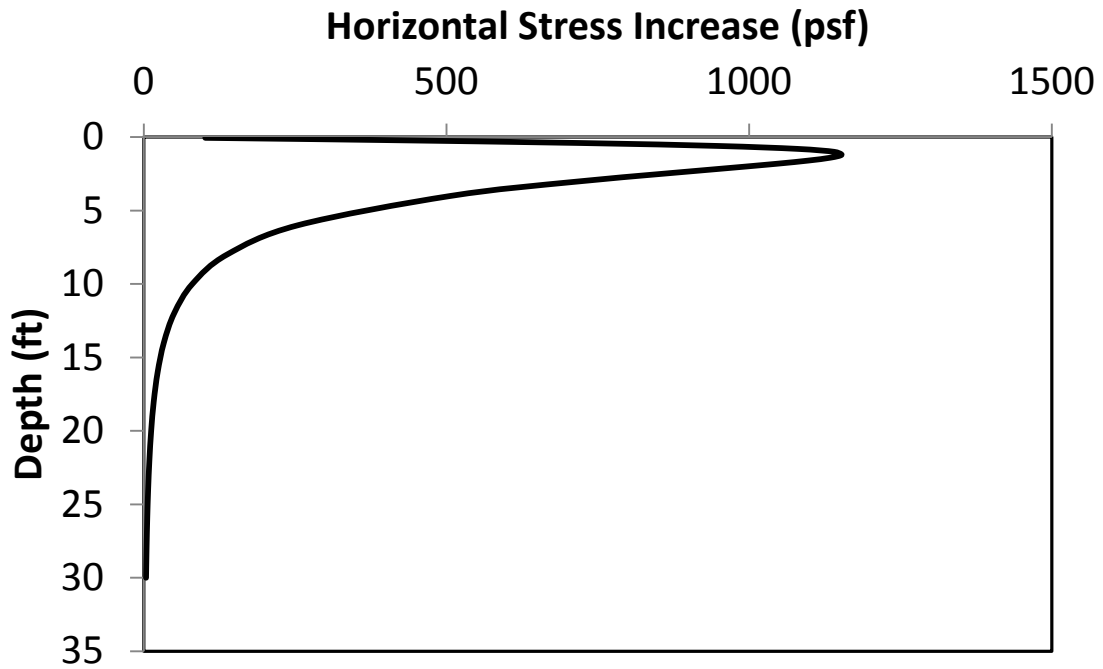
Figure 42. Equation. Increase in lateral pressure $\Delta\sigma$ subscript h.

Where α and δ are angles defined as shown in figure 43. Assuming a 4-ft- (1.2-m-) wide footing with a 1-ft (.3-m) setback, the increase in lateral pressures on the CMU blocks are highest within the top 3 ft (1 m) from the facing as shown in figure 44. The maximum lateral stress was only 1,150 psf (55.1 kPa), which is 29 percent of the applied load.



1 psf = 0.048 kPa

Figure 43. Drawing. Definition of angles α and δ .



1 ft = 0.3 m
1 psf = 0.048 kPa

Figure 44. Chart. Increase in lateral stress due to 4,000-psf (191.5-kPa) vertical stress on a 4-ft- (1.2-m-) wide footing with a 1-ft (.3-m) setback.

Figure 42 and figure 44 assume a flexible wall that is free to displace laterally. If the wall were rigid (i.e., unable to displace laterally), then the pressures in figure 42 and figure 44 should be doubled.

SUMMARY

- Lateral stresses in a reinforced soil are higher than those in the same soil unreinforced.
- Just below a critical depth, measured lateral stresses in a reinforced soil or on the facing of a reinforced soil wall appear to be constant with depth. However, it should be cautioned that this observation is based on very limited reliable data.
- Wu and Soong and Koerner postulated theories that estimate the lateral pressure on the face of reinforced soil walls.^(25,79) Their magnitudes depend on the reinforcement spacing, the soil shear strength parameters, and the soil unit weight only. A constant reinforcement spacing will lead to a constant lateral pressure distribution with depth.
- Lateral stresses on the GRS facing will increase if the GRS is loaded vertically, as in the case of a bridge footing on a GRS abutment, even with a frictionally connected facing as seen in Mitchell's experiments.⁽⁷⁷⁾ For the example above, assuming linear elastic theory applies, the lateral pressure was not more than 30 percent of the applied vertical stress.

CHAPTER 6. W EQUATION

The W equation is used to estimate the vertical capacity of footings on a GRS wall and was first published by Pham in his Ph.D. thesis entitled *Investigating Composite Behavior of Geosynthetic Reinforced Soil (GRS) Mass.*⁽⁸⁵⁾ In this equation, the W term accounts for the fact that an increase in the reinforcement strength does not have the same effect as a proportional decrease in the reinforcement spacing, as has been traditionally assumed in simplified GMSE design. This is a significant difference between GMSE and GRS design. Results of mini-pier experiments performed by Adams, Adams et al., and Elton and Patawaran, and plane strain tests on GRS performed by Pham, showed that the contributions of the reinforcement spacing to the strength of the GRS is much greater than that of the reinforcement strength. (See references 86, 6, 87 through 91, and 85.) The various terms in the W equation and previous research and theory leading to its development are discussed. The reliability of this equation is demonstrated based on load test results from the literature.

W EQUATION

In reality, the capacity of a GRS is related to the effects of confinement (due to CISs and the lateral restraint offered by the reinforcement internally, and confining stress at the facing), reinforcement spacing, strength and stiffness, shape and location of the failure surface, stress-strain behavior of the soil, and degree of mobilization of shear resistance along an assumed failure plane. The W equation was derived using limit equilibrium analysis. This type of analysis assumes a linear failure surface, assumes a rigid-plastic soil behavior, neglects soil-reinforcement stiffness, and assumes full mobilization of shear strength along the failure surface. Despite the many assumptions that may not reflect reality, limit equilibrium analysis is popular among practitioners because it provides a solution that is simple and easy to use.

The W equation can be derived by first considering the Mohr-Coulomb failure envelope and the Mohr circle at failure for an unreinforced cohesionless soil (figure 45).

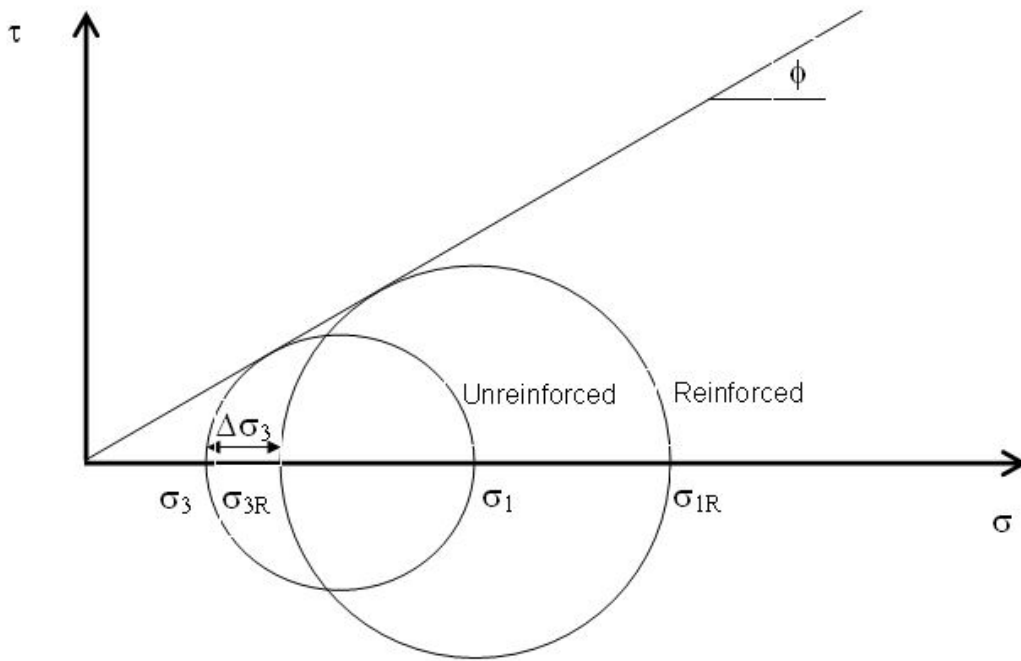


Figure 45. Drawing. Mohr circles for unreinforced and reinforced soil.

If the soil friction angle is ϕ , the equation in figure 46 shows that at failure:

$$\sigma_1 = \sigma_3 \frac{1 + \sin \phi}{1 - \sin \phi} = \sigma_3 K_p$$

Figure 46. Equation. Major principal stress σ subscript 1.

σ_1 and σ_3 are the major and minor principal stresses respectively, and K_p equals the Rankine passive earth pressure coefficient. If the soil were reinforced, Yang indicated that the friction angle of the reinforced soil is approximately the same as the unreinforced soil if no slippage occurs between the soil and reinforcement.⁽⁶⁴⁾ A GRS is stronger than the unreinforced soil, and hence the major principal stress at failure is higher than σ_1 , say σ_{1R} in figure 45.

For this to occur, the confining stress in the soil must effectively increase due to the presence of the reinforcement as shown in the equation in figure 47:

$$\sigma_{3R} = \sigma_3 + \Delta\sigma_3$$

Figure 47. Equation. Confining stress due presence of reinforcement σ subscript 3R.

The reinforcement restrains lateral movement of the soil. Thus, $\Delta\sigma_3$ represents the additional confining stress that is imposed due to the reinforcement. Therefore, the capacity of the GRS can be expressed as the equation in figure 48:

$$\sigma_{1R} = \sigma_{3R} K_p = (\sigma_3 + \Delta\sigma_3) K_p$$

Figure 48. Equation. Capacity of the GRS σ subscript 1R.

$\Delta\sigma_3$ is analogous to a prestress in the reinforced soil equal to the frictional force developed between the soil and the reinforcement with a maximum value determined by the tensile strength of the reinforcing material. At failure, this prestress will be at its maximum and is related to the reinforcement tensile strength per unit wall length (T_f). If it is assumed that one-dimensional expansion in the horizontal direction occurs over a tributary area of reinforcement equal to spacing S_v per unit wall length, then $\Delta\sigma_3$ can be expressed as shown in figure 49:⁽⁹²⁾

$$\Delta\sigma_3 = \frac{T_f}{S_v}$$

Figure 49. Equation. Additional confining stress as function of reinforcement tensile strength divided by the reinforcement spacing $\Delta\sigma$ subscript 3.

Implied in the equation in figure 49 is that a GRS with reinforcement strength T_f at spacing S_v will have the same capacity as a GRS with reinforcement strength $2T_f$ at spacing $2S_v$, which has been shown to be untrue by Adams, Adams et al., Elton and Patawaran, Ziegler et al., and Pham. (See References 86, 6, 87 through 91, 93, and 85.) Instead, S_v has a bigger influence on the capacity than T_f . This led Pham to propose a modified version of the equation in figure 49 as shown in figure 50:

$$\Delta\sigma_3 = W \frac{T_f}{S_v}$$

Figure 50. Equation. Modified version of the equation in figure 49 for additional confining stress, $\Delta\sigma$ subscript 3 imposed with the W factor.

W is the factor that amplifies the contribution of S_v to the GRS capacity. The W factor was semi-empirically derived and is calculated using the equation in figure 51:

$$W = 0.7 \frac{S_v}{6D_{\max}}$$

Figure 51. Equation. W factor.

D_{\max} is the maximum particle size of the GRS backfill used as a normalizing parameter to make the exponent dimensionless. Note that the 0.7 factor in figure 51 was theoretically derived while the exponent was empirically derived. Using the concept of “average stresses” proposed by Ketchart and Wu to estimate the average and maximum forces in a reinforcement, Pham showed, based on a load-transfer analysis, that the average reinforcement force is about 70 percent of the maximum reinforcement tensile strength; hence the 0.7 factor in figure 51.^(62,85) For details on this derivation, refer to Pham.⁽⁸⁵⁾

The exponent of figure 51 is a function of S_v and D_{\max} . Because the base term is less than unity, W , and hence the capacity, increases with decreasing S_v and increasing D_{\max} . This is logical

because one would expect a GRS with closer reinforcement spacing and larger maximum aggregate size to have a higher capacity.

Therefore, combining the equations in figure 48, figure 50, and figure 51, the capacity of the GRS can be expressed as the equation in figure 52:

$$\sigma_{1R} = \left(\sigma_3 + 0.7 \frac{S_v}{6D_{\max}} \frac{T_f}{S_v} \right) K_p$$

Figure 52. Equation. Capacity of the GRS, σ subscript 1R.

If the soil has cohesion, c , then the equation in figure 52 can be expanded to the equation in figure 53:

$$\sigma_{1R} = \left(\sigma_3 + 0.7 \frac{S_v}{6D_{\max}} \frac{T_f}{S_v} \right) K_p + 2c\sqrt{K_p}$$

Figure 53. Equation. Expansion of the equation in figure 52 for the capacity of the GRS, σ subscript 1R, to include cohesion.

According to Pham, for a GRS wall with a dry stacked modular block facing, σ_3 equals the lateral stress exerted by the facing on the GRS mass, which is γ_{bl} times D times $\tan\delta$.⁽⁸⁵⁾ γ_{bl} equals the bulk unit weight of the facing block, which is the weight of block/volume of the block assuming it is not hollow. (For a 7.625- by 7.625- by 15.625-inch (19.368- by 19.368- by 39.688-cm) CMU block weighing 42 lbs (19.1 kg), γ_{bl} equals 80 pcf). D equals the depth of the facing block perpendicular to the wall face. δ equals the friction angle between geosynthetic reinforcement and the top or bottom surface of the facing block. The equation in figure 53 can also be rearranged and solved for the required reinforcement strength ($T_{f,req}$) given the loads on the particular GRS composite for design.

RELIABILITY OF THE W EQUATION

A database consisting of 19 load tests on GRS from the literature (table 7) was used to examine the reliability of the W equation or the equation in figure 52. In addition to the references already cited in this synopsis, the table contains tests from Adams et al.⁽⁶⁾ A plot of predicted versus measured capacities is shown in figure 54. It can be seen that overall, the coefficient of determination was 0.853 with a slope of 0.913 for this dataset when the regression line was forced through the origin. To illustrate the importance of the W term, a plot of predicted versus measured capacities is shown in figure 55 with the W term eliminated from the equation in figure 53. It is apparent that the capacities are severely overpredicted with a less than desirable fit. This validates the necessity of the W term in the equation in figure 53.

Table 7. Prediction data for large-scale tests.

No.	Test	Test Results		Facing		Reinforcement		Aggregate					Geometry	Reference
		$q_{ult,emp}$ (kPa)	$q_{ult,calc}$ (kPa)	σ_c (kPa)	Block Type	S_v (m)	T_f (kN/m)	D_{max} (m)	c (kPa)	Φ_{test} (degrees)	Φ Method	K_p		
1	GSGC 2	3,400	2,182	34	N/A	0.2	70	0.0330	70	50	TX	7.55	PS	85 (Pham (2009))
2	GSGC 3	2,040	1,615	34	N/A	0.4	140	0.0330	70	50	TX	7.55	PS	
3	GSGC 4	1,785	936	34	N/A	0.4	70	0.0330	70	50	TX	7.55	PS	
4	GSGC 5	2,034	1,925	0	None	0.2	70	0.0330	70	50	TX	7.55	PS	
5	Elton 1	230	133	0	None	0.15	9	0.0127	28	40	DS	4.60	Cylindrical	91 (Elton and Patawaran (2005))
6	Elton 2	129	33	0	None	0.3	9	0.0127	28	40	DS	4.60	Cylindrical	
7	Elton 3	306	207	0	None	0.2	14	0.0127	28	40	DS	4.60	Cylindrical	
8	Elton 4	292	222	0	None	0.2	15	0.0127	28	40	DS	4.60	Cylindrical	
9	Elton 5	402		0	None	0.2	19	0.0127	28	40	DS	4.60	Cylindrical	
10	Elton 6	397	296	0	None	0.2	20	0.0127	28	40	DS	4.60	Cylindrical	
11	Elton 7	459	370	0	None	0.2	25	0.0127	28	40	DS	4.60	Cylindrical	
12	NCHRP 1	420	275	0.97	CMU	0.2	21	0.0254	0	36.5	LSDS	3.94	PS	94 (Wu et al. (2006))
13	NCHRP 2	850	908	0.97	CMU	0.2	70	0.0254	0	36.5	LSDS	3.94	PS	
14	Defiance 1	542	580	0.97	CMU	0.2	35	0.0127	0	50.7	LSDS	7.84	Column	89 (Adams et al. (2007))
15	Defiance 2	1,213	1,153	0.97	CMU	0.2	70	0.0127	0	50.7	LSDS	7.84	Column	
16	Vegas	1,008	1,231	2.35	SRW	0.2	35	0.0254	70	50	TX	7.55	Column	88 (Adams et al. (2002))
17	MP A	225	284	0	None	0.6	70	0.0254	0	53.5	LSDS	9.20	Column	89 (Adams et al. (2007))
18	MP B	170	671	0	None	0.4	70	0.0254	0	53.5	LSDS	9.20	Column	
19	MP C	460	634	0	None	0.2	21	0.0254	0	53.5	LSDS	9.20	Column	

GSGC =Generic Geosynthetic Soil Composite

NCHRP = National Cooperative Highway Research Program

MP = Mini-Pier

TX = Triaxial

DS = Direct Shear

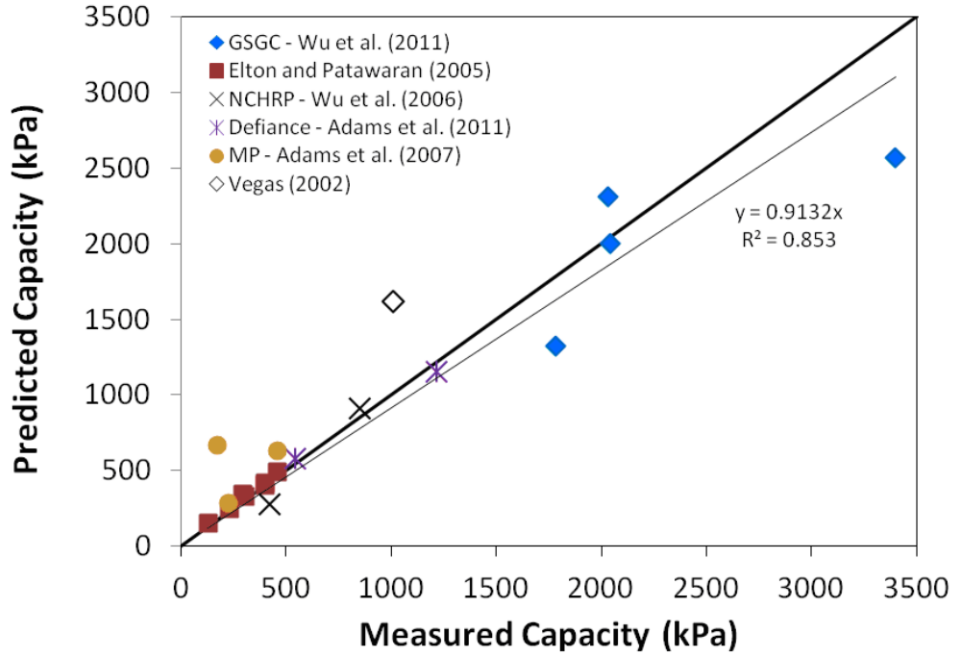
LSDS = Large-Scale Direct Shear

PS = Plane Strain

1 kPa = 20.89 psf

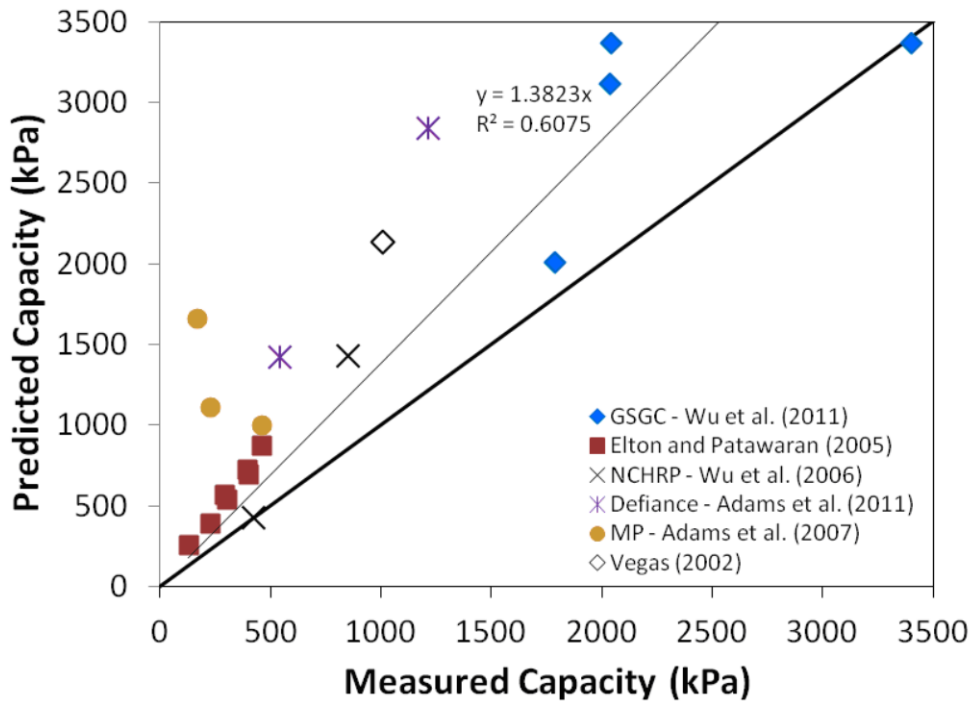
1 m = 3.28 ft

1 kN/m = 68.6 lb/ft



1 kPA = 20.89 psf

Figure 54. Graph. Predicted versus measured capacity of large-scale GRS tests using the equation in figure 52.



1 kPA = 20.89 psf

Figure 55. Graph. Predicted versus measured capacity of large-scale GRS tests using the equation in figure 52 without the W term.

CHAPTER 7. REDUCTION FACTORS

Current design methods for GRS walls and abutments (e.g., AASHTO guideline, FHWA NHI manual, and NCMA manual) typically stipulate that design strength of geosynthetic reinforcement should be determined by applying reduction factors for installation damage, creep, and durability to the ultimate strength of geosynthetic reinforcement.^(1,2,3) The equation in figure 56 expresses the allowable reinforcement design strength, T_a :

$$T_a = \frac{T_{ult}}{FS \times RF} = \frac{T_{ult}}{FS \times RF_{ID} \times RF_{CR} \times RF_D} = K \times T_{ult}$$

Figure 56. Equation. Allowable reinforcement design strength, T subscript a .

T_{ult} is the ultimate wide-width strip tensile strength of the geosynthetic (in accordance with ASTM D4595) based on the minimum average roll value (MARV) for the product. (MARV is commonly defined as the strength that is two standard deviations below the mean tensile strength). FS is an overall safety factor to account for uncertainty. RF is a combined factor to account for geosynthetic strength loss during the wall design life and is equal to RF_{ID} times RF_{CR} times RF_D , where RF_{ID} is a reduction factor for installation damage, RF_{CR} is a reduction factor for creep, and RF_D is a reduction factor for chemical and biological degradation.

In the FHWA NHI manual, $RF_{ID} = 1.1$ to 3.0 , $RF_{CR} = 1.6$ to 5.0 , and $RF_D = 1.1$ to 2.0 are recommended, resulting in $K = 3$ to 50 percent.⁽²⁾ Different state transportation departments have adopted some variations for the reduction factors and safety factor, hence the K -value range. CDOT, for example, has adopted the following values: the allowable design strength is on the order of 10 to 24 percent of MARV for preapproved products and 5 percent of MARV for not preapproved products. This type of practice has practically excluded the use of all geotextiles in reinforced soil wall applications, even though many GRS walls and abutments constructed with geotextiles as reinforcement have performed successfully.

This synopsis addresses the issue of geosynthetic reinforcement reduction factors. The available research on the use of cumulative reduction factors is reviewed, and current practices are discussed. In addition, brief comments about the K -stiffness method, a working stress design method intended to address long-term behavior of geosynthetic reinforcement of reinforced soil walls, are provided.

RESEARCH AND CASE HISTORIES

Degradation

Aging of buried geosynthetics by processes such as hydrolysis, oxidation, and abrasion may result in long-term strength loss of geosynthetic reinforcement. Elias evaluated 24 geosynthetics from 12 retrieval sites, and confirmed that little, if any, chemical degradation had occurred in the geosynthetic reinforcement in those full-scale structures, some of which were up to 25 years old.^(95,96) This has been further confirmed by Allen and Bathurst.⁽⁹⁷⁾ They indicated that the greatest contributors to strength loss and reduced wall performance (i.e., increased deformation)

for the geosynthetic reinforcement products in use today are installation damage and possibly creep.

Installation Damage

Numerous field studies regarding the installation survivability of geosynthetics have been performed. They have shown that the level of installation damage depends on polymer type, manufacturing method, and geosynthetic coating.^(96,98) The level of damage has also been shown to be affected by the weight, type, and number of passes of the construction and compaction equipment, the graduation, angularity, and condition of the fill material and the lift thickness. (See references 99 through 102.)

Allen and Bathurst show that installation damage has limited impact on the initial working stress performance of geosynthetic walls.⁽¹⁰³⁾ For most geosynthetics used as reinforcement (i.e., woven geotextiles and geogrids), their load-strain-time behavior is not significantly affected by installation damage at typical or even relatively high working strains for the levels of installation damage observed in full-scale walls. The data provided by Allen and Bathurst indicate that installation damage does not severely affect modulus, if at all, until damage levels become quite high for woven geotextiles and geogrids.⁽¹⁰³⁾

Bathurst et al. describe how to compute bias statistics from project-specific installation damage trials for use in reliability-based design for the reinforcement rupture limit state, or by using data from multiple sources for LRFD calibration.⁽¹⁰⁴⁾ A database of results from field installation damage trials on 103 different geosynthetic products was collected from 20 different sources. The computed reduction factors for installation damage (RF_{ID}) of their study confirm earlier recommendations by Elias that woven and nonwoven geotextiles with mass per unit area less than 7.96 oz/yd² (270 g/m²) should not be used in combination with Type 1 soil (with $D_{50} > 19$ mm (.74 inches)).⁽⁹⁵⁾ For a certain soil type, there were detectable differences in the calculated RF_{ID} values depending on the geosynthetic type.

Hufenus et al. conducted a series of field installation tests and concluded that, in applications where only the tensile strength at relatively low elongations is relevant, the effects of moderate installation damage is very limited, and the factor RF_{ID} can be designated as very close to unity (1.0 to 1.1) based on product-specific test data.⁽¹⁰⁵⁾

Allen and Bathurst investigated the combined effect of polymeric creep and installation damage using a database of constant sustained load (creep) data for both undamaged and installation damaged geosynthetic specimens.⁽¹⁰⁶⁾ They concluded that multiplication of creep reduction (RF_{CR}) and installation damage factors (RF_{ID}) may be conservative and hence results in errors on the safe side for current ASD practice. Greenwood came to the same conclusion based on stepped isothermal creep-rupture tests performed on a polyester geosynthetic material in undamaged and damaged states.⁽¹⁰⁷⁾

Creep

Major types of geosynthetics used in GMSE and GRS structures are polypropylene, polyethylene, and polyester. These geosynthetics, manufactured with various types of polymers, are creep-sensitive. Stress level, polymer type, manufacturing method, and temperature have

been known to affect the creep potential of a geosynthetic material. In general, polypropylene and polyethylene exhibit larger creep deformation than polyester and polyvinyl alcohol under otherwise identical conditions.

As noted above, the allowable reinforcement tensile load employed in current design guidelines is determined by applying a safety factor and a combination of reduction factors to a limiting strength determined from short- and/or long-term laboratory tests. These tests are conducted by applying uniaxial tensile forces directly to the geosynthetic reinforcement (in a confined or unconfined condition) without regard to the soil-geosynthetic interaction behavior. It is important to point out that conducting uniaxial creep tests in the confinement of soil does not mean soil-geosynthetic interaction is accounted for. Wu indicates that long-term creep behavior of geosynthetic reinforcement in a reinforced soil structure must be determined by allowing soil-geosynthetic interaction to take place in a manner mimicking the field conditions.⁽¹⁰⁸⁾

McGowan et al. developed a fairly sophisticated uniaxial tension test device to measure creep behavior of geotextiles under soil confinement.⁽¹⁰⁹⁾ Wu and Ling et al. developed a simplified confined creep test method, in which a constant sustained tensile force is applied to a membrane-confined geosynthetic specimen (without inducing artificial soil-geosynthetic interface friction).^(110,111) Various geotextiles under different confining pressures have been tested. The results indicated that pressure confinement gave various degrees of improvement in creep behavior for different geotextiles. The greatest improvement was for needle-punched nonwoven geotextiles, while the improvement in woven geotextiles and geogrids was negligible.

Boyle manufactured a plane strain test device similar to that developed at Massachusetts Institute of Technology by Abramo and Whittle.^(112,113) In the test, a geosynthetic specimen was embedded in soil and subjected to a plane strain loading condition. The loads at both ends of the geosynthetic material were measured. Creep tests using sand as confining soil indicated that the geosynthetic material experienced stress relaxation. After creep deformation had diminished, the force in the geosynthetic material would reduce with time. The practical implication is that such GRS structures will have increasing safety margins as time progresses.

Crouse and Wu synthesized measured field behavior of seven reinforced soil walls that had been monitored for extended periods of time for assessment of their long-term performance characteristics.⁽¹¹⁴⁾ The GRS walls represented a variety of wall types using granular backfill. The walls were: (1) the Glenwood Canyon wall; (2) the Tanque Verde—Wrighttown—Pantano Roads project wall; (3) the Norwegian Geotechnical Institute (NGI) project, NGI wall; (4) the Japan Railway Test Embankment project, JR wall; (5) the Highbury Avenue, London Ontario project, Highbury wall; (6) the FHWA Algonquin wall; and (7) the Seattle Preload Fill project, Seattle wall. (See References 115 through 124, 7, 125, 54, 126, and 127.) The maximum creep strains in the reinforcements measured by strain gauges for all the walls were less than 1.5 percent, and the creep strain rate in all cases decreased with time in that there was a linear relationship between log-[creep rate] and log-[time]. Crouse and Wu also proposed a creep equation for predicting long-term creep deformation of GRS walls.⁽¹¹⁴⁾

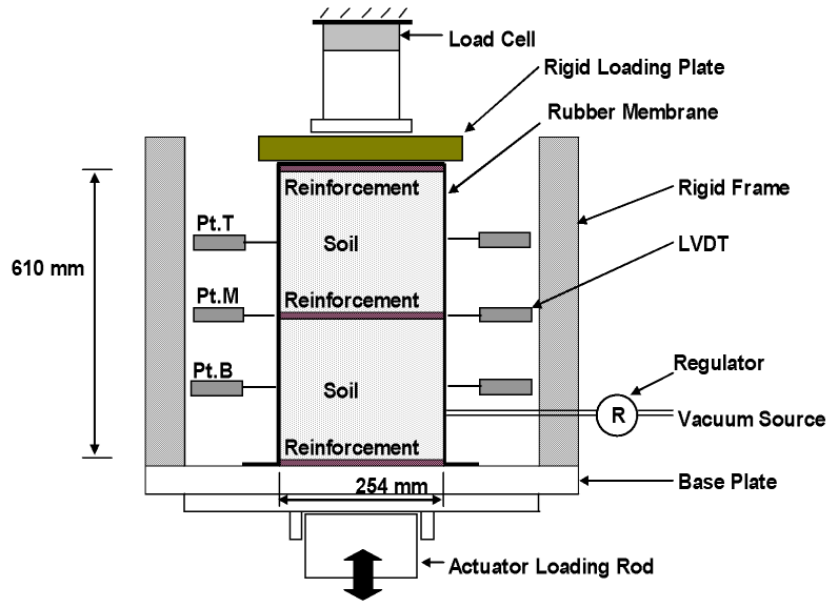
Allen and Bathurst analyzed the long-term creep data from 10 full-scale geosynthetic wall case histories.⁽⁹⁷⁾ Post-construction, long-term wall face deformation data show that geosynthetic wall face deformations, if the wall is properly designed, will generally be less than 0.98 to 1.17 inches

(25 to 30 mm) during the first year of service and less than 1.37 inches (35 mm) during the design lifetime for walls lower than 42.64 ft (13 m). Allen and Bathurst et al. studied reinforcement strains measured in geosynthetic-reinforced walls and slopes.^(128,129) The maximum strains were on the order of 1 to 2 percent or less.

Helwany and Wu performed finite element analysis on two 9.84 (3-m) high geosynthetic-reinforced retaining walls.⁽¹³⁰⁾ The walls were identical in every respect except that one was with a clayey backfill and the other with a granular backfill. In the clay-backfill wall, the maximum strain in the geosynthetic reinforcement increased by 3.5 percent from the end of construction to 15 years later. In the granular-backfill wall, the increase in maximum strain over the same time period was negligible. Note that the difference occurs in spite of comparable levels of load for the two walls. The analysis strongly suggests that the backfill played a very important role in creep deformation of a soil-geosynthetic composite. The finding was supported by studies conducted by Li and Rowe, Skinner and Rowe, Rowe and Taechakumthorn, Bergado and Teerawattanasuk, Liu and Won, Liu et al., and Li et al. (See references 131 through 139.)

Recognizing that the interaction between soil and geosynthetic reinforcement must be used as the basis for a rational design, Wu and Helwany developed a soil-geosynthetic long-term performance test, also referred to as the Soil-Geosynthetic Interactive Performance (SGIP) test.⁽¹⁴⁰⁾ The test has two important features. First, the stresses applied to the soil are transferred to the geosynthetic material in a manner similar to the typical load transfer mechanism in GRS structures (i.e., loads in reinforcement are transferred from soil through soil-geosynthetic interface bonding to geosynthetic material, rather than being applied directly to geosynthetic material). Second, both the soil and geosynthetic material are allowed to deform in an interactive manner under plane strain conditions. Two carefully conducted long-term performance tests, one using a clayey backfill and the other a granular backfill, have been reported. An element test on the geosynthetic material alone underestimated the maximum strain by 250 percent in the clay-backfill test, and overestimated the maximum strain by 400 percent in the sand-backfill test. It is noteworthy that creep deformation essentially ceased within 100 min after the sand-backfill test began; whereas the clay-backfill test experienced creep deformation over the entire test period (18 days), at which time shear failure occurred in the soil.

The SGIP test subsequently evolved to accommodate taller specimens, as shown in figure 57.⁽¹⁴¹⁾ A number of geosynthetic/granular road base composites have been tested, with a few under elevated temperatures to accelerate creep of the geosynthetic materials. For a nonwoven geotextile embedded in a road base material (with 20 percent of fines, prepared at 95-percent R.C. and 2-percent wet-of-optimum moisture) subject to an average surcharge of 15 psi (103 kPa) and in a 125 °F (52 °C) environment (note that the creep rate of the geotextile was about 150 times faster at 125 °F (52 °C) than at the ambient temperature, as measured in a series of long-term creep tests), creep deformation of the soil-geotextile composite was very small and decreased rapidly with time. Creep deformation ceased completely in 12 days and gave an accumulative average strain of 0.58 percent.



©K. Ketchart and J.T.H. Wu

1 mm = 0.039 inches

Figure 57. Illustration. Schematic diagram of a SGIP test.⁽¹⁴¹⁾

DISCUSSION

This discussion addresses five points regarding long-term design consideration of GRS walls and abutments: (1) long-term degradation, (2) construction damage, (3) creep, (4) current practice, and (5) the K -stiffness method.

Long-Term Degradation

Studies conducted by Elias and Allen and Bathurst have indicated that long-term degradation of geosynthetics in reinforcement applications during exposure to the in-soil environment appear to be very small.^(95,97)

A full-scale experiment conducted by the PWRI of Japan is enlightening in terms of long-term degradation. The experiment was to examine the failure mechanism of a 19.7-ft- (6.0-m-) high GRS wall. The wall face was segmental concrete blocks, and the backfill was a sandy soil reinforced with six layers of 11.5-ft- (3.5-m-) long polymer grid. The reinforcement inside the wall was severed at selected sections after the wall was constructed (for details, see chapter 3). The maximum horizontal movement due to cutting of the reinforcements was nearly zero until the cut was approximately $0.2H$ from the wall face, at which time the movement increased from 30 mm to 40 mm. The result of the PWRI experiment reveals the fundamental concept of GRS—the reinforcement serves not as tiebacks but as improvements to stiffness and strength properties. It also suggests that long-term degradation of the reinforcement is not a design issue. The cutting of reinforcements can be viewed as an extremely severe state of degradation in that the reinforcement has been degraded into small pieces and is not continuous.

Installation Damage

Most study on installation damage indicates that such damage does not severely affect load-strain behavior for woven geotextiles and geogrids, if at all, until damage levels become quite high. In applications where only the tensile strength at relatively low elongations is relevant, the effects of moderate installation damage is very limited. It has been suggested that RF_{ID} should be designated as being close to unity, on the order of 1.0 to 1.1.⁽¹⁰⁵⁾

Allen and Bathurst provided strong evidence that installation damage would have little, if any, effect on creep strains and rates for typical levels of installation damage in full-scale structures.⁽¹⁰⁶⁾ They stated that “in many cases, installation damage will have a negligible effect on the long-term strength at working stress levels (i.e., the geosynthetic behaves as if it is not damaged).”

Creep

Most geosynthetic materials are susceptible to creep under sustained loads. Stress level, polymer type, manufacturing method, and temperature have been known to affect the creep potential of a geosynthetic material. However, it can be drastically misleading to evaluate the creep potential of geosynthetic reinforcement based on tests performed by applying a sustained tensile force to geosynthetic specimens, as has been done by current design guides. If the confining soil has a tendency to deform faster than the geosynthetic reinforcement along its direction of elongation, the geosynthetic material will impose a restraining effect on the time-dependent deformation of the soil through the interface bonding forces. Conversely, if the geosynthetic reinforcement in isolation tends to deform faster than the confining soil, then the confining soil will restrain creep deformation of the reinforcement. This restraining effect is a direct result of soil-reinforcement interaction wherein redistribution of stresses in the confining soil and changes in tensile forces in the reinforcement occur over time in an interactive manner. Field-measured data reveal that geosynthetic creep deformation is not a design issue when well-compacted granular fill is used as backfill in the reinforced soil zone.

Current Practice

In an attempt to accommodate the effects of installation damage, creep, and durability, current practice applies a combined reduction factor to short-term reinforcement strength in design. The combined factor is obtained by multiplying individual reduction factors for each effect, which is unwarranted for closely spaced GRS. First, soil-geosynthetic interaction is critical to the susceptibility of geosynthetic creep; the current design approach is based on tests in which forces are applied directly to geosynthetic materials without regard to the soil. Second, creep is a deformation problem; the current design approach uses a somewhat arbitrary reduction factor for creep and treats it as a strength problem. Third, installation damage has been shown to have little effect on long-term creep, i.e., there is no compounding effect of installation damage and creep; also RF_D for geosynthetic materials has been found to be near unity.^(106, 105)

When well-compacted granular fill is employed, a single safety factor can be used to account for long-term effects, uncertainty, and ductility. It is an indisputable fact that creep of geosynthetic reinforcement in a GRS is strongly affected by the time-dependent behavior of the fill. When

time-dependent properties of a given fill material are in question, a laboratory test similar to the SGIP test (see figure 57) may be conducted to evaluate potential creep “deformation” of a GRS wall or abutment.

REFERENCES

1. American Association of State Highway and Transportation Officials, *LRFD Bridge Design Specifications*, 5th Edition, 2010.
2. Berg, R.R., Christopher, B.R., and Samtani, N.C., *Design of Mechanically Stabilized Earth Walls and Reinforced Soil Slopes, Design & Construction Guidelines*, FHWA-NHI-00-043, Federal Highway Administration, McLean, VA, March 2009.
3. National Concrete Masonry Association, *Design Manual for Segmental Retaining Walls*, 3rd Edition, J.G. Collin (ed.), 2009.
4. Geotechnical Engineering Office (GEO), *Guide to Reinforced Fill Structure and Slope Design, Draft, Geoguide 6*, Civil Engineering Department, Government of the Hong Kong Special Administrative Region, 2002.
5. British Standards Institution (BSI), *Code of Practice for Strengthened/Reinforced Soils and Other Fills*, BS8006, 1995 (amended 1999).
6. Adams, M.T., Nicks, J., Stabile, T., Wu, J.T.H., Schlatter, W., and Hartmann, J., *Geosynthetic Reinforced Soil Integrated Bridge System—Synthesis Report*, FHWA-HRT-11-027, Federal Highway Administration, McLean, VA, 2011.
7. Tatsuoka, F., Murata, O., and Tateyama, M., 1992, “Permanent Geosynthetic-Reinforced Soil Retaining Walls Used for Railway Embankments in Japan,” *Geosynthetic-Reinforced Soil Retaining Walls*, Denver, Colorado, 8–9 August 1991, Wu (ed.), A.A. Balkema Publishers, Rotterdam, The Netherlands, 1992, pp. 101–130.
8. Tatsuoka, F., Tateyama, M., Uchimura, T., and Koseki, J., “Geosynthetic-Reinforced Soil Retaining Walls as Important Permanent Structures,” *Mechanically-Stabilized Backfill*, Wu (ed.), A.A. Balkema Publishers, Rotterdam, The Netherlands, 1997, pp. 3–24.
9. Tatsuoka, F., “Recent Practice and Research of Geosynthetic-Reinforced Earth Structures in Japan,” *Journal of GeoEngineering*, 3(3), June 2008, pp. 77–100.
10. Segrestin, P., “GRS Structures with Short Reinforcements and Rigid Facing—Discussion of Previous Papers Published by Prof. F. Tatsuoka, M. Tateyama, and O. Murata,” *Proceedings, Recent Case Histories of Permanent Geosynthetic-Reinforced Soil Retaining Walls*. Tatsuoka and Leshchinsky (eds.), A.A. Balkema Publishers, Rotterdam, The Netherlands, 1994, pp. 323–342.
11. Bastick, M.J., “Reinforced Earth Narrow Walls and Abutments Correlation of Measured Performance with Design,” *Performance of Reinforced Soil Structures*, McGowan, Yeo, and Andrawes (eds.), British Geotechnical Society, Glasgow, Scotland, September 1990, pp. 59–63.

12. Lawson, C.R., and Yee, T.W., "Reinforced Soil Retaining Walls With Constrained Reinforced Fill Zones," *Geo-Frontiers 2005, ASCE Geotechnical Special Publication 140: Slopes and Retaining Structures Under Seismic and Static Conditions*, 2005.
13. Fukuoka, M., Imamura, Y., and Nishimura, J., "Fabric Faced Retaining Wall With Multiple Anchors," *Geotextile and Geomembranes*, 4, 1986, pp. 207–221.
14. Brandl, H., "Multi-anchored Soil Retaining Walls With Geosynthetic Loop Anchors," *Proceedings, 6th International Conference on Geosynthetics*, Atlanta, GA, Industrial Fabrics Association International (IFAI), 2, 1998, pp. 581–586.
15. Lin, C.C., Hsieh, T.J., Tsao, W.H., and Wang, Y.H., "Combining Multi-Nailings With Soil Reinforcement for Construction," *Mechanically Stabilized Backfill*, Wu (ed.), A.A. Rotterdam, The Netherlands, Publishers, 1997, pp. 255–257.
16. Vulova, C., Effects of Geosynthetic Reinforcement Spacing on the Behavior of Mechanically Stabilized Earth Walls, Ph.D. Dissertation, Department of Civil Engineering, University of Delaware, 2000.
17. Morrison, K.F., Harrison, F.E., Collin, J.G., Dodds, A., and Arndt, B., *Shored Mechanical Stabilized Earth (SMSE) Wall Systems Design Guidelines*, Central Federal Lands Highway Division, FHWA-CFL/TD-06-001, Federal Highway Administration, McLean, VA, 2006.
18. Chew, S.H., Schmertmann, G.R., and Mitchell, J.K., "Reinforced Soil Wall Deformations by Finite Element Method," *Performance of Reinforced Soil Structures*, McGowan, Yeo, and Andrawes (eds.), Thomas Telford Ltd, 1991, pp. 35–40.
19. Ling, H.I., and Leshchinsky, D., "Finite Element Parametric Study of the Behavior of Segmental Block Reinforced Soil Retaining Walls," *Geosynthetics International*, 10(2), 2003, pp. 77–94.
20. Liu, H., "Long-Term Lateral Displacement of Geosynthetic Reinforced Soil Segmental Retaining Walls," *Geotextiles and Geomembrances*, 32, 2012, pp. 18–27.
21. Wu, J.T.H., Lee, K.Z.Z., Helwany, S.B., and Ketchart, K., "Design and Construction Guidelines for Geosynthetic-Reinforced Soil Bridge Abutments with a Flexible Facing," *NCHRP Report 556*, Transportation Research Board, 2006.
22. Wu, J.T.H., Ketchart, K., and Adams, M., "Two Full-Scale Loading Experiments of Geosynthetic-Reinforced Soil (GRS) Abutment Wall," *International Journal of Geotechnical Engineering*, 2(4), 2008, pp. 305–317.
23. Tatsuoka, F., Tateyama, M., Aoki, H., and Watanabe, K., "Bridge Abutment Made of Cement-Mixed Gravel Backfill," *Ground Improvement, Case Histories*, Indradratna and Chu (eds.), Elsevier Geo-Engineering Book Series, 3, 2005, pp. 829–873.
24. Morishima, H., Saruya, K., and Aizawa, F., "Damage to Soils Structures of Railway and Their Reconstruction," Special Issue on Lessons from the 2004 Niigata-ken Chu-Etsu

- Earthquake and Reconstruction, *Foundation Engineering and Equipment (Kiso-ko)*, October, 2005, pp.78–83 (in Japanese).
25. Wu, J.T.H., *Revising the AASHTO Guidelines for Design and Construction of GRS Walls*, Colorado Department of Transportation, Report No. CDOT-DTD-R-2001-16, 2001.
 26. Thomas, D., and Wu, J.T.H., *Analysis of Geosynthetic-Reinforced Soil Walls With a Truncated Base*, Technical Report, Department of Civil Engineering, University of Colorado at Denver, 2000.
 27. Woodruff, R., *Centrifuge Modeling for MSE-Shoring Composite Walls*, Master of Science Thesis, Department of Civil Engineering, University of Colorado, Boulder, 2003.
 28. Vulova, C., and Leshchinsky, D., *Effects of Geosynthetic Reinforcement Spacing on the Behavior of Mechanically Stabilized Earth Walls*, FHWA Report No. FHWA-RD-03-048, Federal Highway Administration, McLean, VA, 2003.
 29. Chou, N.N.S., and Wu, J.T.H., *Investigating Performance of Geosynthetic-Reinforced Soil Walls*, Report No. CDOT-DTD-93-21, Colorado Department of Transportation, 1993.
 30. Lee, K., Jones, C.J.F.P., Sullivan, W.R., and Trolinger, W., “Failure and Deformation of Four Reinforced Soil Walls in Eastern Tennessee,” *Geotechnique*, 4(3), 1994, pp. 397–426.
 31. Huang, B.Q., Numerical Study and Load and Resistance Factor Design (LRFD) Calibration for Reinforced Soil Retaining Walls, Ph.D. Dissertation, Queen’s University, Kingston, Ontario, Canada, 2010.
 32. Wilson-Fahmy, R.F., Koerner, R.M., Harpur, W.A., “Long-Term Pullout Behavior of Polymeric Geogrids,” *Journal of Geotechnical Engineering*, American Society of Civil Engineers, 121(10), 1995, pp. 723–728.
 33. Bergado, D.T., Shivashankar, R., Alfaro, M.C., Chai, J-C., and Balasubramaniam, A.S., “Interaction Behavior of Steel Grid Reinforcements in a Clayey Sand,” *Geotechnique*, 43(4), 1993, pp. 589–603.
 34. Khoury, C.N., Miller, G.A., and Hatami, K., “Unsaturated Soil-Geotextile Interface Behavior,” *Geotextiles and Geomembranes*, 29, 2011, pp. 17–28.
 35. Bobet, A., *Design of MSE Walls for Fully Saturated Conditions*, FHWA/IN/JTRP-2002/13, Joint Transportation Research Program, Indiana Department of Transportation and Purdue University, Federal Highway Administration, McLean, VA, 2002.
 36. Sobhi, S., and Wu, J.T.H., “An Interface Pullout Formula for Extensible Sheet Reinforcement,” *Geosynthetic International*, 3(5), 1996, pp. 565–582.
 37. Abu-Farsakh, M.Y., Farrag, K., Almoh’d, I., and Mohiuddin, A., “Evaluation of Interaction Between Geosynthetics and Marginal Cohesive Soils From Pullout Tests,”

Advances in Geotechnical Engineering with Emphasis on Dams, Highway Materials, and Soil Improvement, ASCE Conference Proceedings. 2004. Available at doi: [http://dx.doi.org/10.1061/40735\(143\)25](http://dx.doi.org/10.1061/40735(143)25).

38. Suah, P.G., and Goodings, D.J., "Failure of Geotextile-Reinforced Vertical Soil Walls With Marginal Backfill," *Transportation Research Record 1772*, 2001, pp. 183–189.
39. Yang, K.H., Zornberg, J.G., Hung, W.Y., and Lawson, C.R., "Location of Failure Plane, and Design Considerations for Narrow Geotextile Reinforced Soil Wall Systems," *Journal of GeoEngineering*, 6(1), 2011, pp. 27–40.
40. Leshchinsky, D., and Vulova, C., "Numerical Investigation of the Effects of Geosynthetic Spacing on Failure Mechanisms in MSE Block Wall," *Geosynthetics International*, 8(4), 2001, pp. 343–365.
41. Tatsuoka, F., "Roles of Facing Rigidity in Soil Reinforcing, Keynote Lecture," *Proceedings of Earth Reinforcement Practice, IS-Kyushu '92*, Ochiai et al. (eds.), 2, 1992, pp. 831–870.
42. Yang, G., Zhang, B., Lv, P., and Zhou, Q., "Behavior of Geogrid Reinforced Soil Retaining Wall With Concrete Facing," *Geotextiles and Geomembranes*, 27, 2009, pp. 350–356.
43. Schlosser, F., and Long, N., "Recent Results in French Research on Reinforced Earth," *Journal of Construction Division, ASCE*, 100(CO3), 1974, pp. 223–237.
44. John, N.W.M., "Collapse Test on a Reinforced Soil Wall," *Failure in Earthworks*, Thomas Telford Ltd., London, 1985.
45. Burwash, W.J., and Frost, J.D., "Case History of a 9 m High Geogrid Reinforced Retaining Wall Backfilled With Cohesive Soil," *Proceedings, Geosynthetics '91 Conference*, Atlanta, GA, 2, 1991, pp. 485–493.
46. Leonards, G.A., Frost, J.D., and Bray, J.D., Collapse of Geogrid-Reinforced Retaining Structure, *Journal of Performance of Constructed Facilities*, ASCE, 8(4), 1994, pp. 274–292.
47. Collin, J.G., "Lessons Learned from a Segmental Retaining Wall Failure," *Geotextiles and Geomembranes*, 19, 2001, pp. 445–454.
48. Yoo, C., and Jung, H.-Y., "Case History of Geosynthetic Reinforced Segmental Retaining Wall Failure," *Journal of Geotechnical and Geoenvironmental Engineering*, ASCE, 132(12), 2006, pp. 1,538–1,548.
49. Leshchinsky, D., "Lessons Learned from Failed MSE Walls," 33rd Annual S. Kapp Dinner Lecture, Manhattan, New York, January 17, 2008.

50. Wendland, S., "When Retaining Walls Fail: The Lessons Learned." Transportation Engineers Association of Missouri (TEAM), PowerPoint presentation, March 17, 2011.
51. U.S. Army Corp of Engineers, *Engineering and Design, Retaining and Flood Walls, Engineer Manual EM 1110-2-250*, USACE, Washington, DC, 1989.
52. AASHTO, *LRFD Bridge Design Specifications*, 2th Edition, 1998.
53. Federal Highway Administration, *Mechanically Stabilized Earth Walls and Reinforced Soil Slopes Design and Construction Guidelines, FHWA Demonstration Project 82, FHWA-SA-96-071*, Washington, DC, 1997.
54. Simac, M.R., Christopher, B.R., and Bonczkiewicz, C., "Instrumented Field Performance of a 6 m Geogrid Wall," *Proceedings, 4th International Conference on Geotextiles, Geomembranes and Related Products*, The Hague, The Netherlands, 1990, pp. 53–59.
55. Bathurst, R.J., Benjamin, D.J., and Jarrett, P.M., "An Instrumented Geogrid Reinforced Soil Wall," *Proceedings, 12th International Conference on Soil Mechanics and Foundation Engineering*, Rio de Janeiro, Brazil, 1989, pp. 1,223–1,226.
56. Canadian Geotechnical Society, *Canadian Foundation Engineering Manual*, 4th Edition, 2006.
57. Koerner, R.M., *Designing With Geosynthetics*, Prentice Hall PTR, Upper Saddle River, NJ, 1998.
58. Barrett, R.K., "Retaining Wall-Dialog: A Tale of Two Walls," *Geosynthetics*, August 2006.
59. Barrett, R.K., and Ruckman, A.C., "GRS—A New Era in Reinforced Soil Technology." *Proceedings, GeoDenver 2007, Geosynthetics in Reinforcement and Hydraulic Applications*, ASCE, 2007.
60. Duncan, J.M., and Seed, R.B., "Compaction-Induced Earth Pressure Under K_0 Conditions," *Journal of Geotechnical Engineering*, ASCE, 112(1), 1986, pp 1–22.
61. Williams, G.W., Duncan, J.M., and Sehn, A.L., *Simplified Chart Solutions of Compaction-Induced Earth Pressures on Rigid Structures*, Geotechnical Engineering Report, Virginia Polytechnic Institute and State University, Blacksburg, VA, 1987.
62. Ketchart, K., and Wu, J. T. H., *Performance Test for Geosynthetic Reinforced Soil Including Effects of Preloading*, FHWA-RD-01-018, Federal Highway Administration, Washington, DC, 2001.
63. Clough, G.W., and Duncan, J.M., 1991, "Chapter 6—Earth Pressures," *Foundation Engineering Handbook*, 2nd Edition, H.Y. Fang, (ed.), Chapman and Hall, New York, pp. 223–235.

64. Yang, Z., *Strength and Deformation Characteristics of Reinforced Sand*, Ph.D. Thesis, University of California at Los Angeles, Los Angeles, CA, 1972.
65. Warren, K., and LeGrand, D., *Installation and Preliminary Evaluation of a GRS Integrated Bridge System Supporting a Large, Single Span, Steel Superstructure in Defiance Ohio*, Phase 1 and 2 Final Report submitted to Federal Highway Administration, 2010.
66. Ahmadi, H., and Hajialilue-Bonab, M., “Experimental and Analytical Investigations on Bearing Capacity of Strip Footing in Reinforced Sand Backfills and Flexible Retaining Wall,” *Acta Geotechnica*, Springer-Verlag, May 2012.
67. Dalton, D.C., Fabric Reinforced Brick Retaining Wall, West Yorkshire Metropolitan County Council, internal report, 1977.
68. Walsh, J.W., *Fabric Reinforced Brick Faced Earth Retaining Walls*, Ph.D. Thesis, University of Leeds, Leeds, United Kingdom, 1987.
69. Pinto, M.I.M., and Cousens, T.W., “Geotextile Reinforced Brick Faced Retaining Walls,” *Geotextiles and Geomembranes*, 1996, pp. 449–464.
70. Saran, S., Garg, K.G., and Bhandari, R.K., “Retaining Wall With Reinforced Cohesionless Backfill,” *Journal of Geotechnical Engineering*, ASCE, 118(12), 1992, pp. 1,869–1,888.
71. Garg, K.G., and Saran, S., “Effective Placement of Reinforcement to Reduce Lateral Earth Pressure,” *Indian Geotechnical Journal* 27(4), 1997, pp. 353–376.
72. Mittal, S., Garg, K.G., and Saran, S., “Analysis and Design of Retaining Wall Having Reinforced Cohesive Frictional Backfill,” *Geotechnical and Geological Engineering*, 24, 2006, pp. 499–522.
73. Garg, K.G., Ramesh, C., Chandra, S., and Ahmad, Z., “Performance of Instrumented Wall Retaining Reinforced Earthfill,” *Indian Geotechnical Journal*, 32(4), 2002, pp. 364–381.
74. Shinde, A.L., and Mandal, J.N., “Behavior of Reinforced Soil Retaining Wall With Limited Fill Zone,” *Geotechnical and Geological Engineering*, 25, 2007, Springer Verlag, pp. 657–672.
75. Won, M.S., and Kim, Y.S., “Internal Deformation Behavior of Geosynthetic-Reinforced Soil Walls,” *Geotextiles and Geomembranes*, Elsevier, 2007, pp. 10–22.
76. Abu-Hejleh, N.M., Zornberg, J.G., Elias, V., and Watcharamonthein, J., Design Assessment of the Founders/Meadows GRS Abutment Structure, Paper No. 03-3268, Transportation Research Board CD ROM, 2003.
77. Mitchell, J.W., Behavior of Geosynthetically Reinforced Soil Bridge Piers, M.S. Report, University of Massachusetts at Amherst, 2002.

78. Yogarajah, I., and Saad, M.A., "Development of Horizontal Earth Pressures and Behavior of Single and Multi Segmented Walls," *Proceedings, Earth Reinforcement*, A.A. Balkema Publishers, Rotterdam, The Netherlands, 1996, pp. 553–558.
79. Soong, T-Y., and Koerner, R.M., "On the Required Connection Strength of Geosynthetically Reinforced Walls," *Geotextiles and Geomembranes*, 15, 1997, pp. 377–393.
80. Ehrlich, M., and Mitchell, J. K., "Working Stress Design Method for Reinforced Soil Walls," *Journal of Geotechnical Engineering*, ASCE, 120(4), 1994, pp. 625–645.
81. Wu, J.T.H., "Lateral Earth Pressure Against the Facing of Segmental GRS Walls," *Proceedings, Geosynthetics in Reinforcement and Hydraulic Application, Geo-Denver 2007: New Peaks in Geotechnics*, American Society of Civil Engineers, 2007, pp. 1–11.
82. Yogarajah, I., and Andrawes, K.Z., "Modeling Construction Effects in Polymeric Grid Reinforced Soil Walls," *Proceedings, 5th International Conference on Geotextiles and Related Products*, Singapore, 1, 1994, pp. 177–182.
83. Barrett, R., <http://www.gcswall.com/>, 2012. Accessed October 30, 2012.
84. Carothers, S.D., "Plane Strain: The Direct Determination of Stress," *Proceedings, Royal Society of London, Series A, Containing Papers of a Mathematical and Physical Character*, 97(682), 1920, pp. 110–123.
85. Pham, T.Q., 2009, *Investigating Composite Behavior of Geosynthetic Reinforced Soil (GRS) Mass*, Ph.D. Thesis, University of Colorado, Denver.
86. Adams, M.T., "Performance of a Prestrained Geosynthetic Reinforced Soil Bridge Pier," *Proceedings, International Symposium on Mechanically Stabilized Backfill*, A.A. Balkema Publishers, Rotterdam, The Netherlands, 1997, pp. 25–34.
87. Adams, M.T., Ketchart K., and Wu, J.T.H., 2007, "Mini Pier Experiments: Geosynthetic Reinforcement Spacing and Strength as Related to Performance," *Proceedings, Geo-Denver 2007*, Denver, CO, American Society of Civil Engineers, Reston, VA, 2007.
88. Adams, M.T., Lillis, C.P., Wu, J.T.H., and Ketchart, K., "Vegas Mini-Pier Experiment and Postulate of Zero Volume Change," *Proceedings, Seventh International Conference on Geosynthetics, Nice, France*, 2002, pp. 389–394.
89. Adams, M.T., Schlatter, W., and Stabile, T., "Geosynthetic Reinforced Soil Integrated Abutments at the Bowman Road Bridge in Defiance County, Ohio." *Proceedings, Geo-Denver 2007*, Denver, CO, American Society of Civil Engineers, Reston, VA, 2007.
90. Elton, D.J., and Patawaran, M.A.B., "Mechanically Stabilized Earth Reinforcement Tensile Strength From Tests of Geotextile-Reinforced Soil," *Journal of the Transportation Research Board*, No. 1868, TRB, National Research Council, Washington DC, 2004. pp. 81–88.

91. Elton, D.J., and Patawaran, M.A.B., Mechanically Stabilized Earth (MSE) Reinforcement Tensile Strength from Tests of Geotextile Reinforced Soil, Alabama Highway Research Center, Auburn University, Auburn, AL, 2005,
92. Hausmann, M.R., "Strength of Reinforced Soil," *Proceedings of the Australian Road Research Board*, Section 13, Vol. 8, 1976, pp. 1–8.
93. Ziegler, M., Heerten, G., and Ruiken, G., "Progress in the Understanding of Geosynthetic/Soil Composite Material Behavior in Geosynthetic Reinforced Earth Structures," *Geoamericas2008, Proceedings, First Pan American Geosynthetics Conference, Cancun, Mexico, 2–5 March 2008*, pp. 1,227–1,236.
94. Wu, J.T.H., Lee, K.Z.Z., Helwany, S.B., and Ketchart, K., Design and Construction Guidelines for GRS Bridge Abutments with Flexible Facing, Report No. 556, National Cooperative Highway Research Program, Washington, DC, 2006.
95. Elias, V., *Corrosion/Degradation of Soil Reinforcements for Mechanically Stabilized Earth Walls and Reinforced Soil Slopes*, FHWA-NHI-00-044, Federal Highway Administration, Washington, DC, 2000.
96. Elias, V., *Long-Term Durability of Geosynthetics Based on Exhumed Samples from Construction Projects*, FHWA Report No. FHWA RD-00-157, Federal Highway Administration, McLean, VA, 2001.
97. Allen, T.M., and Bathurst, R.J., Prediction of Reinforcement Loads in Reinforced Soil Walls. Final Research Report, Washington State Department of Transportation and Federal Highway Administration, 2003.
98. Sprague, C.J., Allen, S., Thornton, S., "Installation Damage Testing, Sensitivity Assessment and Derivation of RF_{ID} ," *Geosynthetics '99 Conference*, Boston, 1999, pp. 1,123-1,132.
99. Watts, G.R.A., Brady, K.C., "Geosynthetics—Installation Damage and the Measurement of Tensile Strength," *Fifth International Conference on Geotextiles, Geomembranes and Related Products, Singapore*, 1994, pp. 1,159–1,164.
100. Brau, G., "Damage of Geosynthetics During Installation—Experience From Real Sites and Research Works," *First European Geosynthetics Conference, Maastricht*, 1996, pp. 145-150.
101. Rainey, T., Barksdale, R., "Construction Induced Reduction in Tensile Strength of Polymer Geogrids," *Proceedings, Geosynthetics '93 Conference*, Vancouver, 1993, pp. 729–742.
102. Richardson, G.N., "Field Evaluation of Geosynthetic Survivability in Aggregate Road Base," *Geotechnical Fabrics Report*, September 1998.

103. Allen, T.M. and Bathurst, R.J., "Characterization of Geosynthetic Load-Strain Behavior After Installation Damage," *Geosynthetics International*, 1(2), 1994, pp. 181–199.
104. Bathurst, R.J., Huang, B., and Allen, T.M., "Analysis of Installation Damage Tests for LRFD Calibration of Reinforced Soil Structures," *Geotextiles and Geomembranes*, 29, 2011, pp. 323–334.
105. Hufenus, R., Ruegger, R., Flum, D., and Sterba, I.J., "Strength Reduction Due to Installation Damage of Reinforcing Geosynthetics" *Geotextiles and Geomembranes*, 23, 2005, pp. 401–424.
106. Allen, T.M., and Bathurst, R.J., "Combined Allowable Strength Reduction Factor for Geosynthetic Creep and Installation Damage," *Geosynthetics International*, 3(3), 1996, pp. 407–439.
107. Greenwood, J.H., "The Effect of Installation Damage on the Long-Term Strength Design Strength of a Reinforcing Geosynthetic," *Geosynthetics International*, 9(3), 2002, pp. 247–258.
108. Wu, J.T.H., "Discussion on Long-Term Clay-Geotextile Interaction," *Recent Case Histories of Permanent Geosynthetic-Reinforced Soil Retaining Walls*, Tatsuoka and Leshchinsky (eds.), A.A. Balkema Publishers, Rotterdam, The Netherlands, 1994, pp. 343–344.
109. McGowan, A., Andrawes, K.Z., and Kabir, M.H., "Load-Extension Testing of Geotextiles Confined in Soil," *Proceedings of the Second International Conference on Geotextiles*, IFAI, 3, Las Vegas, NV, August 1982, pp. 793–798.
110. Wu, J.T.H., "Measuring Inherent Load-Extension Properties of Geotextiles for Design of Reinforced Structures," *ASTM Geotechnical Testing Journal*, 1991, pp. 157–165.
111. Ling, H., Wu, J.T.H., and Tatsuoka, F., "Short-Term Strength and Deformation Characteristics of Geotextiles Under Typical Operational Conditions," *Geotextiles and Geomembranes*, 11(2), 1992, pp. 185–219.
112. Boyle, S.R., "Unit Cell Tests on Reinforced Cohesionless Soils," *Proceedings, Geosynthetics '95*, IFAI, 3, Nashville, Tennessee, February 1995, pp. 1,221–1,234.
113. Abramento, M., and Whittle, A.J., "Experimental Evaluation of Pullout Analyses for Planar Reinforcements," *ASCE Journal of Geotechnical Engineering*, 1995, pp. 486–492.
114. Crouse, P., and Wu, J.T.H., "Geosynthetic-Reinforced Soil (GRS) Walls," *Journal of Transportation Research Board*, No. 1849, 2003, pp. 53–58.
115. Bell, J.R., Barrett, R.K., and Ruckman, A.C., "Geotextile Earth-Reinforced Retaining Wall Test: Glenwood Canyon, Colorado," *Transportation Research Record*, No. 916, Washington, DC, 1983, pp. 59–69.

116. Derakhashandeh, M., and Barrett, R.K., Evaluation of Fabric Reinforced Earth Wall, Colorado Department of Highway Report, CDOH-DTP-R-86-16, 1986.
117. Bell, J.R., and Barrett, R.K., "Survivability and Durability of Geotextiles Buried in Glenwood Canyon Wall," *Transportation Research Record*, No. 1474, National Academy Press, Washington, DC, 1995, pp. 55–63.
118. Berg, R.R., Bonaparte, R., Anderson, R.P, and Chouery, V.E., "Design, Construction, and Performance of Two Geogrid Reinforced Soil Retaining Walls," *Proceedings, Third International Conference on Geotextiles*, Vienna, Austria, 1986, pp. 401–406.
119. Bonaparte, R., and Gross, B.A. *Tensar Geogrid-Reinforced Soil Wall*, FHWA-EP-90-001-005, Federal Highway Administration, Washington, DC, 1989.
120. Fishman, K.L., Desai, C.S., and Sogge, R.L., "Field Behavior of Instrumented Geogrid Soil Reinforced Wall," *Journal of Geotechnical Engineering*, 119(3), August 1993, pp. 1,293–1,307.
121. Collin, J.G., Bright, D.G., and Berg, R.R., "Performance Summary of the Tanque Verde Project–Geogrid Reinforced Soil Retaining Walls," *Proceedings, Earth Retaining Session, ASCE Convention*, Atlanta, GA, 1994.
122. Bright, D.G., Collins, C.G., and Berg, R.R., "Durability of Geosynthetic Soil Reinforcement Elements in Tanque Verde Retaining Wall Structures," *Transportation Research Record*, No. 1439, Washington, DC, 1994, pp. 46–54.
123. Fannin, R.J. and Hermann, S. "Performance Data for Sloped Reinforced Soil Retaining Walls," *Canadian Geotechnical Journal*, 27(5), 1990, pp. 676–686.
124. Fannin, R.J., and Hermann, S., "Geosynthetic Strength–Ultimate and Serviceability Limit State Design," *Proceedings of the ASCE Specialty Conference on Stability and Performance of Slopes & Embankments II*, University of California, Berkeley, CA, 1992, pp. 1,411–1,426.
125. Bathurst, R.J., "Case Study of a Monitored Propped Panel Wall," *Geosynthetic-Reinforced Soil Retaining Walls* Wu, (ed.), A.A. Balkema, Rotterdam, The Netherlands, 1992, pp. 159–166.
126. Christopher, B.R., Bonczkiewicz, C., and Holtz, R.D., "Design, Construction and Monitoring of Full-Scale Test Soil Walls and Slopes," *Recent Case Histories of Permanent Geosynthetic Reinforced Soil Retaining Walls*, Tatsuoka and Leshchinsky (eds.), A.A. Balkema, Rotterdam, The Netherlands, 1994, pp. 45–60.
127. Allen, T.M., Christopher, B.R., and Holtz, R.D., "Performance of a 12.6 m High Geotextile Wall in Seattle, Washington," *Geosynthetic-Reinforced Soil Retaining Walls*, Wu (ed.), A.A. Balkema, Rotterdam, The Netherlands, 1992, pp. 81–100.

128. Allen, T.M., “Determination of Long-Term Strength of Geosynthetics: a State-of-the-Art Review,” *Proceedings of Geosynthetics '91*, IFAI, 1, Atlanta, GA, February 1991, pp. 351-379.
129. Bathurst, R.J., Benjamin, D.J., and Jarrett, P.M., “Laboratory Study of Geogrid Reinforced Soil Walls,” *Geosynthetics for Soil Improvement*, Holtz (ed.), ASCE Geotechnical Special Publication No. 18, Nashville, Tennessee, May 1988, pp. 178–192.
130. Helwany, S., and Wu, J.T.H., “A Numerical Model for Analyzing Long-Term Performance of Geosynthetic-Reinforced Soil Structures,” *Geosynthetics International*, 2(2), 1995, pp. 429–453.
131. Li, A.L., and Rowe, R.K., “Influence of Creep and Stress-Relaxation of Geosynthetic Reinforcement on Embankment Behavior,” *Geosynthetics International*, 8(3) 2001, pp. 233–270.
132. Li, A.L., Rowe, R.K., “Effects of Viscous Behaviour of Geosynthetic Reinforcement and Foundation Soils on Embankment Performance,” *Geotextiles and Geomembranes*, 26(4), 2008, pp. 317–334.
133. Skinner, G.D., and Rowe, R.K., “Design and Behaviour of Geosynthetic Reinforced Soil Walls Constructed on Yielding Foundations,” *Geosynthetics International*, 10(6), 2003, pp. 200–214.
134. Skinner, G.D., and Rowe, R.K., “Design and Behaviour of a Geosynthetic Reinforced Retaining Wall and Bridge Abutment on a Yielding Foundation,” *Geotextiles and Geomembranes*, 23(3), 2005, pp. 235–260.
135. Rowe, R.K., and Taechakumthorn, C., “Combined Effect of PVDs and Reinforcement on Embankments Over Rate-Sensitive Soils,” *Geotextiles and Geomembranes*, 26(3), 2008, pp. 239–249.
136. Bergado, D.T., and Tearawattanasuk, C., “2D and 3D Numerical Simulations of Reinforced Embankments on Soft Ground,” *Geotextiles and Geomembranes*, 26(1), 2008, pp. 39–55.
137. Liu, H., and Won, M.S., “Long-Term Reinforcement Load of Geosynthetic-Reinforced Soil Retaining Walls,” *Journal of Geotechnical and Geoenvironmental Engineering*, ASCE, 135(7), 2009, pp. 875–889.
138. Liu, H., Wang, X., and Song, E., “Long-Term Behavior of GRS Retaining Walls with Marginal Backfill Soils,” *Geotextiles and Geomembranes*, 27, 2009, pp. 295–307.
139. Li, F.L., Peng, F.L., Tan, Y., Kongkitkul, W., and Siddiquee, M.S.A., “FE Simulation of Viscous Behavior of Geogrid-Reinforced Sand Under Laboratory Scale Plane-Strain-Compression Testing,” *Geotextiles and Geomembranes*, 2011. Available at doi:10.1016/j.geotexmem. 2011.09.005.

140. Wu, J.T.H., and Helwany, S., "A Performance Test for Assessment of Long-Term Creep Behavior of Soil-Geosynthetic Composites," *Geosynthetic International*, 3(1), 1996, pp. 107–124.
141. Ketchart, K., and Wu, J.T.H., "A Modified Soil-Geosynthetic Interactive Performance Test for Evaluating Deformation Behavior of GRS Structures," *ASTM Geotechnical Testing Journal*, 25(4), 2002, pp. 405–413.

